Aus dem Adolf-Butenandt-Institut
Lehrstuhl: Molekularbiologie
Im Biomedizinischen Centrum der
Ludwig-Maximilians-Universität München
Direktor: Prof. Dr. Peter B. Becker
Arbeitsgruppe: Prof. Dr. Gunnar Schotta

Dominant role of DNA methylation over H3K9me3 in ERV silencing during embryonic endoderm development

Dissertation zum Erwerb des Doktorgrades der
Naturwissenschaften (Dr. rer. nat.) an der
Medizinischen Fakultät der
Ludwig-Maximilians-Universität München
vorgelegt von

Zeyang Wang

aus Jilin, China

München, 2020

Gedruckt mit Genehmigung der Medizinischen
Fakultät der Ludwig-Maximilians-Universität München

Betreuer: Prof. Dr. rer. nat. Gunnar Schotta

Zweitgutachter: Prof. Dr. Olivier Gires

Dekan: Prof. Dr. med. dent. Reinhard Hickel

Tag der mündlichen Prüfung: 15.04.2020

Eidesstattliche Versicherung

Ich erkläre hiermit an Eides statt, dass ich die vorliegende Dissertation mit dem Thema

“Dominant role of DNA methylation over H3K9me3 in ERV silencing during embryonic endoderm development”

selbständig verfasst, mich außer der angegebenen keiner weiteren Hilfsmittel bedient und alle Erkenntnisse, die aus dem Schrifttum ganz oder annähernd übernommen sind, als solche kenntlich gemacht und nach ihrer Herkunft unter Bezeichnung der Fundstelle einzeln nachgewiesen habe.

Ich erkläre des Weiteren, dass die hier vorgelegte Dissertation nicht in gleicher oder in ähnlicher Form bei einer anderen Stelle zur Erlangung eines akademischen Grades eingereicht wurde.

__Xiamen, 25,04,2020__ _____

Ort, Datum Unterschrift Zeyang Wang

The work presented in this thesis is being assembled into a manuscript for publication in a peer-reviewed journal.

Dominant role of DNA methylation over H3K9me3 in ERV silencing during embryonic endoderm development.

Wang, Z.*, Fan, R.*, Cernilogar, F.M., Nuber A., Silvia Schirge, S., Lickert, H. and Schotta, G.

* These authors contributed equally to this work.

While carrying out my PhD thesis I collaborated with colleagues to support other scientific projects, which led to the following publications:

Cernilogar, F.M., Hasenoder, S. *, **Wang, Z**. *, Scheibner, K. *, Burtscher, I., Sterr, M., Smialowski, P., Groh, S., Evenroed, I.M., Gilfillan, G.D., et al. Pre-marked chromatin and transcription factor co-binding shape the pioneering activity of Foxa2. Nucleic Acids Res. 2019 Jul 27. PMID: 31350899

* These authors contributed equally to this work

I. Table of contents

II. Abstract

Balanced endogenous retroviruses (ERVs) expression is important for early embryonic development. Dysregulation of ERV expression is often associated with severe damage to cells leading to defective development. ERVs expression is tightly regulated by epigenetic mechanisms such as the histone H3 lysine 9 trimethylation (H3K9me3) and DNA methylation. H3K9me3 is considered primarily responsible for silencing ERVs including Intracisternal A-particle (IAP) elements in mouse embryonic stem cells, whereas DNA methylation is considered more important in differentiated cells. Recently, Setdb1, a major silencing factor for ERVs, was identified as a dominant factor in control of distinct ERV families including the VL30-class but not IAPs in differentiated cells. However, the roles of Setdb1 mediated H3K9me3 in ERV silencing remain unclear in early embryonic lineage decisions.

To assess roles of Setdb1 in ERV silencing during early embryonic lineage decisions, Setdb1 was specifically deleted in endoderm cells using a Sox17-driven Cre recombinase ($Setdb1^{END}$). ERV expression analysis showed that only visceral endoderm (VE) which is a specific subtype of endoderm cells with distinct developmental origin but similar morphology and function but not definitive endoderm (DE) displayed ERV derepression in $Setdb1^{END}$ embryos. To molecularly characterize ERV silencing in these two endoderm subsets, I performed *in vitro* differentiation of $Setdb1^{END}$ ES cells to either extra-embryonic endoderm (XEN) cells which is the progenitor of visceral endoderm or definitive endoderm cells. Notably, transcriptome analysis of *in vitro* differentiated cells completely reflected the *in vivo* situation with many ERV families being up-regulated in mutant XEN cells and very minor ERV derepression in DE cells. These findings correlate with pronounced reduction of H3K9me3 in mutant XEN cells while this modification was less affected in mutant DE cells, suggesting redundant H3K9me3 pathways in DE. Similar to H3K9me3, DNA methylation on ERVs was reduced in XEN cells but maintained in DE cells.

However, interestingly, ERV derepression was observed in both XEN and DE cells upon depletion of Dnmt1. Moreover, the loss of DNA methylation leads to a reduction of H3K9me3 at imprinted genes but not on ERVs in both types of endoderm cell.

Altogether our data suggest redundant cell-type-specific H3K9me3 pathways in endoderm cells. Moreover, these findings shed light on the H3K9me3 repressive mechanisms through DNA methylation in ERV silencing and indicate a dominant role of DNA methylation in ERV silencing during early embryonic endoderm commitment.

III. Zusammenfassung

Die ausgeglichene Expression endogener Retroviren (ERVs) ist wichtig für die frühe embryonale Entwicklung. Eine Fehlregulation der ERV-Expression ist häufig mit schweren Schäden an den Zellen verbunden, die zu einer fehlerhaften Entwicklung führen. Die Expression von ERVs wird durch epigenetische Mechanismen wie die Histon H3 Lysin 9 Trimethylierung (H3K9me3) und die DNA-Methylierung streng reguliert. H3K9me3 ist in erster Linie für die Stummschaltung von ERVs, einschließlich Intracisternale A-Partikel (IAP) -Elemente, in embryonalen Stammzellen der Maus verantwortlich, wohingegen der DNA-Methylierung in differenzierten Zellen eine wichtigere Rolle zugeordnet wird. Kürzlich wurde Setdb1, ein Hauptfaktor der ERV Stummschaltung, als dominanter Faktor bei der Kontrolle verschiedener ERV-Familien einschließlich der VL30-Klasse, jedoch nicht der IAPs, in differenzierten Zellen identifiziert. Dennoch ist die Rolle von Setdb1-vermitteltem H3K9me3 bei der ERV-Stummschaltung während Entscheidungen der frühen embryonalen Abstammungslinien unklar.

Um die Rolle von Setdb1 bei der ERV- Stummschaltung bei Entscheidungen über frühe embryonale Abstammungslinien zu bewerten, haben wir Setdb1 in Endodermzellen unter Verwendung einer Sox17-gesteuerten Cre-Rekombinase (Setdb1^{END}) spezifisch entfernt. Wir haben die ERV-Expression analysiert und stellten fest, dass nur das viszerale Endoderm (ein spezifischer Subtyp von Endodermzellen mit unterschiedlichem Entwicklungsursprung, aber ähnlicher Morphologie und Funktion), aber nicht das definitive Endoderm (DE) in Setdb1^{END}-Embryonen eine ERV-Derepression aufwies. Um die ERV-Stummschaltung in diesen beiden Endoderm-Untergruppen molekular zu charakterisieren, führten wir eine In-vitro-Differenzierung von Setdb1^{END}-ES-Zellen entweder zu einem extraembryonales Endoderm (XEN), den Vorläufer des viszeralen Endoderms (VE) Zellen sind, oder eines definitiven Endoderms Zellen durch. Insbesondere die Transkriptomanalyse von *in vitro* differenzierten Zellen spiegelte die *in vivo*-Situation vollständig wider, wobei viele ERV-Familien in mutierten XEN-Zellen hochreguliert waren und in DE-Zellen eine sehr geringe ERV-Derepression auftrat. Diese Ergebnisse korrelieren mit einer ausgeprägten Reduktion von H3K9me3 in mutierten XEN-Zellen, während diese Modifikation in mutierten DE-Zellen weniger betroffen war, was auf redundante H3K9me3-Wege in DE hindeutet. Ähnlich wie bei H3K9me3 wurde die DNA-Methylierung auf ERVs in XEN-Zellen reduziert, in DE-Zellen jedoch beibehalten.

Interessanterweise wurde jedoch eine ERV-Derepression sowohl in XEN- als auch in DE-Zellen nach Verringerung von Dnmt1 beobachtet. Darüber hinaus führt der Verlust der DNA-Methylierung zu einer Reduktion von H3K9me3 an geprägten Genen, jedoch nicht an ERVs in beiden Arten von Endodermzellen.

Insgesamt deuten unsere Daten auf redundante zelltypspezifische H3K9me3-Pfade hin. Darüber hinaus geben diese Ergebnisse Aufschluss über die H3K9me3-Repressionsmechanismen durch DNA-Methylierung bei der ERV-Stummschaltung und weisen auf eine dominante Rolle der DNA-Methylierung bei der ERV-Stummschaltung während der frühen Festlegung des embryonalen Endoderms hin.

1. Introduction

1.1. Lineage decision during early embryonic development

The development of the mouse embryo, as a commonly used mammalian model system, shows a distinct progression over time. At around 3 days after fertilization (E3.0) the embryonic cells form a compact morula with first lineage specifications, which get more distinct at blastulation stage by ~E3.5 when the inner cell mass (ICM) and the trophectoderm (TE) begin to separate. The ICM contains epiblast (Epi) and primitive endoderm (PrE) cells, which give rise to visceral endoderm (VE) and parietal endoderm cells (Zernicka-Goetz et al., 2009) (Figure 1.1A). Primitive endoderm is the epithelial layer of cells that lines the blastocoelic surface of the ICM. Visceral endoderm cells envelop the epiblast of the post-implantation embryo and displace proximally to the extraembryonic yolk sac (Rossant and Tam, 2009; Srinivas, 2006) (Figure 1.1B). Visceral endoderm cells are shown to remain associated with the epiblast and incorporated into the early gut tube (Kwon et al., 2008). By ~E6.5 which is called gastrulation stage, ectoderm derived from the anterior epiblast and the posterior proximal epiblast develop into the primitive streak, which then forms mesoderm and endoderm (Lawson et al., 1991). Each of the three germ layers forms its own structure and they contain all progenitors for the future body plan. Definitive endoderm (DE) contributes tissues to the visceral organs associated with the gut, such as the liver and pancreas (Grapin-Botton, 2008).

In vitro embryonic stem (ES) cells and extraembryonic endoderm stem (XEN) cells can be derived from the Epi and PrE lineages, respectively. ES cells maintain the pluripotency and are able to differentiate into any embryonic cell types. XEN cells retain the property of primitive endoderm cells and can contribute to primitive endoderm derivatives including *in vivo* visceral endoderm cells in chimeras (Kunath et al., 2005). XEN cells, as a progenitor of visceral endoderm cells, share similar transcriptome features, but show difference in expression of some transcription factor such as AFP, Gata6 and so forth. ES cells can be reprogrammed to XEN cells by overexpression of transcription factors such as the ones from the GATA family (Niakan et al., 2013; Wamaitha et al., 2015). ES cells can also differentiate to DE cells by stimulation with a high concentration of Activin A (Kubo et al., 2004). Moreover, it has been shown that Activin A/Smad2/3 signaling synergizes with the Wnt pathway to promote the activation of mesendoderm genes (Singh et al., 2012). Also others have shown that the canonical Wnt signaling is required during late stages of activin-induced development of Sox17-expressing endodermal cells (Hansson et al., 2009).

Visceral endoderm and definitive endoderm share similar molecular properties of many key endoderm marker genes. However, they can be distinguished using different markers both *in vivo* and *in vitro*. AFP can be used as a marker to monitor the dynamics of visceral endoderm cell dispersal to distinguish it from definitive endoderm *in vivo* (Kwon et al., 2008; Viotti et al., 2014). Gsc has been used to monitor the generation of Gsc–Sox17+ visceral endoderm and Gsc+Sox17+ definitive endoderm and to define culture conditions to differentiate (Yasunaga et al., 2005).

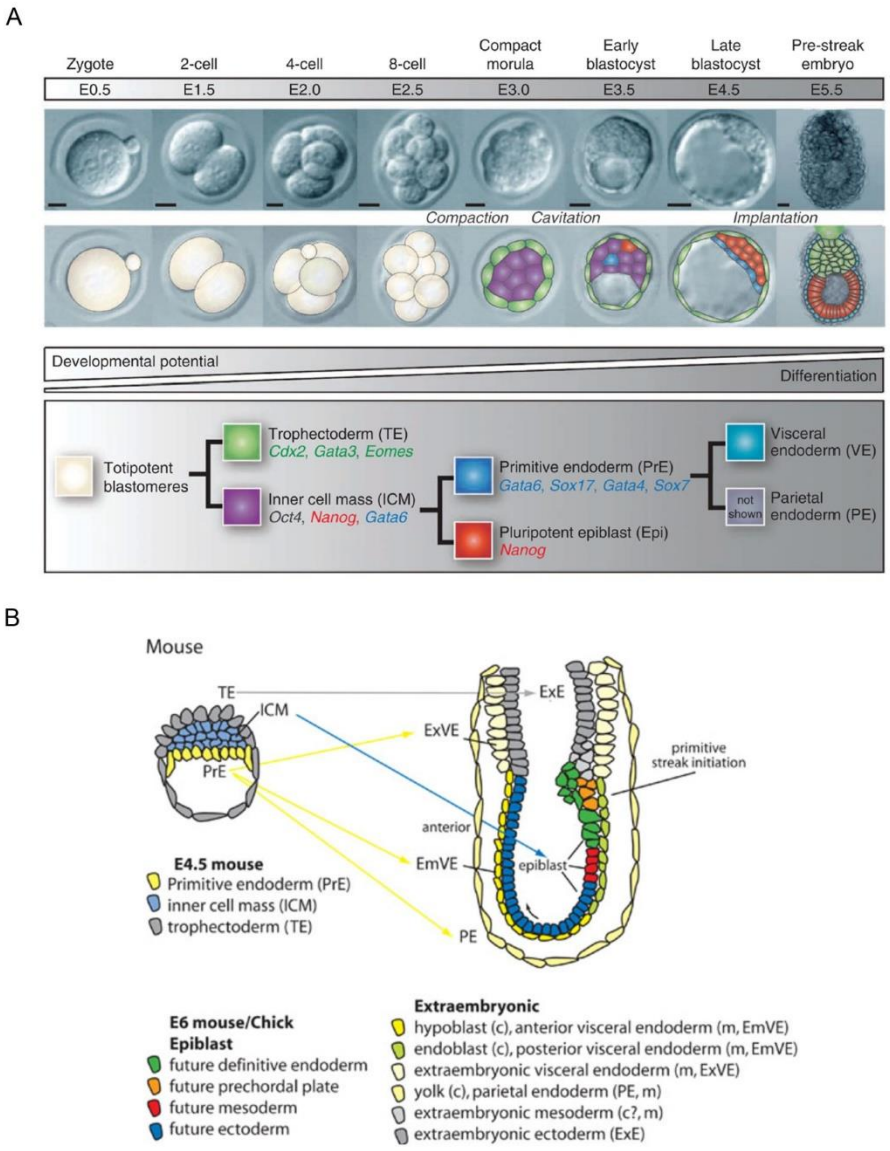

Figure 1.1 Overview of early embryonic development and the organization of endoderm

A. Overview of early embryonic development. The morula first gives rise to trophectoderm and inner cell mass, the inner cell mass develops into primitive endoderm and epiblast. The PrE differentiates into visceral and parietal endoderm. Lineage-associated gene expression is noted below each cell type (Niakan et al., 2013). Scale bars, 50 μm.

B. Organization of endodermal progenitors and extraembryonic endoderm at the start of gastrulation in mouse embryos. The epiblast gives rise to ectoderm, mesoderm and endoderm. Extraembryonic endoderm lineages and the fate of epiblast cells are color-coded (Grapin-Botton, 2008).

1.2. Epigenetic modifications and gene expression

Epigenetics is the study of heritable changes that affect gene expression without alterations in the DNA sequence. Early embryonic development is accompanied by extensive epigenetic reprogramming. Epigenetic phenomena in animals are mediated by DNA methylation and stable chromatin modifications such as methylation, acetylation or other chemical modifications of histone proteins. This epigenetic modification, by chemical alterations of DNA and histones, can affect the expression of genes. For instance, acetylation of the histone 3 tail at lysine 27 (H3K27ac) and trimethylation of lysine 4 of histone 3 (H3K4me3) are usually considered to mark active transcription. However, DNA methylation and H3K9me3 are considered to be associated with silenced states. The dynamic structure of chromatin responds to epigenetic modification changes, especially by changing histone modifications, cells can modulate the nucleosome mobility and chromosome accessibility accordingly (Figure 1.2). Modifications associated with gene silencing can help to reduce nucleosome mobility. For instance, H3K9me3 favors heterochromatin formation when bound by heterochromatin protein 1 (HP1). Highly repeated DNA sequences such as tandem-repeat satellites, retrotransposons and endogenous retroviruses (ERVs) are kept physically inaccessible by packaging them in condensed heterochromatin termed “constitutive heterochromatin”. They are traditionally thought to be universally silenced across developmental lineages (Saksouk et al., 2015). By contrast, cell-type-specific genes are dynamically silenced during development and can be compacted into “facultative heterochromatin” (Trojer and Reinberg, 2007).

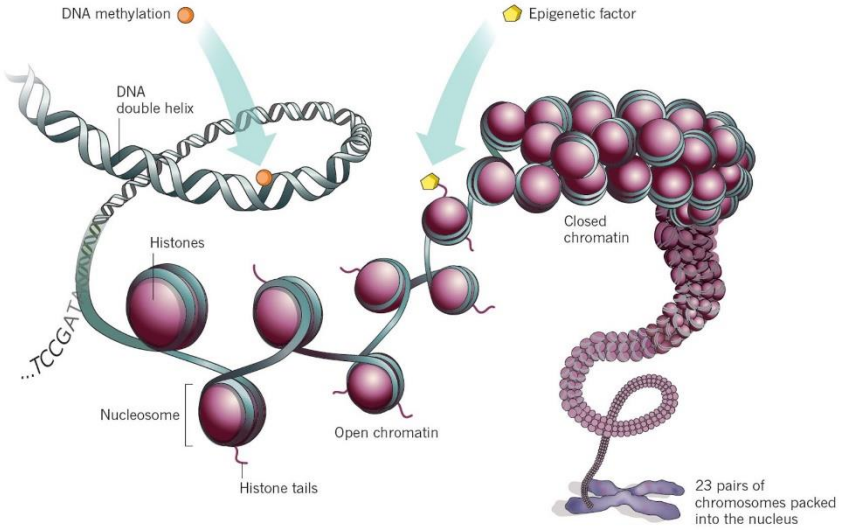

Figure 1.2 Epigenetic modifications in the context of chromatin structure

In eukaryotes, double strand DNA wraps around histone octamer to form nucleosome, the fundamental unit of chromatin. Nucleosome is compacted into higher order chromatin structure in the nucleus. Epigenetic regulators dynamically add or remove epigenetic marks on DNA or histone tails to regulate gene expression (Marx, 2012).

1.3. Transposable elements

Transposable elements (TE) are DNA sequences that can change their position within a genome. These repetitive elements accumulate while the evolutionary complexity of their host increases. They make up 38 and 41 % of the mouse and human genome, respectively (Figure 1.3A) (Garcia-Perez et al., 2016; Kidwell, 2002; Mouse Genome Sequencing et al., 2002). Based on the mechanism of transposition, they can be divided into two classes: Retrotransposons, which mobilize through a copy-and-paste mechanism and DNA transposons, which mobilize through a cut and paste mechanism.

1.3.1 Retrotransposons

Retrotransposons can be subdivided into two subclasses: long terminal repeat (LTR) retrotransposons and non-LTR retrotransposons. The chromosomal integration of LTR retrotransposons are catalyzed by a retroviral like integrase, whereas non-LTR retrotransposons, which consist of long and short interspersed nuclear elements (LINEs and SINEs), are catalyzed by a reverse transcriptase. Non-LTR retrotransposons predominate in both mouse and human and make up to ~35 % of the genome. LINE-1 retrotransposons account for ~17 % of the mouse and human genome. In contrast, LTR retrotransposons only constitute ~10 % of the mammalian genome (Figure 1.3A) (Garcia-Perez et al., 2016; Kidwell, 2002). Although the abundance of retrotransposons in the mouse and human genome are quite similar, the activities of these retrotransposons are very different. Many of these retrotransposons maintain the ability to retrotranspose (Jern and Coffin, 2008; Maksakova et al., 2006). Most of LINE1 elements lost their activity and only 80-100 L1 elements are still active in human genome. But a few thousand L1 elements remain active in mouse genome.

1.3.2 Endogenous retroviral elements

Endogenous retroviruses (ERVs) are derived from retroviral infections of germ line cells, then became endogenized and obtained the ability to retrotranspose. In mammals, all LTR-retrotransposons belongs to the ERVs superfamily which makes the term endogenous retrovirus synonymous to the term LTR-retrotransposons (Stocking and Kozak, 2008). ERVs have a retroviral structure compromised of gag, pro, pol and env genes flanked by LTRs but

loss of their envelope gene in mice (Figure 1.3B) (Bannert and Kurth, 2006). The pol gene, which is the most conserved region, encodes a reverse transcriptase (RT). The env gene encodes the envelope protein involved in virus entry, and the gag gene encodes structural proteins for the viral core. The LTR regions can act as promoters and can be bound by transcription factors to regulate the expression of ERVs (Kato et al., 2018). Based on the phylogenetic relationship and sequence similarity, ERVs can be classified into ERV1/HERVH(W), ERVK/HERVK and ERVL/HERVL families in mouse and human, respectively. HERV-K might be the only family to retain activity in human. In contrast to the human ERVs, which are almost extinct, most of the ERV families are still active in mouse. The most active ERVs in mouse are intracisternal A-type particles (IAP) elements with a total number of about 1000 copies (Barbot et al., 2002). Mouse IAPs have lost the env gene present in their infectious progenitors. Many of the IAP copies are truncated and only one third of the IAPs have the full coding gag pro and pol genes for retrotransposition (Figure 1.3B). Due to the active transposition, ongoing activities of several families of LTR elements are causing 10–15 % of all inherited mutations and genetic polymorphisms in murine lab strains (Maksakova et al., 2006).

1.3.3 Physiological roles of endogenous retrovirus

ERVs were considered as parasitic and selfish elements. By now, numerous studies have proved that the host can utilize these elements to fulfill new functions. And they are now considered as a source of genetic variation for the evolution of higher species (Friedli and Trono, 2015).

On the one hand, a subset of ERVs serves as gene promoters to initiate transcription from LTR regions and could also generate chimeric transcript for proper neighboring gene expression. Recent studies using next-generation sequencing (NGS) analysis have shown that 6-30 % of the mouse or human RNAs start within repetitive elements. ERVs are able to affect both neighboring genes and distant loci by either acting as alternative promoters or enhancers, respectively (Figure 1.3C). One well studied example shows a significant number of two-cell (2C) stage-specific transcripts are initiated from the LTR region in mouse ES cells. The ERVs can be used as a reporter restricted to the zygote/2C stage cells (Macfarlan et al., 2012). In Setdb1 knockout mESCs, ~15 % up-regulated genes are associated with derepression of promoter-proximal ERVs and half of them are in the context of chimeric transcripts, that initiate in LTR region of ERVs and splice into canonical genic exons (Karimi et al., 2011). A MaLR initiated aberrant transcript of colony-stimulating factor 1 receptor

(CSF1R) gene contributes to the tumor survival in human lymphomas (Lamprecht et al., 2010)

On the other hand, a subset of ERVs serves as enhancers to regulate the expression of genomically distant genes. Therefore, ERVs need to be well controlled for proper gene expression. Targeting LTR5HS, an ape-specific class of HERVK, with CRISPR activation and interference showed reciprocal up- and down-regulation of hundreds of genomically distant genes in human embryonal carcinoma (NCCIT) cells (Fuentes et al., 2018). Though, ERVs are enriched by cell-type specific transcription factor binding motifs, the motif itself does not reflect the enhancer potential. When using CRISPR interference to target the family of RLTR13D6 elements in mESCs, a minority of the ERVs show significant enhancer roles in gene regulation (Todd et al., 2019).

In summary, ERV initiated transcripts contribute to the pluripotency in both mice and human embryonic stem cells (Macfarlan et al., 2012; Wang et al., 2014). Additionally, increasing roles of onco-exaptations of ERVs have been supported by numerous studies in different human tumor cells (Lamprecht et al., 2010; Lock et al., 2014; Wiesner et al., 2015). Improper silencing of ERVs also impairs cell survival through abnormal production of ERV proteins. For instance, derepression of MLV copies in Setdb1 deficient pro-B cells associated with production of MLV proteins results in activation of unfolded protein response and leads to pro-B cells death through apoptosis (Pasquarella et al., 2016).

Considering all that, it becomes obvious that mammals were required to develope numerous ways to repress the endogenous retrovirus.

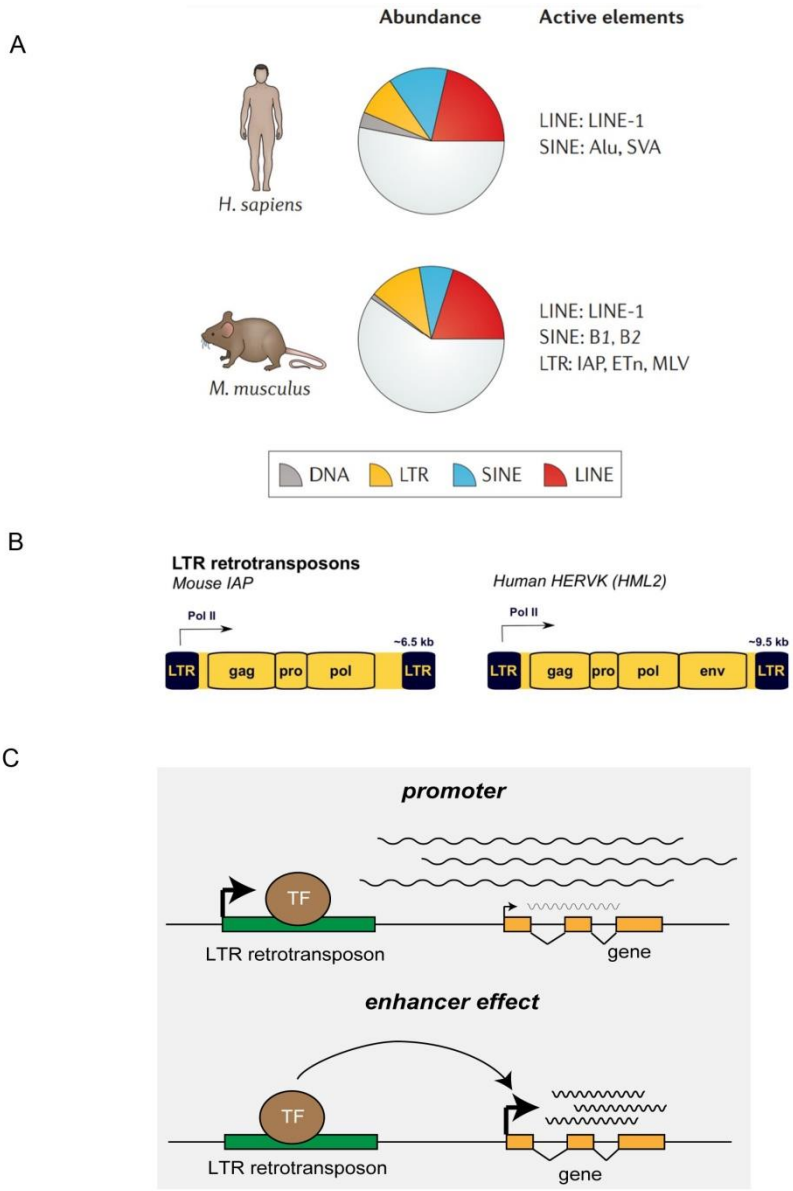

Figure1.3 Structure and function of transposable elements in the mammalian genome

A. Similar percentage of the human and mouse genomes are occupied by different types of transposable elements. LINEs are active in both mouse and human but ERVs are mainly active in mouse (Deniz et al., 2019).

B. Mouse IAP have lost the env gene present in their infectious progenitors.

C. Transcription factor (TF) binds to LTR retrotransposon that locates at upstream of the gene and serves as promoter or enhancer to regulates gene expression.

1.4 Silencing mechanisms of endogenous retroviral elements

Repetitive elements are regulated by context-specific patterns of chromatin marks. Around 29 epigenetic modifiers are identified as significantly involved in regulating these repetitive elements (He et al., 2019). Two major chromatin modifications, H3K9me3 and DNA methylation have been implicated in ERV silencing, however, their roles in ERV silencing

may differ in different cell types. DNA methylation has been thought to be dominant in ERV silencing in somatic tissues (Walsh et al., 1998). Global DNA demethylation occurs in the early embryo and germline, which is mediated by Ten-eleven translocation (Tet) enzymes (Smith et al., 2012). ERVs are accordingly released from DNA methylation repression. Since balanced ERV expression is important for early embryonic development, ERVs are suppressed by an alternative repressive KRAB ZnF-Trim28-Setdb1 pathway during the extensive DNA methylation. Certain ERV sequences can mediate recruitment of KRAB-ZnFs, which in turn interact with Trim28 to recruit Setdb1 to establish H3K9me3 and silence ERVs. Despite of stable H3K9me3, the H3K27me3 mark is also shown to accumulate at transposons in response to DNA methylation loss when converting primed ESCs to naïve ESCs (Walter et al., 2016).

In this thesis, I focus on the primary silencing mechanism of a subclass of LTR-retrotransposons. Therefore, I will give an overview over our current knowledge about DNA dependent and DNA-independent (H3K9me3) LTR-retrotransposon silencing in the following chapter.

1.4.1 DNA methylation mediated ERV silencing

DNA methylation is a repressive mark involving the transfer of a methyl group to the C-5 of the cytosine residue by DNA methyltransferase. Most DNA methylation is critical for normal development in terms of genomic imprinting, X-chromosome inactivation and repetitive element suppression. DNA methylation is regulated by a family of DNA methyltransferases (DNMT): DNMT1, DNMT2, DNMT3A, DNMT3B, and DNMT3L in mammals.

Dnmt1 as a maintenance DNA methyltransferase is thought to be recruited to sites of replication by its partner Uhrf1 and uses the parental strand as template to modify the synthesized daughter strand (Hermann et al., 2004) (Figure 1.4). Dnmt3 (including Dnmt3a and Dnmt3b) as de novo methyltransferases are primarily responsible for establishing genomic DNA methylation patterns. Cells with functional Dnmt1 but lack of Dnmt3a and Dnmt3b show hemi-methylation of up to 30 % of the CG sites in repeat region. This illustrates a strong cooperativity between Dnmt3a and/or -3b and Dnmt1 in methylation maintenance at repeats (Liang et al., 2002). Despite the concerted action of Dnmt enzymes in methylation maintenance and establishment, an unexpected division role of Dnmt1 and Dnmt3a/b in methylating LTR and LINE elements is also observed (Li et al., 2015).

Knocking out Dnmt1 in the post-implantation embryo leads to lethality at E13.5. The embryos show global demethylation and strong activation of IAP endogenous retroviruses which indicate a dominate role of DNA methylation in ERV silencing (Li et al., 1992; Walsh et al.,

1998). However, this activation of IAP ERVs has not been observed in Dnmt1 knockout primordial germ cells (PGCs) (Walsh et al., 1998). As PGCs undergo progressive DNA demethylation and reach a low point at E13.5 (Hajkova et al., 2002). A DNA methylation independent mechanism mediated by H3K9me3 is responsible for ERV silencing at this stage. A similar phenomenon has also been observed in ES cells as epiblast cells undergo similar demethylation. ERVs including IAPs remained silenced in Dnmt1 knockout ES cells and are only activated when they differentiated (Hutnick et al., 2010). Dnmt triple-knockout (Dnmt TKO) ES cells show that ERVs are minimally derepressed and Setdb1 mediated H3K9me3 is maintained even when the DNA methylation is severely reduced (Matsui et al., 2010). mES cells lacking G9a show no derepression of retrotransposons with significant loss of DNA methylation and moderate decrease of H3K9me2, however, the H3K9me3 remains unchanged (Dong et al., 2008).

Reversion of mESCs from primed state to naïve state correlates with genome wide demethylation. However, regions including IAPs and satellites are resistant to demethylation and correlate with the presence of H3K9me3 (Habibi et al., 2013). But repeats including not only LINE1 and MERVL but also IAP are transiently moderate derepressed followed with efficiently re-silencing. This is accompanied by broad and stable H3K9me3 over IAPEz and specific accumulation of H3K27me3 over LINE and MERVL (Walter et al., 2016).

Uhrf1 (also known as NP95) bind hemi-methylated DNA through its SET and RING finger associated (SRA) domain and recruit Dnmt1 to replicating heterochromatic regions. Embryos lacking Uhrf1 show global demethylation and transcriptional activation of endogenous retrotransposons (Sharif et al., 2007). Uhrf1 binds methylated histone H3 lysine 9 (H3K9) through its tandem Tudor (TTD) domain which is required for DNA methylation maintenance (Rothbart et al., 2012). Both Dnmt1 and Uhrf1 conditional knockout embryos and ESCs showed widespread DNA demethylation. However, acute loss of Dnmt1 but not Uhrf1 induced derepression of ERVs including CpG-rich IAPs. This paradoxical result involved the interaction between Uhrf1 and Setdb1. In the absence of Dnmt1, the binding of Uhrf1 to hemimethylated DNA disrupts Setdb1 dependent H3K9me3 deposition and IAP repression (Sharif et al., 2016).

During early development and gametogenesis, two de novo methyltransferases Dnmt3a and Dnmt3b are dominant for DNA methylation. Dnmt3a and Dnmt3b double-knockout (DKO) embryos die by E11.5 indicating that they are also crucial for mouse development, but show modest demethylation and a very mild effect on endogenous retrovirus silencing in the DKO embryos (Okano et al., 1999). However, Dnmt3L is essential for IAP repression in the male germ line and it facilitates the de novo DNA methylation of IAP elements by Dnmt3a and 3b (Bourc'his and Bestor, 2004; Kato et al., 2007).

Dnmt1 conditional knockout Six2+ nephrons progenitor cells show marked demethylation mostly on transposable elements associated with ERV upregulation (Li et al., 2019). Consistently, DNA methyltransferase inhibitors (DNMTi) treated MEF cells induce strong IAP derepression accompanied with mild decrease of DNA methylation (Rowe et al., 2013a). Similarly, DNMTi treatment of ovarian cancer cells show up-regulation of ERV transcripts associated with DNA demethylation (Chiappinelli et al., 2015).

These studies highlight the importance of H3K9me3 in cells that undergo intensive DNA methylation changes but also indicate a more important role of DNA methylation in ERV silencing in differentiated cells. However, it is still unclear how H3K9me3 changes upon decrease of DNA methylation in different cell types.

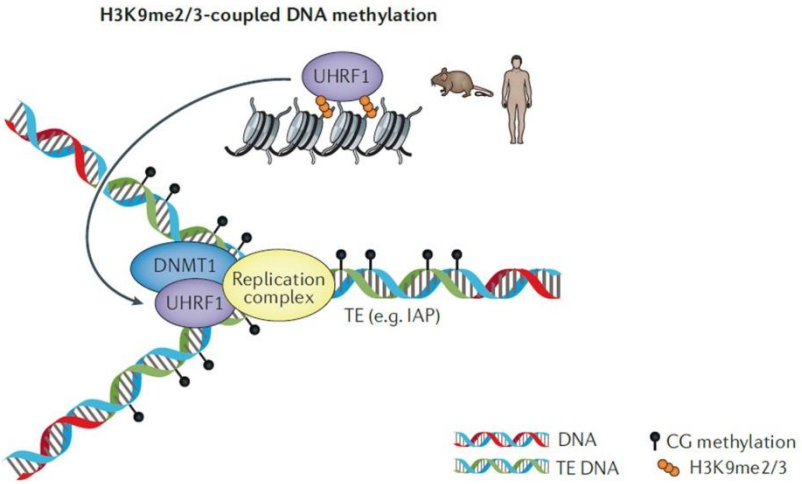

Figure 1.4 Transposon- silencing mechanisms by DNA methylation

Uhrf1 is a crucial cofactor of Dnmt1 and essential for maintenance of DNA methylation. UHRF1 binds H3K9me3 by its tandem Tudor domain and subsequently recruits DNMT1 to DNA replication foci. Transposons such as Intracisternal A particles (IAPs) are protected from passive demethylation and silenced by DNA methylation (Deniz et al., 2019).

1.4.2 H3K9me3 mediated ERV silencing

Trimethylation of histone H3 at the lysine position 9 (H3K9me3), a histone modification associated with compacted chromatin regions, contributes to gene regulation by forming large repressive domains on the chromosomes termed heterochromatin. H3K9me3 control a broad spectrum of transposons in a DNA methylation independent manner when DNA methylation changes intensively. H3K9me3 also suppress the expression of lineage-specific transcription factors through preventing the binding of diverse transcription factors. H3K9me3

domains can be dynamic in mammalian development and constitute a major barrier of cell fate changes (Becker et al., 2016).

H3K9me3 is regulated by a family of H3K9me3 methyltransferases: Suv39h1, Suv39h2 and Setdb1. Suv39h enzymes are responsible for catalyzing H3K9me3 at pericentric heterochromatin. In contrast, Setdb1 (Eset) is the responsible enzyme for catalyzing H3K9 methylation at endogenous retroviruses of euchromatin (Figure 1.5). Interestingly, *in vitro* analysis showed that G9a exhibit H3K9m3 activity, but only H3K9me1 and H3K9me2 levels are reduced when G9a is deleted (Collins et al., 2005; Kubicek et al., 2007). G9a null embryos die at E8.5 (Tachibana et al., 2002). Accompanied with decreased levels of H3K9me2, de novo methylation and proper silencing of newly integrated proviruses are impaired in G9a deficient mESCs, which indicates that G9a is required for establishing the silencing of newly integrated proviruses. Setdb1 is also required for silencing newly integrated proviruses (Leung et al., 2011).

Suv39-h null embryos show impaired viability (~33 %), high chromosomal instability and an increased incidence of lymphoma (Peters et al., 2001). The homozygous mutations of Setdb1 results in peri-implantation lethality between E3.5 and E5.5, however, no global change of H3K9me3 and DNA methylation at IAP ERV is observed in knockout blastocyst outgrowths (Dodge et al., 2004).

Recent studies show that Suv39h-dependent H3K9me3 marks the majority of the ~8150 intact LINEs and ERVs but the minority of more than 1.8million truncated LINEs/ERVs (Bulut-Karslioglu et al., 2014). Setdb1 can collaborate with Suv39h in a multimeric complex (Fritsch et al., 2010) and more detailed analysis indicates that Setdb1 is the primary methyltransferase to initiate H3K9me3 at ERV elements and to silence their transcription (Bulut-Karslioglu et al., 2014; Karimi et al., 2011).

H3K9me3 is primarily responsible for silencing ERVs when cells undergo an intensive change in DNA methylation such as PGC and ES cells. mESCs lacking Setdb1 or KAP1 but not DNMT TKO lines show genome wide reactivation of the same families of ERVs (Karimi et al., 2011; Matsui et al., 2010; Rowe et al., 2010). Deletion of Setdb1 in ES cells leads to significant ERV derepression including ERV1 (MLV) and ERVK (IAP and MusD), whereas the non-LTR retrotransposon LINE-1 and the ERVL are only weakly derepressed. Setdb1 mediated H3K9me3 is decreased at these regions but the DNA methylation is either unchanged at 5' LTR region of IAP and LINE or moderately decreased at 5' LTR region of MusD and MLV class. However, using the exogenous retrovirus expression system, these elements are derepressed upon Setdb1 depletion and associated with reduced levels of proviral H3K9me3 and DNA methylation (Matsui et al., 2010). Setdb1 knockout primordial

germ cells display derepression of many ERVs including MLV from ERV1 and IAP/ MusD from ERVK in the context of a decreased level of H3K9me3 as well as aberrant DNA methylation pattern at marked ERVs and LINE element. Notably, the ERVs highly enriched for H3K9me3 show a decrease of DNA methylation. And the proximal internal region of the consensus IAPEz shows a near-complete loss of methylation across a short stretch of CpGs just 3' of the 5' LTR (Liu et al., 2014).

In fetal forebrains of Setdb1 conditional knockout mice, IAPs are highly derepressed with decrease of H3K9me3. And the overall DNA methylation of global IAP LTR does not change whereas significant DNA demethylation is observed in IAP-LTR which adjacent to specific genes (Tan et al., 2012). But when I re-analyzed the published RNA-seq data from Setdb1 conditional knockout neurons, IAPs are relatively mild changed compared to Setdb1 knockout ESC (Jiang et al., 2017).

Strong derepression of murine leukemia virus (MLV) copies associated with partial loss of H3K9me3 and unchanged DNA methylation is observed in Setdb1 deficient B cells (Collins et al., 2015; Pasquarella et al., 2016). Similarly, upon Setdb1 deletion in MEF cells, a few distinct families such as VL30-class of ERVs including MLV are significantly induced, but IAP, MusD and LINE-1 elements are not derepressed. Moreover, VL30 activation requires the cell-type-specific transcription factor Elk-1 and Ets1 (Kato et al., 2018; Matsui et al., 2010).

Loss of Setdb1 in hematopoietic stem cells (HSPCs) results in a significant but milder reduction of H3K9me3 at repetitive regions such as ERVK including IAP, ERV1 and LINEs compared to the changes in mESCs. The DNA methylation at these repetitive regions remains unchanged. Correspondingly, the expression of IAP and ERV1 remains unchanged but LINEs show slight up-regulation which is similar as in Setdb1 knockout ESCs (Koide et al., 2016). The low level expressed IAP and MusD elements are mildly derepressed in Setdb1 knockout thymocyte (Takikita et al., 2016).

Considering all that, a broad set of ERVs, including IAPs, are regulated by Setdb1 when cells undergo intensive DNA methylation changes. They remain silent when Setdb1 is deleted in differentiated cells. However, a few distinctive sets of ERVs including the VL30-class of ERVs required Setdb1 for proper silencing in differentiated cells.

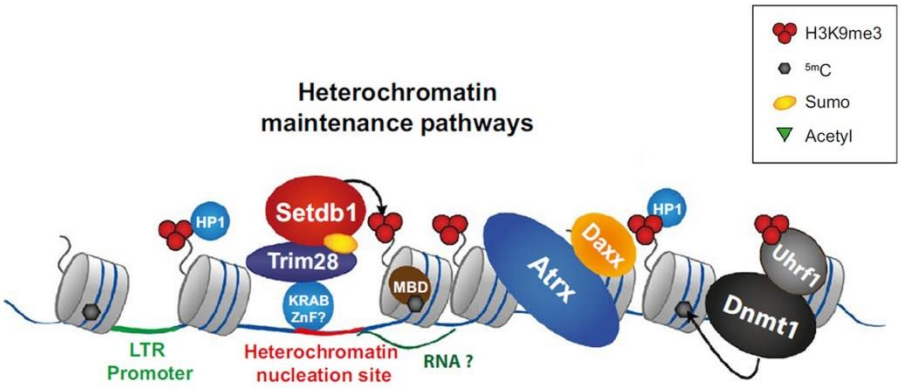

Figure 1.5 Transposon- silencing mechanisms by KRAB ZnF-Trim28-Setdb1 pathway

KRAB Znf proteins specifically bind to ERVs via its C2H2 type zinc finger array and subsequently recruits Trim28/Setdb1 complex. Setdb1 catalyses H3K9me3 methylation for the binding of chromatin regulator such as HP1, thus facilitates establishment and maintenance of chromatin.

1.4.3 Crosstalk between Setdb1 mediated H3K9me3 and Dnmt1 mediated DNA methylation in ERV regulation

Endogenous IAP retrotransposons are marked with H3K9me3 (Mikkelsen et al., 2007). Since trimethylation of H3K9 is shown to direct DNA methylation in Neurospora crassa (Tamaru and Selker, 2001; Tamaru et al., 2003). Suv39 double knockout cells show partial loss of DNA methylation at MaeII sites of pericentromeric heterochromatin but not on ERVs (Lehnertz et al., 2003). Further, DNA methylation of retrotransposons and densely methylated CpG-rich promoters is proved to depend on G9a in ES cells (Dong et al., 2008). Accordingly, a number of studies have focused on the DNA methylation level of retrotransposon upon Setdb1 deletion.

As mentioned above, DNA methylation at 5' LTR of ERV remains unchanged in several Setdb1 knockout studies (Dodge et al., 2004; Matsui et al., 2010). However, introduced ERV sequences require Trim28 and Setdb1 to induce de novo DNA methylation. Loss of Trim28 in embryos also shows a decreased level of DNA methylation (Rowe et al., 2013a). The proximal internal region of the endogenous consensus IAPEz showed a near-complete loss of methylation across a short stretch of CpGs just 3' of the 5' LTR in Setdb1 knockout primordial germ cells but a modest increase of DNA methylation is observed in 5'UTR and

ORF1 regions of L1Md_T. However, DNA methylation levels in knockout PGCs are 2.5 fold higher than heterozygous at global level (Liu et al., 2014). It is unclear to which extent DNA methylation of endogenous ERV sequences is affected by Setdb1 loss.

A few studies have reported the crosstalk between H3K9me3 and DNA methylation. For instance, Suv39h1 interacts with Dnmt3a and Dnmt1 through the recruitment of HP1beta to reinforce H3K9me3 (Fuks et al., 2003). In Dnmt3a/3b DKO mESCs, thousands of regions keep a higher DNA methylation level than the average and are therefore termed enriched residual methylation loci (ERML). A large proportion of ERML (41 %) overlapped with H3K9me3-marked regions and is also enriched for ERV1 and ERVK. As ERV1 and ERK are highly derepressed in Setdb1 knockout mESCs, these ERV1 and ERVK which overlap with ERML defined in Dnmt3a/3b DKOs show significant demethylation with gain of 5hmc in Setdb1 knockout mESCs. This gain of 5hmc is consistent with a significant increase of Tet1 binding. However, ERVL and non-LTR elements which are not marked by H3K9me3 show an even DNA hypermethylation. In summary, this indicates an antagonistic relationship between Setdb1 mediated H3K9me3 and 5mC removal through Tet enzymes (Leung et al., 2014).

Mutant Uhrf1 alleles deficient in binding either hemi-methylated CpG or H3K9me2/3, used to rescue Uhrf1 null mESCs, are still able to associate with pericentric heterochromatin to recruit Dnmt1. But coordinately binding of both hemi-methylated CpG and H3K9me2/3 leads to a efficient recruitment of Dnmt1. It reflects the fact that Uhrf1 recruits Dnmt1 to replicating DNA, to maintained DNA methylation, through binding either hemi-methylated CpG or H3K9me2/me3. It indicates that Uhrf1 mediated the crosstalk between H3K9 methylation and DNA methylation and revealed that H3K9me3 might facilitate Dnmt1-dependent DNA methylation (Liu et al., 2013). Uhrf1 knockin (KI) mice which specifically lost the H3K9me2/3 binding activity show moderate (~10 %) reduction of DNA methylation. Demethylation does not restrict the H3K9me2/3 enriched repetitive elements but occurred globally. In an *in vitro* system, Uhrf1 preferentially binds nucleosomes with hemi-mCpGs than with H3K9me3, but both H3K9me3 and hemi-mCpGs enhance the binding of Uhrf1 to nucleosomes. Thus, this study supports that H3K9me3 promotes the DNA methylation through Uhrf1 but DNA maintenance by Dnmt1 is largely independent of H3K9me3 (Zhao et al., 2016).

In contrast, the question how DNA methylation could be affected by the level of H3K9m3 in different cell types of Dnmt knockout cells remains unclear. Using chemical hypomethylating culture conditions for mESCs to mimic a rapid and extensive demethylation, broad domains of H3K9me3 remain stable at IAPEz but accumulation of H3K27me3 at LINE1, MMERGLN and MERVL are observed (Walter et al., 2016). H3K9 methylation only found to be dependent on DNA methylation in human cancer cells. Colorectal cancer cells lacking Dnmt1

and Dnmt3b show removal of histone H3K9 methylation by the loss of DNA methylation (Bachman et al., 2003). Additionally, HCT-116 colon cancer cells lacking Dnmt1 show alterations of nuclear architecture and decrease of H3K9me2/me3 (Espada et al., 2004).

In summary, H3K9me3 has a broad role in DNA methylation maintenance. However, it is unclear how DNA methylation in mammals is affected by H3K9me3.

1.5 Setdb1 and Dnmt1 in cancer cells

Chromatin remodeling and transcription regulation are tightly controlled under physiological conditions. Abnormal epigenetic control is a common early event in tumor progression. Treatment with inhibitors prompt tumor cells to undergo apoptosis, cell-cycle arrest, cell differentiation, anti-angiogenesis and autophage. DNA demethylation reagents lead to induction of dsRNAs derived from ERVs and cause an interferon response in ovarian cancer (OC) and colorectal cancer-initiating cells (CICs). Overexpression of ERVs and transfection with dsRNAs shows similar effects as DNMT inhibitor treatment. This highly expressed interferon-response genes associated with anti-viral response induce immunogenic cell death and appear as an emerging opportunity to immune checkpoint therapy in cancer (Chiappinelli et al., 2015; Roulois et al., 2015). Treatment of human lung cancer cell lines with both DNMT and HDAC inhibitors leads to the emergence of cryptic transcription of thousands of treatment-induced non-annotated TSSs (TINATs) in long terminal repeats. TINATs may splice into protein-coding exons to encode chimeric transcripts that are then translated into aberrant protein isoforms. Most of these TINATs arose from solitary repeats of LTR12 family which are usually epigenetically repressed in healthy/untreated cells (Brocks et al., 2017).

Loss of Setdb1 in acute myeloid leukemia (AML) human cells also results in derepression of ERVs and LINEs coincident with induction of double-stranded RNAs (dsRNAs). It triggers the viral sensing machinery and interferon-mediated cell death (Cuellar et al., 2017).

In summary, ERV silencing seems essential for cancer survival and ERV derepression through DNMT and Setdb1 inhibition is associated with interferon response to open new therapeutic avenues for cancer treatment.

1.6. Aim of the thesis

In summary, H3K9me3 mediated by Setdb1 is required for silencing a broad set of ERVs in ES cells with minor effects on DNA methylation maintenance. But it is necessary for the tight control of a few distinct sets of VL-30 class ERVs expression in differentiated cells without perturbing DNA methylation. However, a few studies support the role of H3K9me3 in DNA methylation maintenance through Uhrf1. Moreover, loss of Setdb1 affects the DNA methylation of a short stretch of CpGs at IAPEz. Therefore, the role of Setdb1 mediated H3K9me3 in ERV regulation during early embryonic development and in which context H3K9me3 affects DNA methylation are not yet clear.

On the other hand, DNA methylation is dispensable for ERV silencing in ES cells but essential for ERV silencing in differentiated cells. In addition, H3K9me3 is stable when converting mESCs from high level of DNA methylation to low level of DNA methylation. But few exceptions showed a decrease of H3K9me3 in human cancer cells lacking DNMT enzymes. However, the involvement of DNA methylation in H3K9me3 changes in most of these cases is not yet known.

Based on these findings, the main goal of this work was to characterize the role of Setdb1 in ERV regulation during early embryonic development. Moreover, an understanding of the crosstalk between H3K9me3 and DNA methylation in ERV regulation is required to elucidate the contexts in which they occur and the mechanisms by which they act.

Therefore, we wanted to establish an efficient *in vitro* endoderm differentiation system for both visceral endoderm cells and definitive endoderm cells.

Secondly, after having an *in vitro* differentiation system, the aim was to use a Setdb1 conditional knockout ES cells to study which ERVs are regulated by Setdb1 during endoderm differentiation.

I also wanted to check the H3K9me3 changes and the correlation between H3K9me3 changes and ERVs expression changes upon Setdb1 deletion in endoderm cells. Additionally, it is also interesting to identify the DNA methylation level at selected ERVs in this system.

Finally, I could characterize the IAP regulation upon Dnmt1 depletion during endoderm differentiation and the crosstalk between DNA methylation and H3K9me3.

2. Results

2.1 *In vivo* ERV expression analysis

Since the Setdb1 knockout embryo dies before three germ layer formation (Dodge et al., 2004), the Setdb1 conditional knockout mouse line and ES cell line was previously generated in our lab by Dr. Rui Fan in order to better understand the role of Setdb1 in ERV regulation upon endoderm differentiation (Fan, Ph.D. Thesis, 2015). Setdb1^{END} embryos did not display notable differences in development until embryonic day E8.0, but showed turning defect by E8.5. The expression of Foxa2 and Sox17 was unchanged in E7.5 embryos suggesting a proper formation of endoderm cells (data not shown).

By analyzing the transcriptome profile generated by Dr. Rui Fan, I found 170 differentially expressed genes by comparing control versus Setdb1 knockout endoderm cells. Most of the genes (166 out of 170) were up-regulated suggesting a repressive role of Setdb1. The top up-regulated genes were testis genes, which were known to be Setdb1 targets and also were observed in other Setdb1 knockout cell lines. Additionally, up-regulated genes were highly overlapping with the dysregulated genes observed in Setdb1 knockout ES cells (Figure 2.1A) (Karimi et al., 2011). To investigate the role of Setdb1 in ERV silencing, I analyzed the expression of ERV families. Notably, MMERVK10C-int and IAPEz-int, the most derepressed ERVs in Setdb1 knockout ES cells, were also highly up-regulated in the Setdb1 knockout endoderm cells (Figure 2.1B). Embryonic endoderm is considered to be mainly derived from definitive endoderm. However, the visceral endoderm was shown to contribute to the embryonic endoderm, which means the embryonic endoderm is of dual origin (Kwon et al., 2008). We wondered if the ERVs were specifically induced in one of these two types of endoderm. We also used anti-IAP-GAG antibody, which specifically recognizes IAPEz, from Bryan Cullen's lab as a representative to detect the ERV derepression. To distinguish visceral endoderm from definitive endoderm, AFP was used as a marker to label visceral endoderm cells based on recent observation (Kwon et al., 2008). Surprisingly, IAP-GAG was expressed only in visceral endoderm cells (Figure 2.1C) (modified from Fan, Ph.D. Thesis, 2015). Since there is no cell-type-specific reporter and surface antibody available for separating these two types of endoderm, it is difficult to study the transcriptome changes and H3K9me3 changes within these types of endoderm cells.

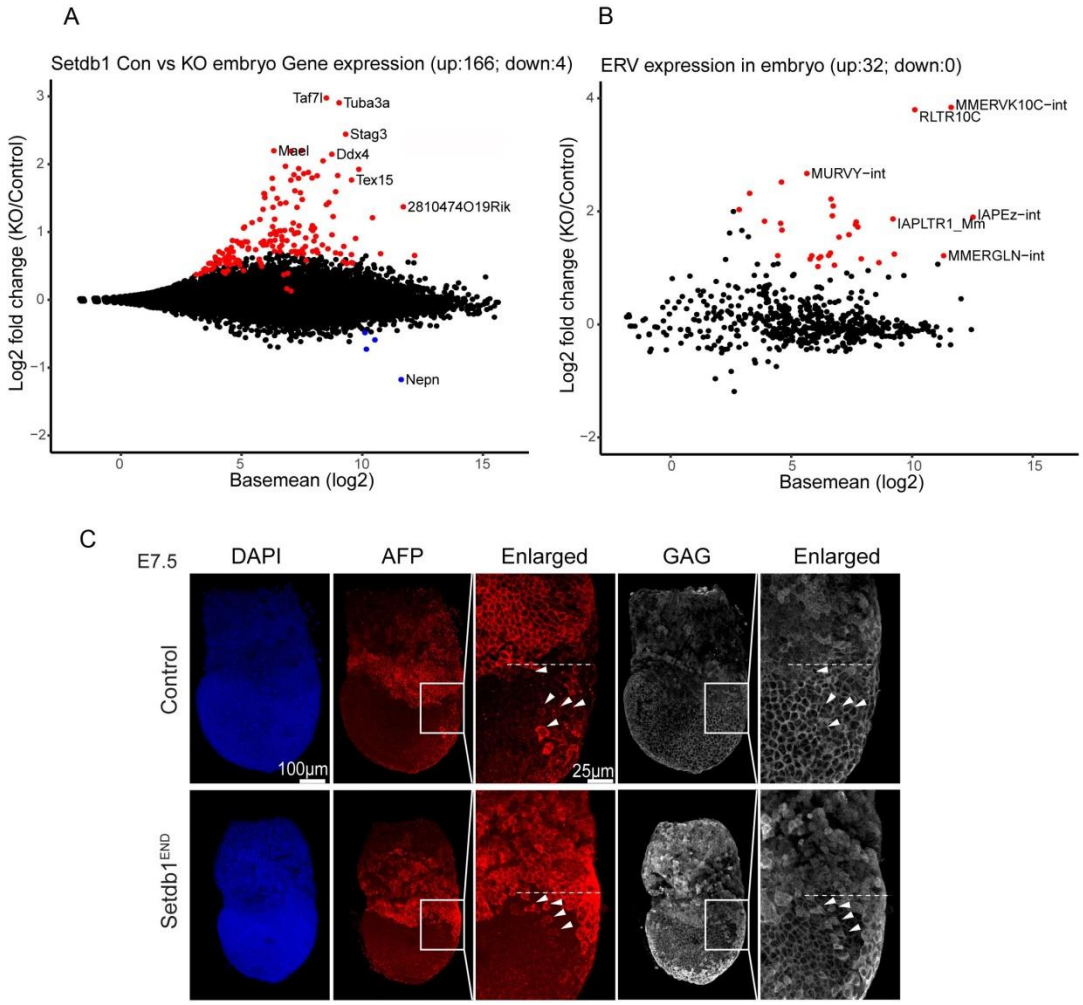

Figure 2.1 Derepression of ERVs in Setdb1 knockout visceral endoderm cells

A. Dot plot showing basemean expression vs. log2-fold change of protein coding genes in embryonic endoderm knockout vs. control cells. Genes with significantly changed expression (adjusted p-value < 0.01; n=3 for each condition) are coloured (red = increased expression in mutant cells, blue = increased expression in control cells). Positions of relevant genes are indicated.

B. Dot plot showing basemean expression vs. log2-fold change of ERVs in embryonic endoderm knockout vs. control cells. Genes with significantly changed expression (adjusted p-value < 0.01, fold change > 2; n=3 for each condition) are coloured (red = increased expression in mutant cells, blue = increased expression in control cells). Positions of relevant ERVs are indicated.

C. Lateral view of E7.5 embryos stained with AFP (red) and IAP-GAG (grey). Up-regulation of AFP and GAG can be observed in mutant embryos. The boxed regions are magnified showing an overlap between AFP and GAG in mutant embryos but not in control embryos. White arrows point the AFP positive cells in embryonic region. White dash lines separate the extraembryonic region and embryonic region.

2.2 Establishment of *in vitro* endoderm differentiation

2.2.1 *In vitro* XEN and DE differentiation

To characterize the role of Setdb1 in ERV silencing and H3K9me3 changes in two different types of endoderm cells (visceral endoderm and definitive endoderm cells) and to overcome the difficulties of separating two types of cells, I established an *in vitro* differentiation system in which I could easily separate progenitors of visceral endoderm cells and definitive endoderm cells. Due to the limited differentiation efficiency, I employed the Setdb1 conditional knockout (CKO) ES cell line containing a GFP reporter. In this cell line, a conditional Setdb1^{flox} allele, where the exon 4 is flanked by loxP sites, was combined with the Sox17-2A-iCre knock-in allele, which expresses Cre recombinase in Sox17 expressing endoderm cells (Engert et al., 2009). The critical exon 4 can be cut out by the introduction of Cre recombinase, when Sox17 is activated (Figure 2.2A). This Setdb1 conditional knockout cell line enables us to do acute deletion of Setdb1 when ES cells differentiate to Sox17-expressing endoderm cells. In order to isolate pure differentiated endoderm cells, an EGFP Cre-reporter was introduced and the EGFP signal is activated by the Cre-mediated excision of a translation stop signal between the CAG promoter and EGFP (Figure 2.2B) (Kawamoto et al., 2000).

By adding Wnt3a and Activin to the endoderm differentiation medium (EDM), the ES cells will progressively restrict their developmental potential by going through an intermediate state, mesendoderm, before becoming definitive endoderm (DE) cells. However, by the overexpression of gata6 using lentivirus transduction, ES cells will progressively differentiate to Extra-embryonic endoderm stem (XEN) cells, it recapitulates the main features of that *in vivo* primitive endoderm cells which is a progenitor of visceral endoderm cells (Figure 2.2C). In contrast to the lethal Setdb1 knockout in ESCs, neither Setdb1-deficient definitive endoderm cells nor extra-embryonic endoderm stem displayed obvious viability or proliferation problems.

I found obvious morphology changes after 4 days of differentiation in both two types of endoderm cells. XEN cells showed a more dispersed and stellate morphology in following days. However, DE cells became flatter without morphology changes. There were no phenotypic changes between mutant and control cells (Figure 2.2D). In contrast to the lethality of Setdb1 knockout ES cells, deletion of Setdb1 in endoderm cells did not show a significant effect in survival rate, which is consistent with the *in vivo* data.

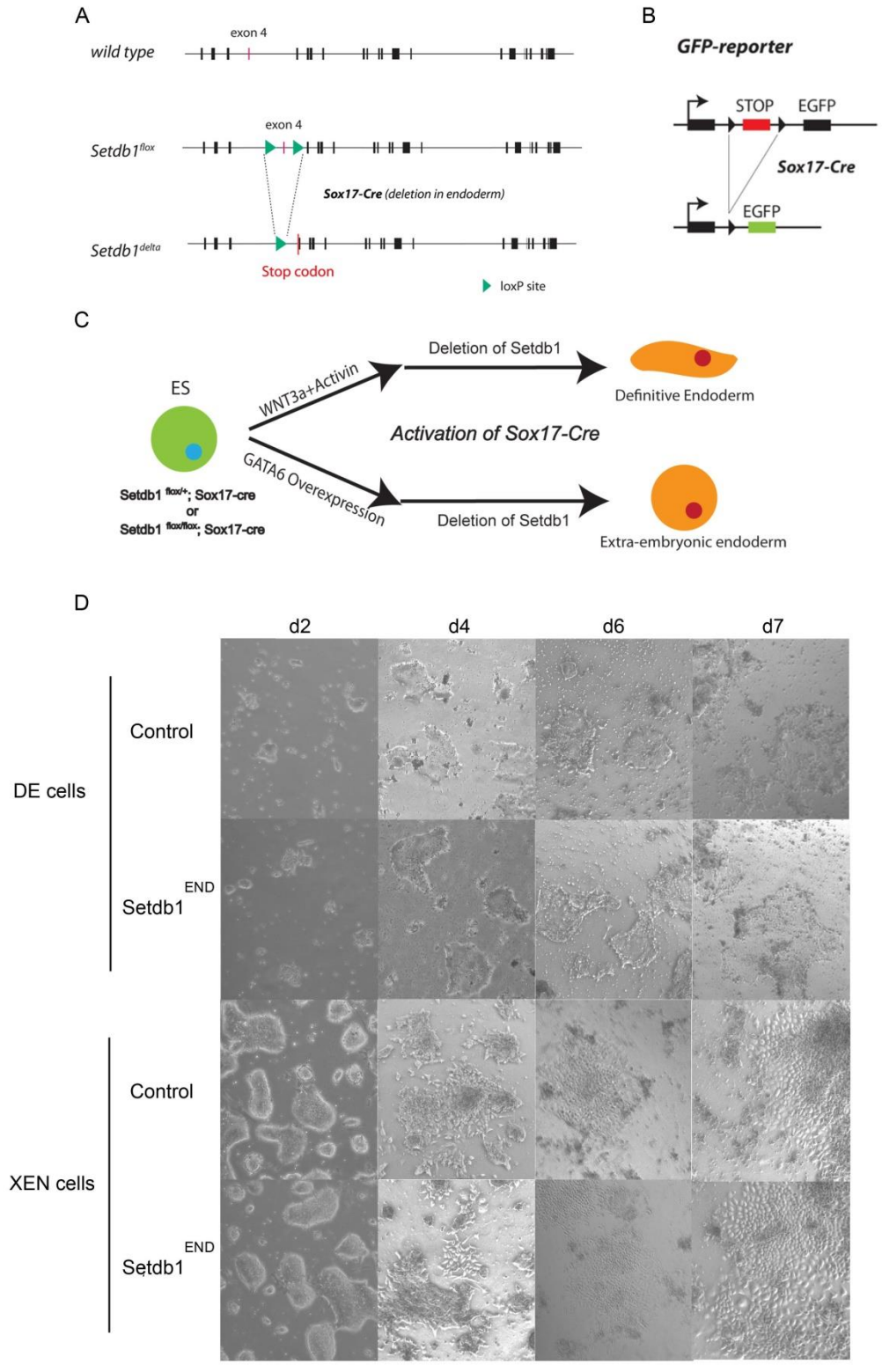

Figure 2.2 Establishment of *in vitro* endoderm cell differentiation with conditional Setdb1 knockout line

A. Schematic show the Setdb1 mutant allele which the 4th exon is flanked by loxp site and deleted when Sox17 is activated.

B. Schematic show the strategy of using CAG-CAT-EGFP reporter to monitor Sox17 activation.

C. Schematic show the strategy of *in vitro* endoderm differentiation that are performed using chemical induction for definitive endoderm differentiation and lentiviral induction for extra-embryonic endoderm differentiation

D. Morphology changes during 7 days differentiation. Both XEN and DE cells are already well differentiated on day5.

2.2.2 Consistent IAP expression *in vitro* by immunostaining

While establishing *in vitro* differentiation system, we wanted to know if the *in vitro* differentiation system could mimic *in vivo* ERV derepression. Immunostaining was performed for GFP which represent the activation of Sox17 and full deletion of Setdb1 in differentiated endoderm cells and for IAP-gag to verify whether the *in vitro* differentiation system could reflect the *in vivo* situation with a dramatic derepression of IAP-gag in visceral endoderm cells. Immunofluorescence staining showed activation of GFP in both DE and XEN cells suggesting a proper Sox17 activation. Moreover, in consistence with the *in vivo* staining data (Figure 2.1C), the IAP-gag was exclusively depressed in XEN mutant cells but not in DE mutant cells (Figure 2.3A, B).

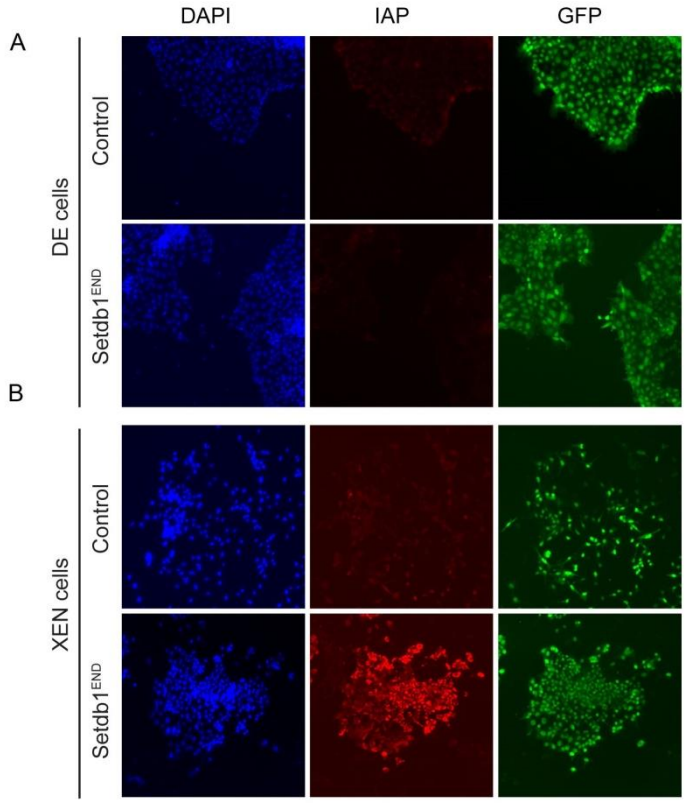

Figure 2.3 *In vitro* differentiation reflect the derepression of IAP-gag only in visceral endoderm cells *in vivo*

A-B. Fluorescent image of 7 days differentiated definitive and extra-embryonic endoderm in control versus mutant cells and immunostained for DAPI (blue), IAP-Gag (red) and GFP (green).

2.3 Characterization of *in vitro* differentiated cells

2.3.1 Fluorescence activated cell sorting indicates differentiation efficiency

To understand the underlying mechanisms contributing to the derepression of IAP-gag in XEN mutant cells but not in DE mutant cells, fluorescence activated cell sorting was used to get pure differentiated cells for subsequent analysis. The expression of Sox17 could be detected as early as three to four days post differentiation. And the differentiation efficiency is already good after five days differentiation in both DE and XEN cells. I utilized 7 days differentiation in order to get a better deletion of Setdb1. But due to the different ways of differentiation, the lentivirus transduction followed with a puromycin selection results in a more homogeneous population with better differentiation efficiency over 50 % up to 80 %. However, the chemical induction was less effective and a low percentage of cell response results in a relative lower differentiation efficiency 30 % to 40 %. Due to the different expression of GFP in control and mutant cell line, I found a consistently lower differentiation efficiency and lower intensity of GFP expression in both XEN and DE control cells (Figure 2.4A, B).

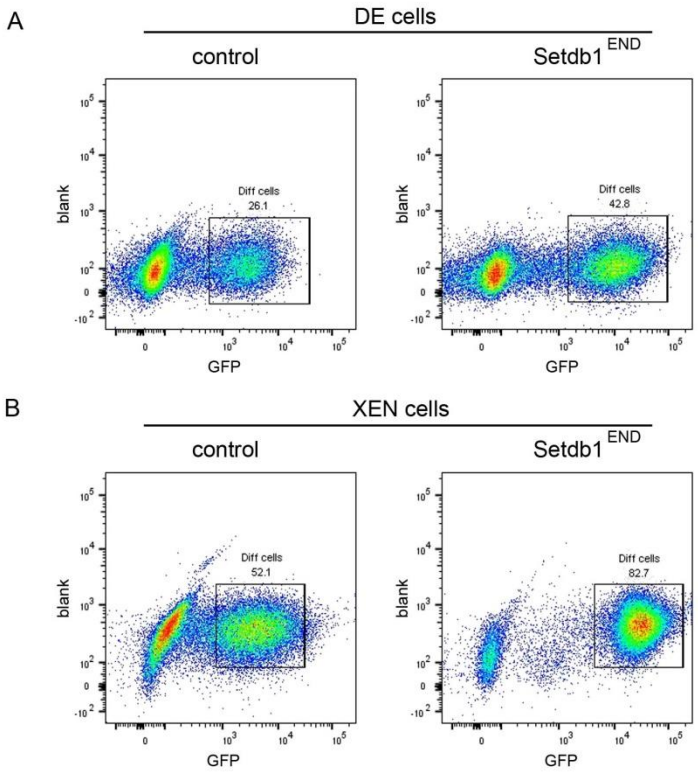

Figure 2.4 *In vitro* differentiation efficiency based on the expression of GFP

A-B. Representative FACS plots of 7 days *in vitro* differentiated visceral and definitive endoderm cells. Trypsinized disassociated differentiated cells were resuspended in PBS containing 0.2 % FBS for sorting. Differentiated cells were sorted based on expression of GFP. 50K cells were recorded in each plot.

2.3.2 Confirmation of Setdb1 deletion and endoderm marker gene expression

Using sorted GFP positive cells, I isolated RNA to check the expression level of Sox17 and Setdb1 deletion by doing a reverse transcription quantitative PCR (RT-qPCR). The expression of Sox17 was not changed in both control and mutant cell lines, which is consistent with the *in vivo* expression of Sox17 by RNA-seq analysis (Figure 2.5A). Primers of IAP were designed based on the consensus sequence of IAPEz family which is at the upstream of IAP-gag region, and the up-regulation of IAP with ~100 times fold change in XEN mutant cells is in consistent with previous findings (Figure 2.5B). Primers of Setdb1 were designed to amplify the 4^{th} exon. The expression of Setdb1 by RT-PCR showed a complete deletion in XEN mutant cells, whereas ~10 % transcript was left in DE mutant cells. As Setdb1 is present in the nucleus, it could be beneficial to use a cellular fractionation protocol to separate the nucleus and cytoplasm. Since I had a limited number of cells, I prepared the whole cell lysate with half million cells for each sample and performed western blot for Setdb1 using tubulin as a loading control. Since I used heterozygous for Setdb1 conditional knockout allele as control for both XEN and DE cells, Setdb1 protein decreased in both XEN and DE control cells compared to undifferentiated ES cells. I observed ~15 % of the Setdb1 protein left in DE mutant cells compared with DE control cells, whereas the protein was not visible in XEN mutant cells (Figure 2.5C). This difference was observed probably due to different ways of differentiation. Upon the XEN differentiation, the cells transduced with lentivirus containing Gata6 could differentiate synchronously and following 2 days puromycin selection could remove the undifferentiated cells and keep a more homogenous population. However, the chemical induction upon DE differentiation could not synchronously differentiate the cells. As soon as the late differentiated cells express Sox17, even Setdb1 transcript and protein was not fully degraded. The GFP positive cells were collected for subsequent analysis. But I could not synchronize the differentiation or separate the late differentiated cells.

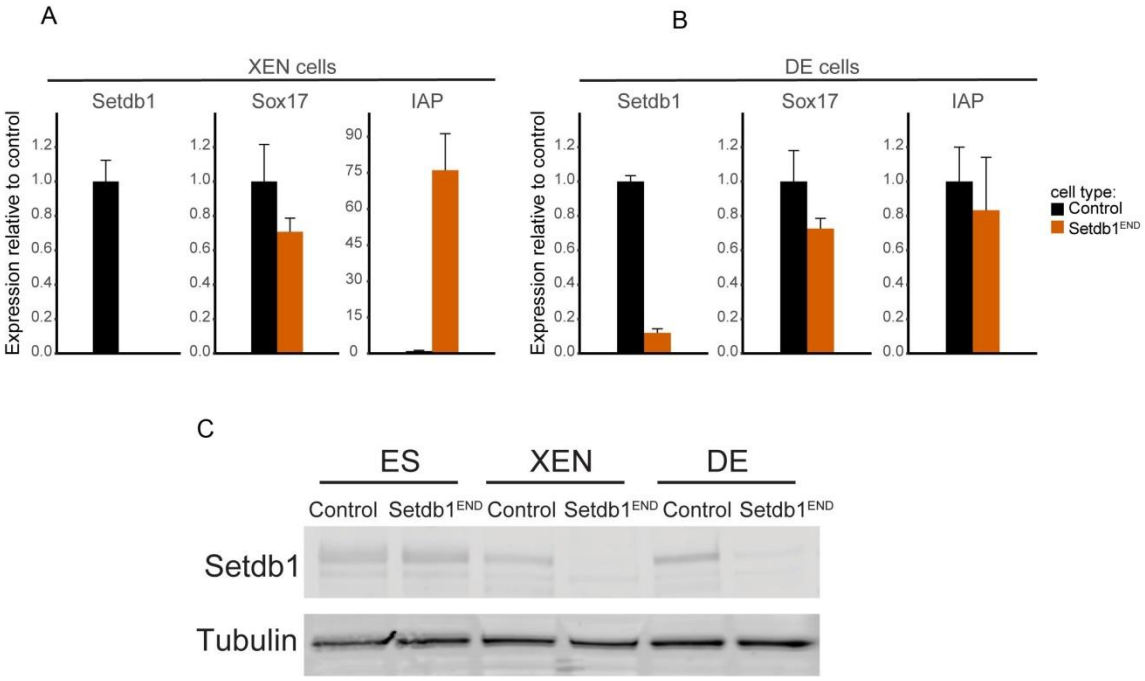

Figure 2.5 Confirmed Setdb1 deletion and no expression change in Sox17.

A-B. Expression levels of Setdb1, Sox17 and IAP by RT-qPCR in Setdb1 knockout endoderm lines compare to control samples. For each replicate, expression was normalized by that of Gapdh and Hprt.

C. Protein expression analysis by western blots confirms the Setdb1 deletion. The membranes were probed with antibody against Setdb1 and tubulin was used as loading control.

2.4 ERV de-repression in Setdb1-deficient visceral endoderm progenitors *in vitro*

2.4.1 PCA analysis and endoderm marker gene expression

To unravel the genome-wide transcription changes, I isolated mRNA from undifferentiated ES and two types of differentiated endoderm cells in both control and mutant cells, and performed RNA-seq using the SMART-Seq Ultra Low Input RNA Kit. Principal component analysis (PCA) showed that each cell type was highly correlated and clustered together, and there were minor differences in control versus mutant for each cell type. However, DE cells and ES cells were more different from each other than XEN cells and ES cells (Figure 2.6A). Transcriptome analysis of these populations by looking at the endoderm marker gene expression revealed a stage specific expression signature. I observed a strong induction of common endoderm maker genes Foxa2 and Sox17 in both two types of endoderm cells and an endoderm cell-type-specific Sox7 and Gsc expression in XEN cells and DE cells, respectively. However, no difference was observed in the endoderm marker gene expression in control versus mutant cells. Notably, I observed a similar expression level of Dppa family, especially Dppa5a in XEN cells compared with ES cells. Also, pluripotency genes like Oct4

and Rex1 were highly expressed only in XEN cells (Figure 2.6B). In summary, established *in vitro* differentiated cells mimic the key features of *in vivo* system and loss of Setdb1 do not impair the expression of stage specific marker gene expression. At the same time, DE cells were more distinct from ES cells, as compared to XEN cells.

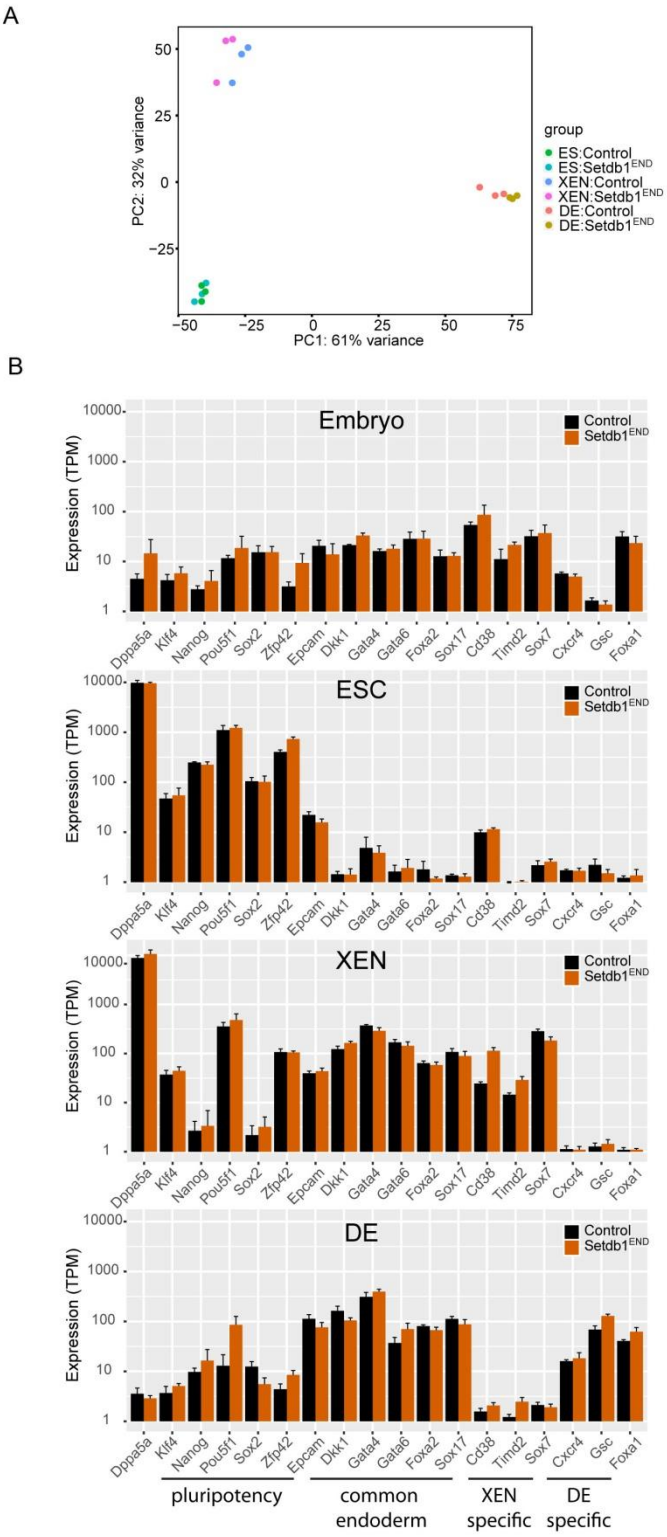

Figure 2.6 PCA analysis and endoderm marker gene expression

A.PCA analysis of ESC and differentiated XEN and DE cells. Each dot represents the dataset originating from one sample. It showed DE cells were more distinct from ES cells, as compared to XEN cells.

B. Average expression levels of selected markers genes detected by RNA-seq for pluripotency, extra-embryonic endoderm and definitive endoderm marker genes in both *in vivo* endoderm cells and *in vitro* differentiated endoderm cells. TPM: Transcripts Per Kilobase Million. Error bars depict standard deviation (n=3).

2.4.2 Transcriptional effect of Setdb1 on gene regulation in differentiated endoderm cells

To characterize the expression patterns of two types of endoderm cells in control and mutant by RNA-seq analysis, I plotted basemean expression versus log2-fold change of all coding genes. 1097 and 1691 genes were found to be significantly dysregulated in XEN and DE knockout cells in comparison to XEN and DE control cells, respectively. The majority (748 out of 1097 genes) was derepressed in XEN knockout cells which showed a similar trend as in the embryonic endoderm knockout cells. I also observed many *in vivo* derepressed genes up-regulated in XEN knockout cells (Figure 2.1A, Figure 2.7A). For example, testis related genes, Gabrr1 and Gm1110 were not only up-regulated in our study but also up-regulated in Setdb1 knockout primordial germ cells and Setdb1 knockout ES cells (Karimi et al., 2011; Liu et al., 2014). Furthermore, the majority of the genes either up-regulated in definitive endoderm knockout cells or XEN knockout cells were also found derepressed in Setdb1 knockout ES cells. Gm1110 and Cd22, chimeric transcripts initiating in LTR elements validated in Setdb1 knockout ES cells, were also highly up-regulated in XEN knockout cells. It indicated a critical role of Setdb1 in inhibiting aberrant gene transcription by suppressing the expression of proximal ERVs in XEN cells (Karimi et al., 2011). Despite less derepression of testis gene in DE knockout cells, Cd22 were also up-regulated in DE knockout cells together with derepression of Setdb1 canonical target gene H19. Ifi27l2a, an Interferon-Induced gene, was also highly derepressed (Figure 2.7B). The up regulated gene sets in XEN knockout cells were enriched for biological process gene ontology (GO) terms related to DNA methylation and meiotic cell cycle (Figure 2.7C). Whereas, up regulated gene sets in DE knockout cells were enriched for biological process gene ontology (GO) terms related to differentiation and cardiac development (Figure 2.7D). Hence, these results indicate the DNA methylation might be affected by the H3K9me3 establishment in XEN cells but not DE cells.

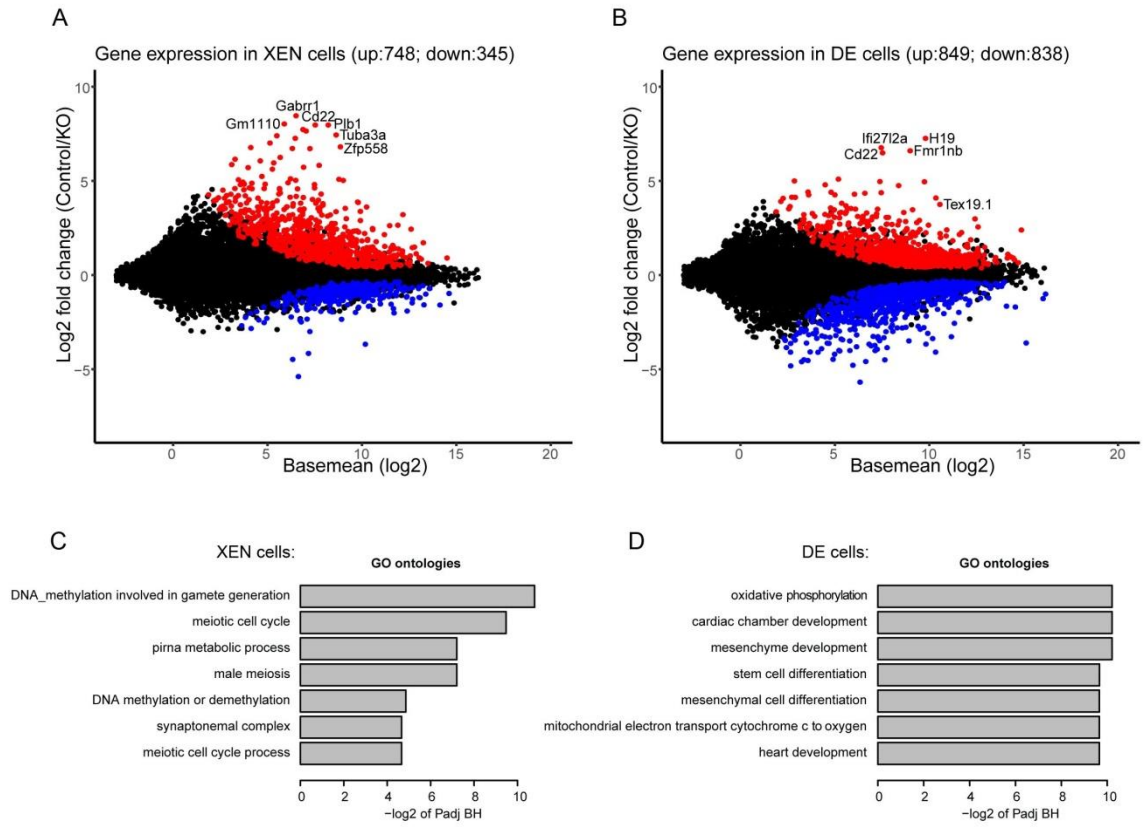

Figure 2.7 Differential gene expression in Setdb1 knockout endoderm cells

A,B. Dot plot showing basemean expression vs. log2-fold change of protein coding genes in differentiated endoderm knockout vs. control cells after 7 days differentiation. Genes with significantly changed expression (adjusted p-value < 0.01; n=3 for each condition) are coloured (red = increased expression in mutant cells, blue = increased expression in control cells).

C,D. GO term enrichment analysis for biological processes of up-regulated genes in either XEN or DE knockout cells. Shown is the probability based on the log2 of adjusted p-value by Benjamini-Hochberg (BH) adjustment.

2.4.3 Transcriptional effect of Setdb1 on repeat regulation in differentiated endoderm cells

Although H3K9me3 enrichment in ERV families have been studied in many cell types (Kato et al., 2018), the cell type specific ERV regulation is not well defined in early differentiation. After the gene expression characterization of these two types of endoderm cells, I focused on the differential expression of repeat classes to understand which families of ERVs are regulated by Setdb1 upon endoderm differentiation. By making use of Homer, all annotated repeat definitions from UCSC were loaded to access the expression levels of different repeat classes. I found a burst of ERVK and ERV1 expression but a mild change of ERVL and LINE-1 expression in XEN cells (Figure 2.8A, C). Interestingly, IAPEz and MMERVK10C, the most derepressed ERVs in Setdb1 knockout ES cells were also most derepressed (Karimi et al., 2011). However, MMVL30, the most derepressed ERV in Setdb1 knockout MEF cells, were mildly changed (Kato et al., 2018). On the other hand, in DE knockout cells ERV1 and

ERVK were mildly derepressed and no change in ERVL and LINEs expression (Figure 2.8B, D). In consistence with the *in vivo* and *in vitro* staining (Figure 2.1C, Figure 2.3), IAPEz was dramatically derepressed in XEN knockout cells but no change was observed in DE knockout cells.

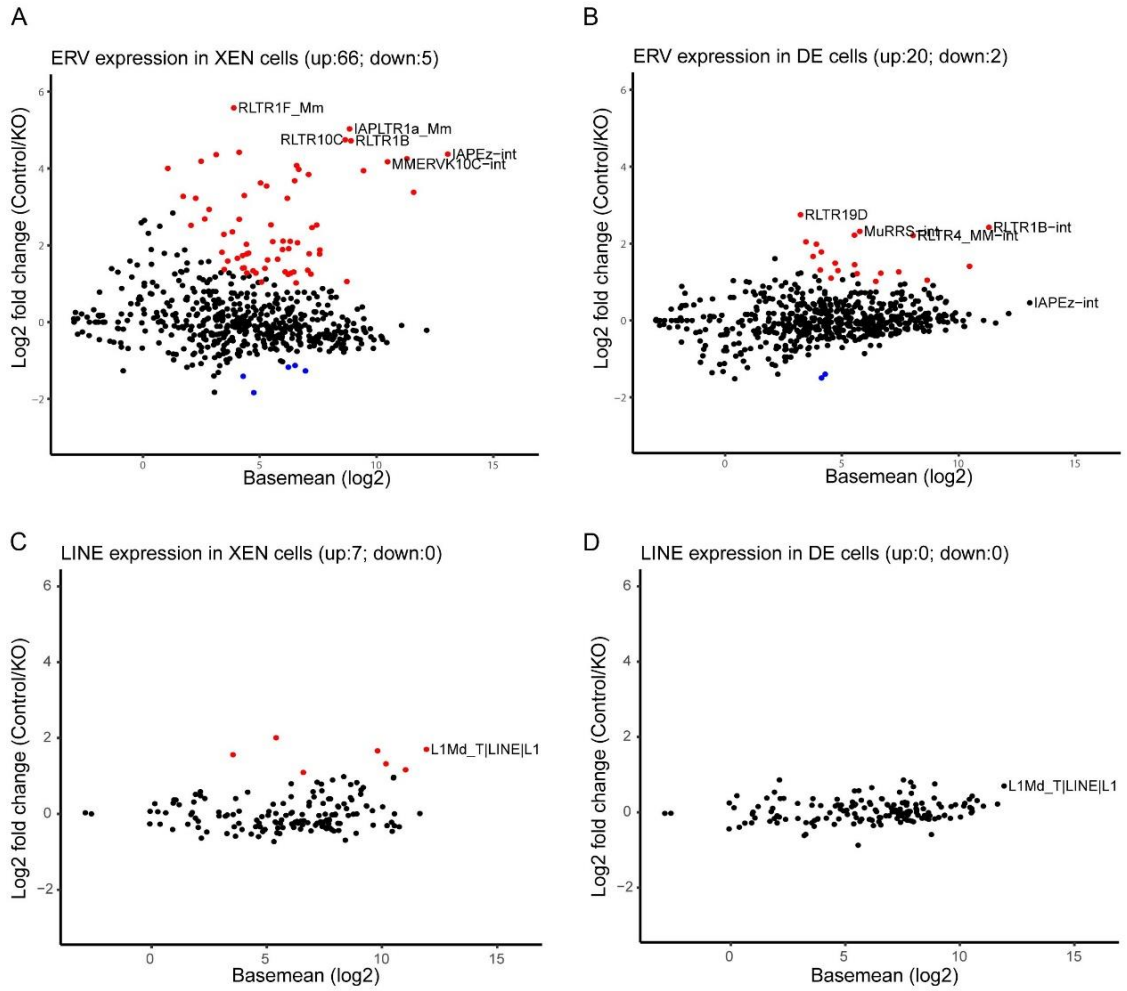

Figure 2.8 Differential retroelements expression in Setdb1 knockout endoderm cells

A,B. Dot plot showing basemean expression vs. log2-fold change of ERV in differentiated XEN and DE cells in knockout vs. control cells after 7 days differentiation. ERVs with significantly changed expression (adjusted p-value < 0.01, fold change > 2; n=3 for each condition) are coloured (red = increased expression in mutant cells, blue = increased expression in control cells).

C,D. Dot plot showing basemean expression vs. log2-fold change of LINEs in differentiated XEN and DE cells in knockout vs. control cells after 7 days differentiation. LINEs with significantly changed expression (adjusted p-value < 0.01, fold change > 2; n=3 for each condition) are coloured (red = increased expression in mutant cells, blue = increased expression in control cells).

2.4.4 *In vitro* differentiation system reflects similar trend of IAP derepression *in vivo*

Since the heterozygous and homozygous for conditional Setdb1 knockout allele were used as control and mutant cells, I compared the expression of all annotated ERVs in each cell line including undifferentiated ES cells to better understand the baseline expression in heterozygous endoderm cells. Embryonic endoderm cells were also included to compare ERV expression level in XEN knockout cells and embryonic endoderm knockout cells. The overall ERV expression is comparable in control and knockout ES cells, though mild decrease in ERV expression upon XEN and DE differentiation in control cells. Consistent with previous result, XEN knockout cells showed strong ERV derepression. However, ERVs were mildly up-regulated in DE knockout cells. Interestingly, the ERV derepression in XEN knockout cells was comparable with the embryonic endoderm cells (Figure 2.9A). I next analyzed the expression of most derepressed ERV family members in different cell types. Despite a mild expression of a few families such as IAPEY4 and MMERVK10D3_LTR in embryonic endoderm control cells, the majority of families were not expressed in either XEN control or DE control cells suggesting that the majority of the ERVs were tightly controlled in control endoderm cells. Notably, most of the families, for example, IAPEz-int and MMERVK10C-int showed consistent strong derepression in XEN knockout cells and embryonic endoderm knockout cells. However, a few families such as IAP1-MM_LTR, MMERVK9C_I-int were also up-regulated in DE knockout cells (Figure 2.9B, C).

In summary, ERVs were tightly controlled in both heterozygous DE cells and XEN cells, and even mildly down-regulated compared with ES cells. Moreover, loss of Setdb1 results in ERV derepression in a comparable level in XEN knockout cells and embryonic endoderm knockout cells. However, loss of Setdb1 leads to only a mild ERV derepression in DE knockout cells.

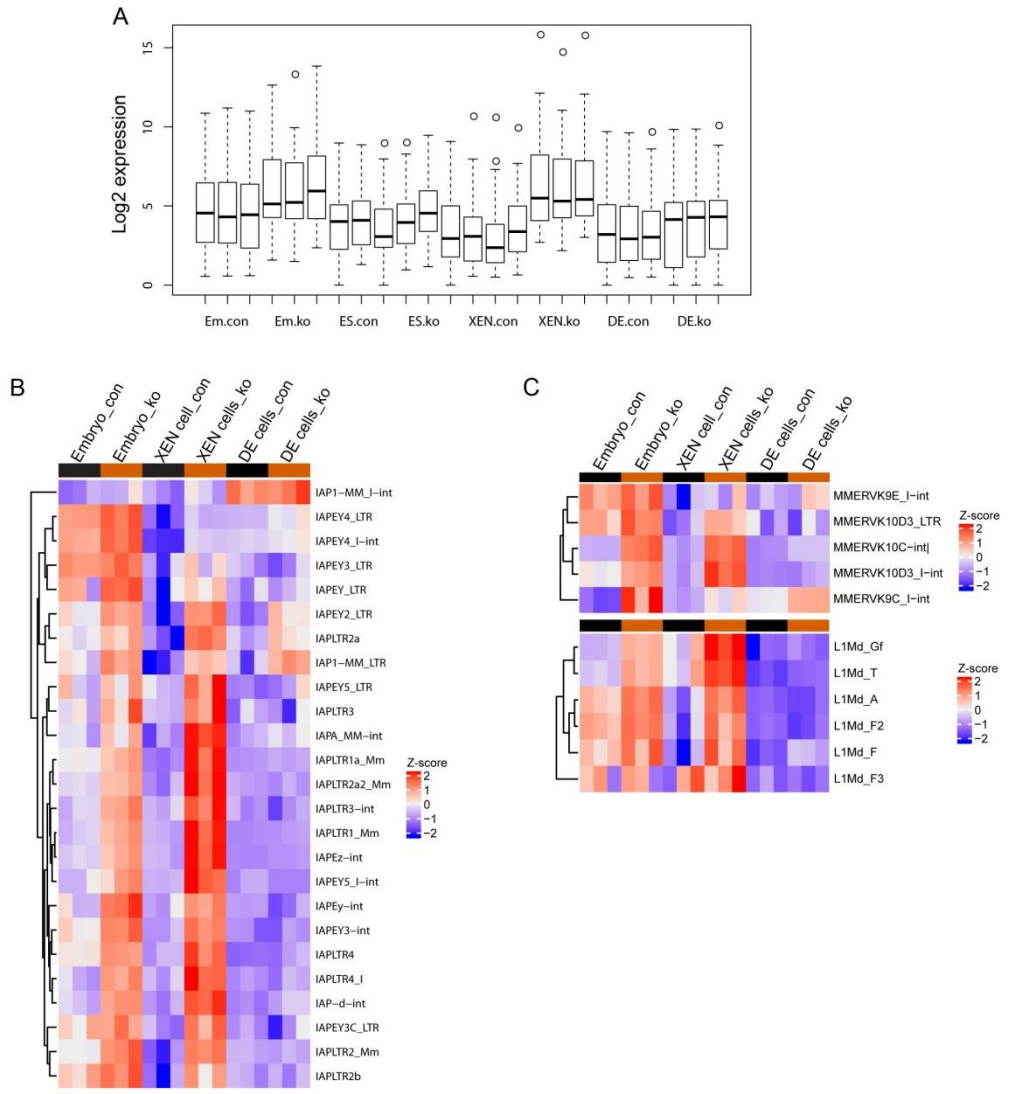

Figure 2.9 Similar ERV derepression in XEN knockout cells and embryonic endoderm knockout cells

A.Boxplot of all ERV expression in embryonic endoderm cells and *in vitro* differentiated endoderm cells.

B-C. Heatmap of the differentially expressed IAP/MMERVK/L1Md families between embryonic endoderm cells and *in vitro* differentiated endoderm cells. Red colour indicate higher expression Z-score. Hierarchical clustering was performed using complete agglomeration method and a Euclidean distance metric (n=3 for each condition).

2.4.5 Strong derepression of ERVs is associated with up-regulation of genes in vicinity

ERVs can affect the neighboring gene expression by providing alternative promoters and initiate the transcription (Buzdin, 2004). Burst expression of ERVs contributed to ~10 % up-regulated genes by generating chimeric transcript in Setdb1 knockout ES cells (Karimi et al., 2011). I applied the GREAT (Genomic regions enrichment of annotations tool) package to identify genes in the vicinity of changed expression of solitary ERVs, and then analyzed the percentage of up-regulated genes in the vicinity of derepressed ERVs. Overall, around 10 % of up-regulated genes were contributed by the closed neighboring (within 20kb) ERVs

derepression (Figure 2.10A). This result reflected what has been observed in Setdb1 knockout ES cells (Karimi et al., 2011). This number goes up to 20 % by setting neighboring criteria to 50kb. But still less than 10 % of genes were up-regulated in vicinity to derepressed ERVs in DE knockout cells. This might be due to the overall mild derepression of ERVs in DE. However, as the ERVs derepression were comparable in both embryonic endoderm knockout cells and XEN knockout cells, the percentage of up-regulated genes affected by the vicinity ERVs derepression is still lower in XEN knockout cells than embryonic endoderm knockout cell. The reason might be that genes were tightly controlled in the *in vivo* system resulting in less up-regulated genes. In the *in vitro* differentiated cells, up-regulated genes may be affected by the indirect effect. Since ERV copies from IAPEz family are highly similar to each other, it is difficult to find an example with unique mapped reads. Thus I showed an example with unique mapped reads where Ccne2 were up-regulated by the derepressed MMERGLN-int and RLTR1A2_MM (Figure 2.10B).

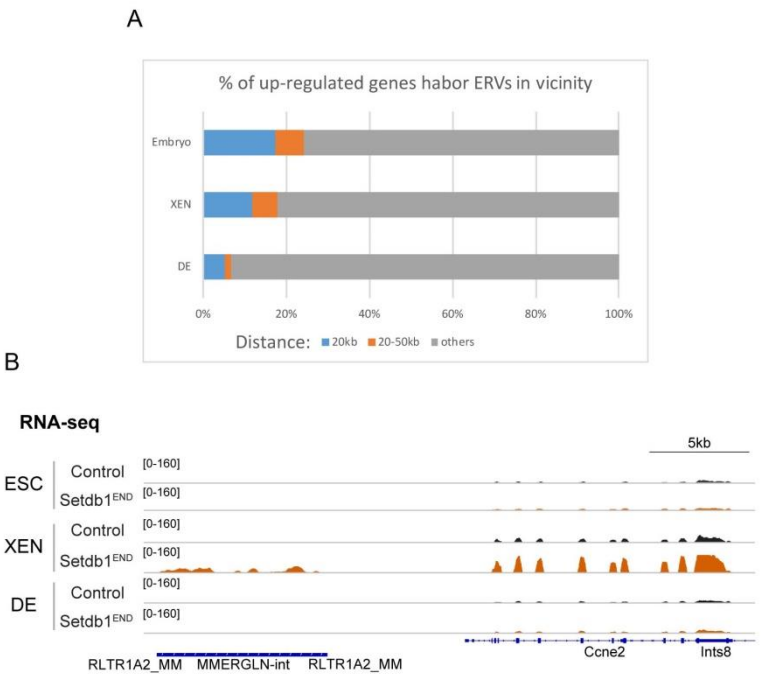

Figure 2.10 Strong derepression of ERVs is associated with vicinity genes up-regulation

A. Percentage of up-regulated genes harbour derepressed ERVs in the vicinity. Distance between genes and ERVs are marked in blue and orange showing 20kb and 20-50kb, respectively.

B. Representative genome browser view of RNA-seq signals in ES, XEN and DE cells at ERVs.

2.5 Impaired repressive marks specifically in Setdb1END XEN cells

2.5.1 Decrease of H3K9me3 at ERVs in Setdb1END XEN cells

To determine the genome wide level of H3K9me3 in two types of endoderm knockout cells and how the H3K9me3 domains could be affected by the loss of Setdb1. The enrichment of H3K9me3 was identified by chromatin immunoprecipitation followed by high throughput sequencing (ChIP-Seq). I plotted the log2 of H3K9me3 reads over input in control versus knockout cells. A few families, such as MURVY-int and RLTR5_mm, showed a strong decrease of H3K9me3 in DE knockout cells. However, 40 ERV families showed a steady decrease of H3K9me3 in XEN knockout cells (Figure 2.11A, B). I further analyzed the enrichment of H3K9me3 over LINEs in two types of endoderm cells. The LINEs covered with low levels of H3K9me3 showed no dramatic decrease in both XEN knockout cells and DE knockout cells (Figure 2.11B, C). This finding is consistent with previously published results which showed that loss of Setdb1 in MEF cells exhibited a slight reduction of H3K9me3 in LINE families (Kato et al., 2018).

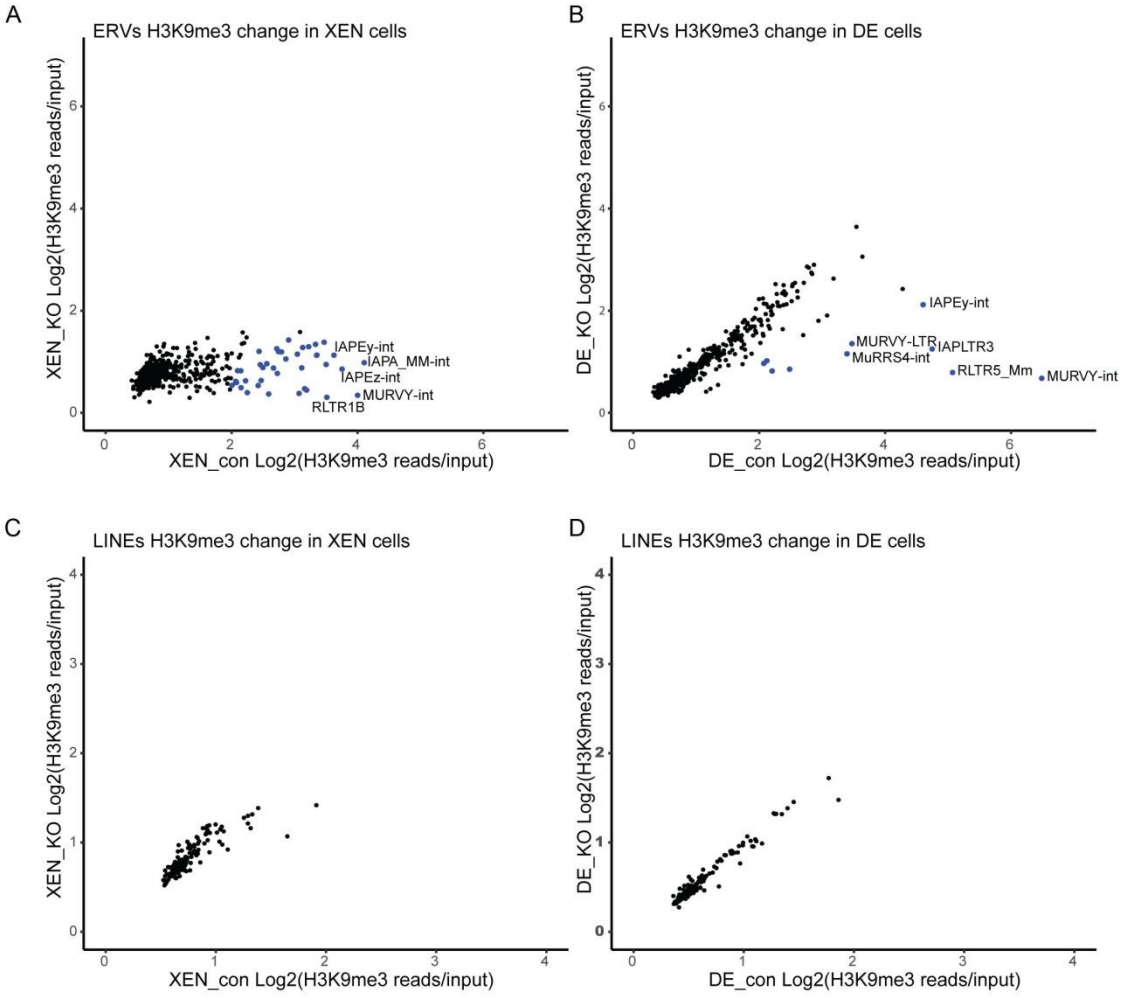

Figure 2.11 Correlation of gene expression and H3K9me3 changes for ERVs and LINEs families

A. Family analysis by plotting log2 of H3K9me3 reads over input in knockout cells versus control cells in XEN and DE. ERVs with significantly changed H3K9me3 enrichment (fold change > 2; n=2 for each condition) are coloured (red = increased H3K9me3 in mutant cells, blue = increased H3K9me3 in control cells). Positions of relevant ERVs are indicated.

B. Family analysis by plotting log2 of H3K9me3 reads over input in knockout cells versus control cells in XEN and DE. LINEs with significantly changed H3K9me3 enrichment (fold change > 2; n=2 for each condition) are coloured (red = increased H3K9me3 in mutant cells, blue = increased H3K9me3 in control cells).

2.5.2 Derepressed ERVs lose H3K9me3 in Setdb1END XEN cells

To address whether the increased ERVs and LINEs expression was the result of decreased H3K9me3 upon Setdb1 deletion. I plotted the log2foldchange of H3K9me3 versus expression. Most of highly derepressed ERVs in XEN knockout cells, such as MMERVK10C-int and IAPEz-int, were released by the decrease of H3K9me3 (Figure 2.12A). This result has been observed in Setdb1 knockout ES cells (Karimi et al., 2011). However, the derepressed ERVs such as RLTR1B-int and MuRRS-int showed less than 2 fold decrease of H3K9me3 in DE knockout cells. MURVY-int and RLTR5_Mm lost H3K9me3 did not result in an increased expression (Figure 2.12B). Consistent with the previously published result, loss of Setdb1 in MEF cells showed a mild decrease of H3K9me3 at many ERV families but did not result in ERV derepression (Kato et al., 2018). Despite the relatively low cover of H3K9me3 on LINEs comparing to ERVs, the mild derepression of LINEs in XEN knockout cells showed no change in H3K9me3. It indicates that the LINE derepression was not controlled by the Setdb1 mediated H3K9me3 but by indirect effect such as dysregulated genes or other repressive marks, for example DNA methylation (Figure 2.12C).

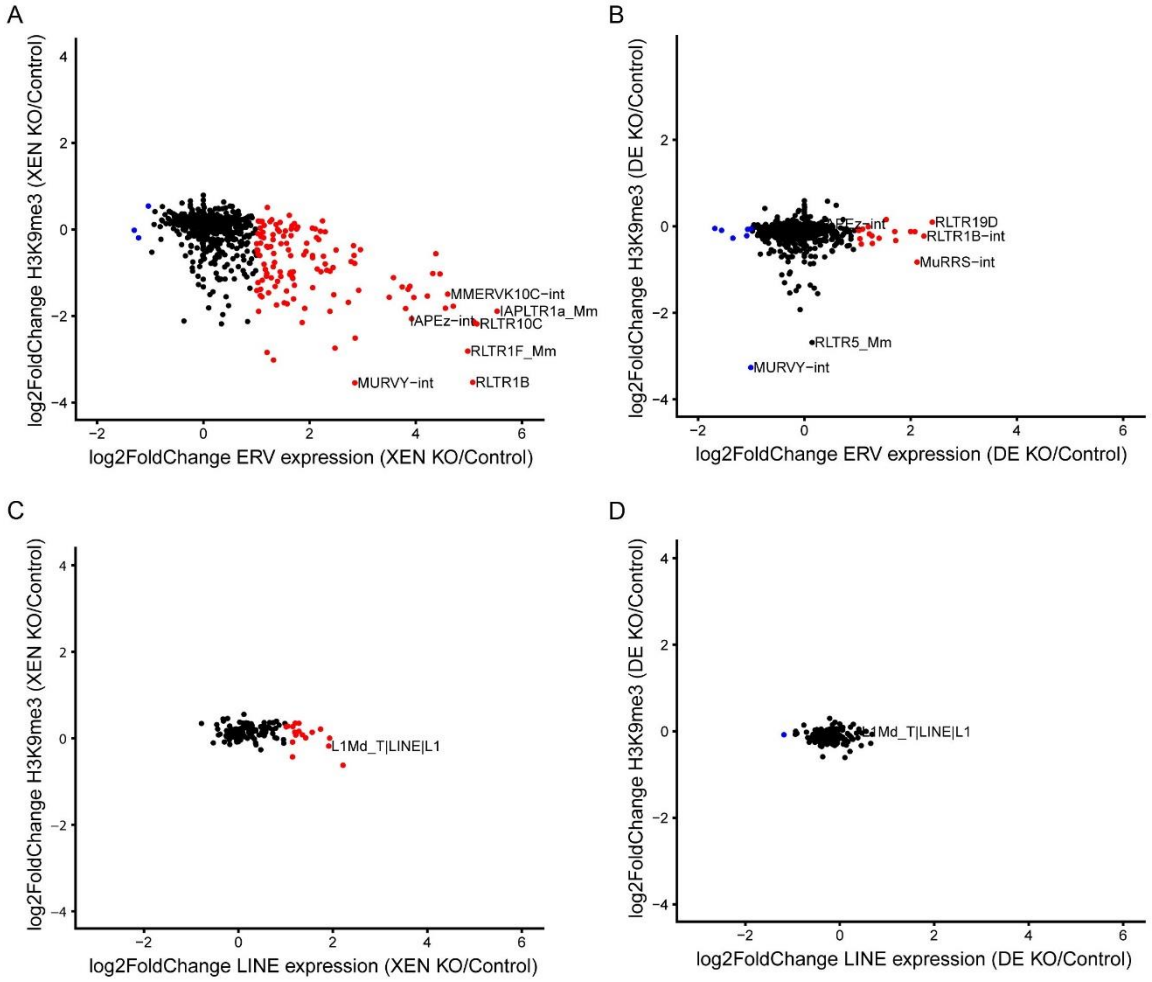

Figure 2.12 Correlation of expression and H3K9me3 changes for ERVs and LINEs families

A-B. Family analysis by plotting log2foldchange of H3K9me3 enrichment over input versus expression log2foldchange in knockout vs. control cells. ERVs with significantly changed expression (fold change > 2; n=2 for each condition) are coloured (red = increased expression in mutant cells, blue = increased expression in control cells). Positions of relevant ERVs are indicated. It reveals that derepressed ERVs showed strong decrease of H3K9me3 only in Setdb1 knockout XEN cells.

C-D. Family analysis by plotting log2foldchange of H3K9me3 enrichment over input versus expression log2foldchange in knockout vs. control cells. LINEs with significantly changed expression (fold change > 2; n=2 for each condition) are coloured (red = increased expression in mutant cells, blue = increased expression in control cells). Positions of relevant LINEs are indicated. It reveals that LINEs were mildly up-regulated without change in H3K9me3 in Setdb1 ko XEN cells and were still repressed in the Setdb1 ko DE cells.

Although all of the RNA-seq and ChIP-seq libraries were sequenced with a read length of 50bp in single-end mode, the data might not be most suitable for solitary ERVs analysis. However, the correlation of expression and H3K9me3 changes for solitary ERVs may help us to figure out if the conclusion from the family analysis is supportive. Accordingly, the conclusion that decreasing of H3K9me3 resulted ERVs derepression in Setdb1 knockout XEN cells was supported by the solitary ERVs analysis (Figure 2.13A). Majority of the single ERVs copies which were derepressed in DE knockout cells were not controlled by H3K9me3

mediated by Setdb1 (Figure 2.13B). This further proves that the mild ERV derepression in DE knockout cell might be due to the indirect effect.

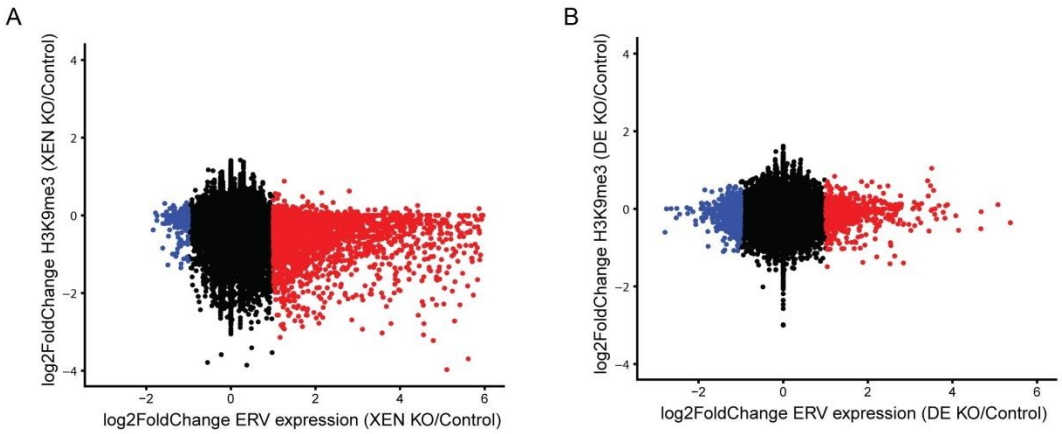

Figure 2.13 Correlation of expression and H3K9me3 changes for solitary ERVs

A-B. Family analysis by plotting H3K9me3 changes versus expression changes reveals that ERV lose H3K9me3 and are derepressed only in the XEN ko cells but not DE ko cells. Derepressed ERV families are shown in red.

IAPs, one of the most well studied transpositionally active ERVs, was used as a representative ERV to investigate the ERV regulation in different cell types (Hutnick et al., 2010; Pastor et al., 2014; Tan et al., 2012). As we used anti-IAP-GAG antibody from Bryan Cullen's lab as a representative to detect the ERV derepression (Figure 2.1C, Figure2.3A, B), I did the cumulative ChIP-seq coverage profiles across IAPEz elements for H3K9me3 and found a strong enrichment of H3K9me3 over IAP-GAG suggesting an important role of IAP-GAG in IAP silencing.

I observed a two times decrease of H3K9me3 in both XEN control and DE control cells compare with undifferentiated ES cells (data not shown). A lower enrichment of H3K9me3 was observed in DE control cells compare with XEN control cells. However, DE knockout cells showed no difference of H3K9me3 compare with DE control cells. while XEN knockout cells were depleted of H3K9me3 (Figure 2.14A). This depletion of H3K9me3 was not only observed in IAPEz but also in other ERV families. Moreover, this exclusive depletion of H3K9me3 in XEN knockout cell was associated with strong ERV derepression. For instance, the loss of H3K9me3 at MMERGLN-int and RLTR1A2_MM results the up-regulation of vicinity gene Ccne2 (Figure 2.14B).

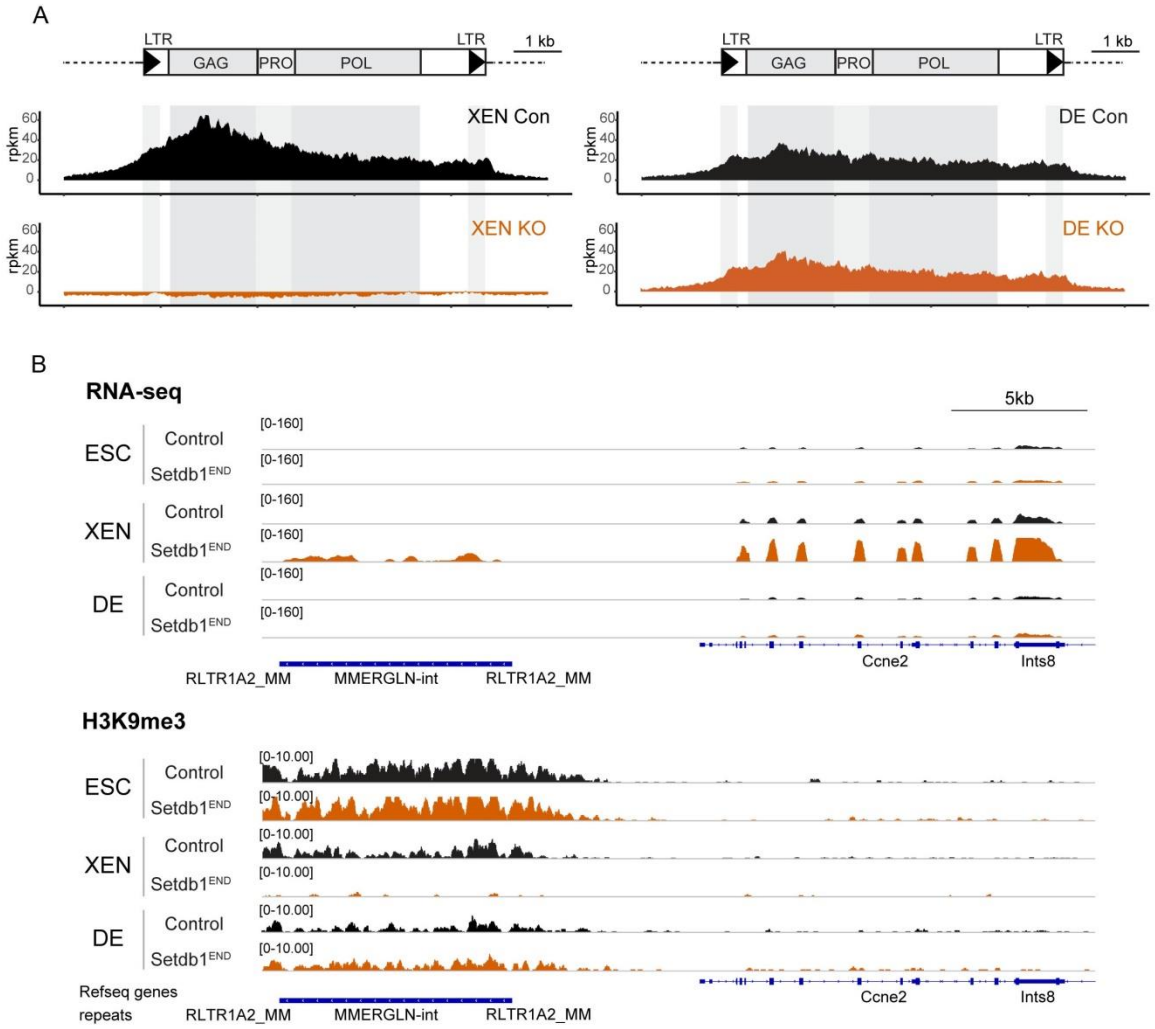

Figure 2.14 Correlation of gene expression, H3K9me3 changes for solitary ERVs

A. Cumulative ChIP-seq coverage profiles across IAPEz elements for H3K9me3, the structure of IAP elements is shown schematically. rpkm, reads per kilobase per million of reads.

B. Representative genome browser view of RNA-seq and H3K9me3 ChIP-seq signals at MMERGLN-int in ES, XEN and DE cells.

2.5.3 Loss of DNA methylation in Setdb1END XEN cells

A heterochromatic screening system was previously established in our lab by Dr. Dennis Sadic. He found that the IAP-GAG region combined with hEF1a and EGFP reporter showed strong silencing effect (Sadic et al., 2015). However, numerous studies focused on the DNA methylation level of IAP LTR region upon loss of Setdb1 and Trim28 and correlation of DNA methylation level of IAP LTR region and IAP expression in different cell types (Bakshi and Kim, 2014; Liu et al., 2014; Rowe et al., 2013b; Shimosuga et al., 2017). Considering all

mentioned above, I used primers specific to IAP LTR, IAP GAG and LINE to detect DNA methylation changes upon loss of Setdb1 in two types of endoderm cells (Figure 2.15A). Due to the decreased complexity of the genomic sequence from bisulfite treatment, I employed bisulfite sequencing coupled with Miseq. It enables us to sequence the whole PCR amplicon following bisulfite treatment of interest regions without mapping problem.

I identified a 300bp sequence from IAP LTR, 500 bp sequence from IAP GAG and 200bp sequence from LINE. I identified 17 CpGs in IAP LTR region and 27 CpGs in the IAP GAG region with nearly 95 % 5mC levels in ES cells which were maintained in both DE control and DE knockout cells. Interestingly, 5mC levels of IAP GAG were dramatically decreased to nearly 50 % in XEN knockout cells whereas the 5mC levels of IAP LTR were mildly decreased. In the case of LINE-1, I identified 9 CpGs with nearly 50 % 5mC levels in ES cells which increased to about 90 % in both DE control and knockout cells. However, the 5mC levels were increased to nearly 70 % in XEN control cells but dramatically decreased in XEN knockout cells (Figure 2.15B). The decrease of DNA methylation upon loss of H3K9me3 in XEN knockout cells supports previous findings that the binding of Uhrf1 to H3K9me3 help to recruit Dnmt1 for DNA methylation maintenance (Liu et al., 2013).

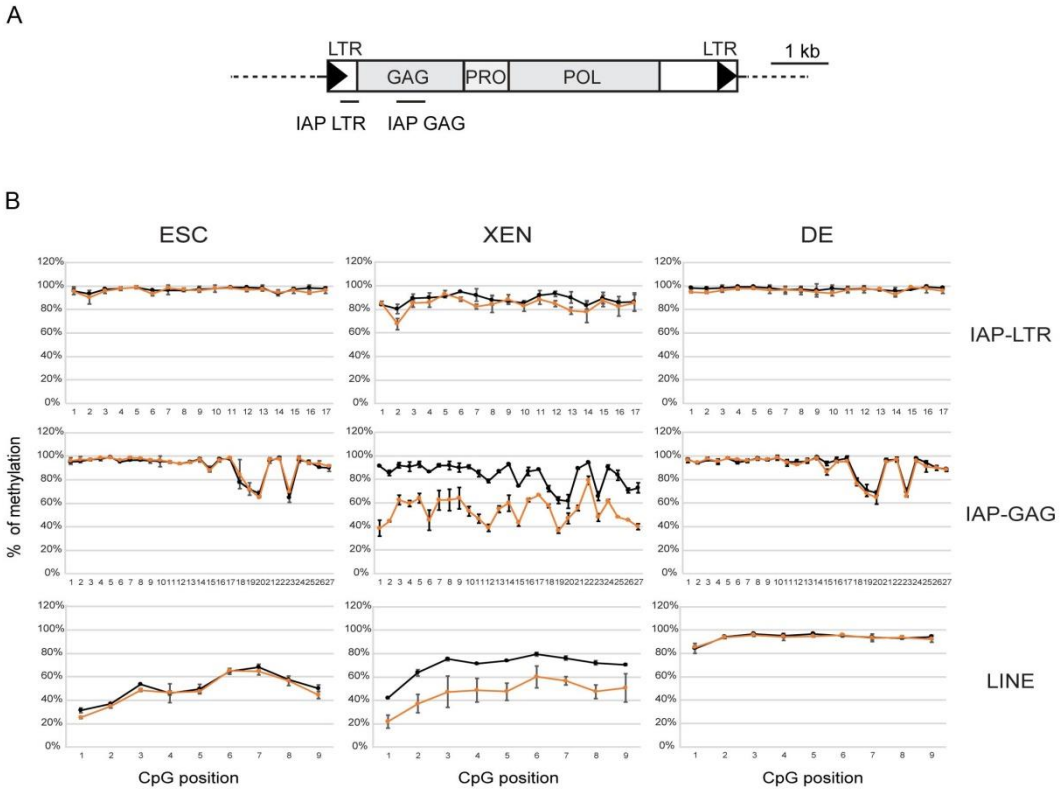

Figure 2.15 loss of DNA methylation in Setdb1 ko XEN

A. Schematic representation of the location of primers detecting IAP LTR and GAG region which represent the promoter region and the region that is sufficient to induce heterochromatin formation to trigger silencing.

B. Graphs depicting the percentage of methylation per CpG in the IAP LTR, GAG and LINE-1 loci in Setdb1 conditional knockout upon 7 days endoderm differentiation and analysed by bisulphite sequencing analysis. Y-axis indicates % of methylation and X-axis indicates individual CpGs.

2.6 Loss of Dnmt1 leads to ERV de-repression in both DE and XEN cells in presence of H3K9me3

2.6.1 IAP derepression in both endoderm cells with ablation of DNMT methyltransferases

I found the derepression of IAPs correlate with a pronounced reduction of DNA methylation associated with decreased level of H3K9me3 in visceral endoderm cells lacking Setdb1 (Figure 2.1C, Figure 2.8A, B, Figure 2.12A, B, Figure 2.15B). However, IAPs remain repressed in definitive endoderm cells upon loss of Setdb1. To figure out if DNA methylation controls the ERVs expression in both viseceral endoderm cells and definitive endoderm cells, I initially utilized Dnmt1/Dnmt3a/Dnmt3b TKO cells, in which DNA methylation is absent, to identify the IAP derepression upon differentiation (Tsumura et al., 2006). Consistent with the previously published result, XEN Dnmt TKO cells were able to differentiate into extra-embryonic endoderm cells but failed in differentiating epiblast lineages (Sakaue et al., 2010). I found strong IAP derepression in this XEN Dnmt TKO cells. But Dnmt TKO cells died 2 days upon definitive endoderm differentiation (data not shown).

I employed Dnmt1 constitutive knockout cells which could differentiate to both XEN and DE cells. Also based on the previous observation, loss of Dnmt1 induces a rapid loss of methylation that stabilizes to ~20 % of the average value, whereas Dnmt3a–/–Dnmt3b–/– ESCs lose nearly all methylation over progressive divisions (Tsumura et al., 2006). However, due to the cell line limit, I could not use GFP reporter to isolate the differentiated cells to perform RNA-seq or RT-qPCR. Thus, I employed the anti-IAP GAG antibody to perform the intracellular staining followed with FACS analysis. The FITC channel was used to distinguish differentiated cells from undifferentiated cells by anti-Sox17 antibody staining. Consistent with the previous result, the XEN differentiation by lentiviral transduction followed with puromycin selection results in a better differentiation (Figure 2.4 A, B). The IAPs were repressed upon XEN and DE differentiation in wild type cells. While Dnmt1 knockout in XEN cells showed strong IAP derepression. Interestingly, a strong increase in IAP expression was observed in Dnmt1 knockout DE cells as well as the Sox17- cells incubated with endoderm differentiation medium (EDM) for 7 days (Figure 2.16A).

I further calculated the fold change through dividing the mean fluorescence intensity of IAP-GAG from differentiated cells by the mean fluorescence intensity of IAP-GAG from undifferentiated ES cells. Both Dnmt1 knockout XEN and DE cells showed significant IAP

derepression (Figure 2.16B). Our finding revealed that ERVs are tightly controlled in definitive endoderm cells by DNA methylation.

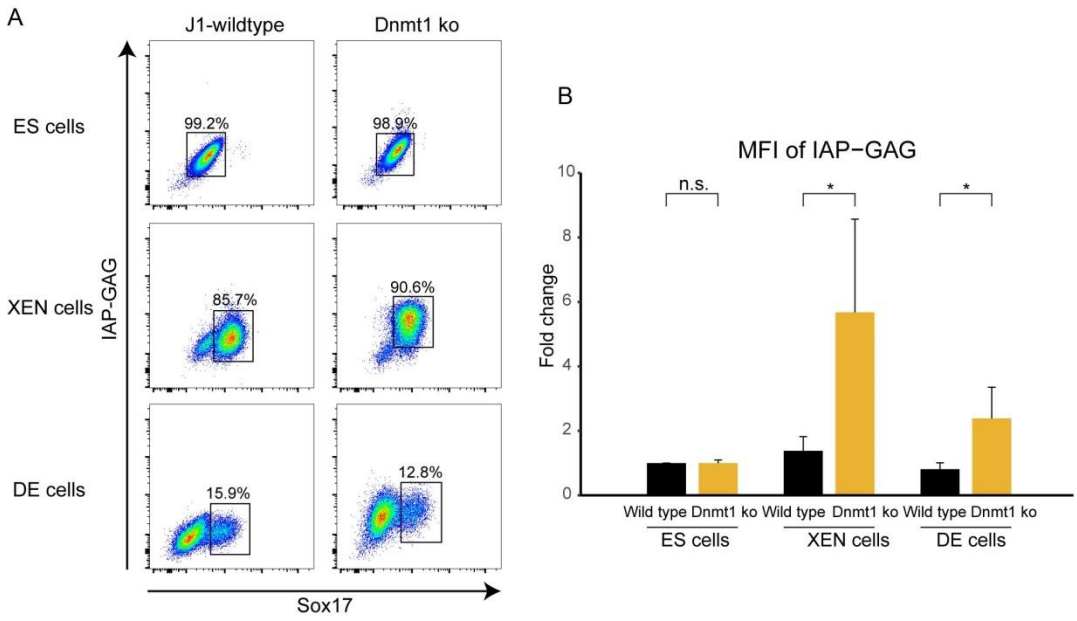

Figure 2.16 Strong expression of IAP in both Dnmt1 XEN and DE KO cells.

A,Flow cytometric analysis of IAP-GAG and Sox17 expression in ES cells, XEN cell and DE cells. The figure is a representative of four experiments with similar results.

B, Fold change of mean fluorescence intensities (MFI) for IAP-GAG staining in differentiated XEN cells and DE cells relative to undifferentiated ES cells. Error bars depict standard deviation (n=4).

2.6.2 No changes of H3K9me3 on ERVs in differentiated Dnmt1 knockout cells

As the decreasing of DNA methylation level on IAP GAG is associated with loss of H3K9me3 upon Setdb1 depletion in XEN cells, I wondered if H3K9me3 and DNA methylation affect each other reciprocally. To answer this question, I tried to detect H3K9me3 level in Dnmt1 knockout cells upon endoderm differentiation. I FACS isolated the intracellular stained Sox17 positive cells and performed chromatin immunoprecipitation experiments followed with qPCR to detect the H3K9me3 levels at imprinted genes and IAPs. I did not only checked IAP GAG but also IAP LTR which represents the promter of IAP and IAP global which is at just 3’ of the 5' LTR. All these three regions showed changes in DNA methylation upon loss of Setdb1 in different cell types (Liu et al., 2014; Matsui et al., 2010). In all three types of cells, the imprinted region showed a strong decrease of H3K9me3. However, H3K9me3 level was not changed at IAP-LTR, IAP-GAG and the surrounding region upon Dnmt1 deletion.

In summary, the loss of DNA methylation results the derepression of IAP retrotransposons without disturbing the level of H3K9me3. Our finding revealed a dominant role of DNA methylation over H3K9me3 in ERV regulation during endoderm differentiation.

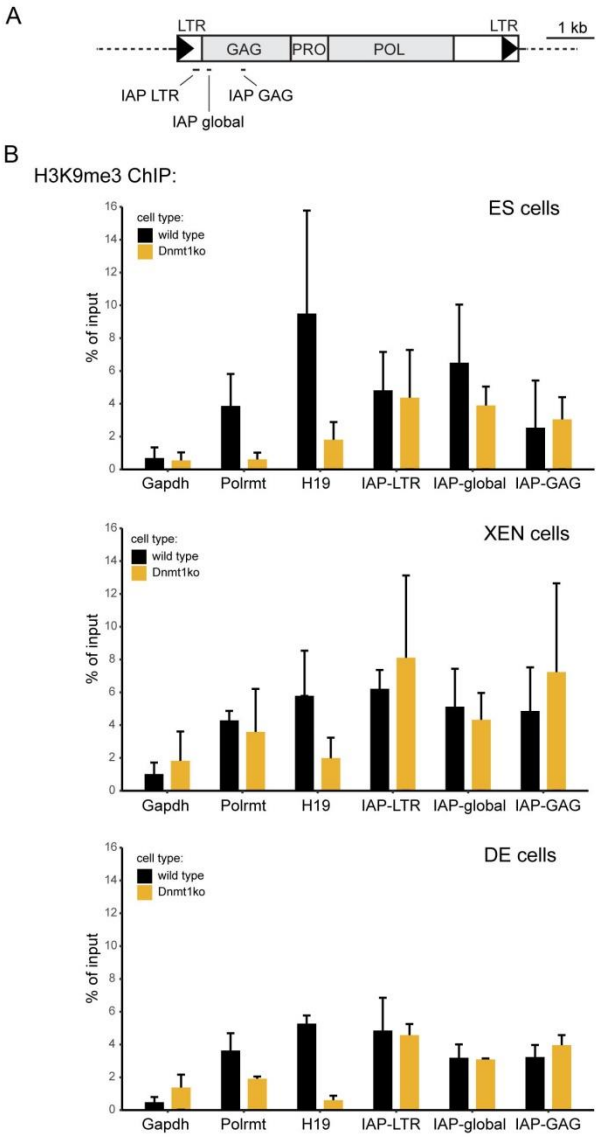

Figure 2.17 No change in H3K9me3 at ERVs

A. Schematic representation of the location of primers detecting IAP LTR, IAP global and GAG region which represent the promoter region, the region at just 3' of the 5' LTR and the region that is sufficient to trigger silencing.

B. ChIP-qPCR analysis for H3K9me3 in wild-type (wt) and Dnmt1 ko ES, XEN and DE cells. Bar plots indicate the mean H3K9me3 enrichment over input of three biological replicates. Error bars indicate the standard deviation. Positive region: Polrmt,H19; Negative region: Gapdh. H3K9me3 is not altered at IAP in Dnmt1 ko cells.

3. Discussion

3.1 An *in vitro* differentiation system models definitive and visceral endoderm differentiation.

During early embryonic development, two events mark the emergence of endoderm cells. At E3.5 ICM cells restrict their fate to epiblast or primitive endoderm by expression of Nanog or Gata6, respectively, in a salt-pepper pattern (Chazaud et al., 2006). Expression of the endoderm marker gene Sox17 is detected as early as the 32-cell stage and with progressing development to the blastocyst stage becomes restricted to certain cells of the ICM and later on primitive endoderm cells (Niakan et al., 2010). The second emergence of endoderm cells, was the ones of the definitive endoderm cells, occurs at the gastrulation stage by at E6.5. While Sox17 mRNA was not detected in embryonic visceral endoderm at E6.25 but it could be identified at mid-streak stage at the anterior end of the primitive streak in definitive endoderm by E7.0 (Kanai-Azuma et al., 2002).

Primitive endoderm contributes to visceral endoderm and parietal endoderm. Visceral endoderm for its part envelops the epiblast of the post-implantation embryo. As the definitive endoderm arises at the anterior primitive streak, visceral endoderm was considered to be displaced proximally to the extra-embryonic yolk sac and important for patterning of the epiblast (Srinivas, 2006). Recently, AFP::GFP mice showed that the visceral endoderm overlying the embryos was dispersed but not displaced by epiblast derived definitive endoderm. These visceral endoderm cells were incorporated into early gut endoderm suggesting its dual origin (Kwon et al., 2008).

Considering the above, the embryonic visceral endoderm and definitive endoderm should express Sox17 at similar stage and, by employing a Sox17 promoter driven Cre recombinase, result in a similar deletion of Setdb1 *in vivo*. Therefore, the different expression of IAP GAG in embryonic visceral endoderm (AFP positive) and definitive endoderm (AFP negative) is due to the different feature of these two type of cells (Figure 2.1B).

A recent detailed single-cell transcriptome analysis of all endoderm populations proved that cells have either embryonic or extra-embryonic endoderm features converged within the nascent gut endoderm and suggested globally similar feature from distinct development trajectories (Nowotschin et al., 2019). However, they observed expression trends of genes with both endoderm factors such as Sox17 and pluripotency-associated factors such as Nanog in visceral endoderm by E5.5. They found the spatial patterning precedes morphological changes within the visceral endoderm which correlate with a subset of cells

and exhibit a more committed state while a majority of the cells exhibit their propensity towards differentiated state. Due to similarities of visceral endoderm and definitive endoderm, an efficient *in vitro* differentiation system could help us to understand the difference within these two types of endoderm cells.

The potential of retinoic acid and activin treatment can promote ES cells to neurons and definitive endoderm cells, respectively. The combination of retinoic acid and activin results a heterogeneous mixture of XEN-differentiated cells. However, the differentiation efficiency is limited and chemical induced XEN (cXEN) cells contributed to the parietal endoderm at early post implantation stages when generating chimera embryos. Another possibility for XEN differentiation is by overexpressing the transcription factor Gata6. However, it has the disadvantage that the constitutive Gata6 expression blocks the differentiation from XEN cells to visceral endoderm cells which only express Gata4 (Niakan et al., 2013).

XEN cells which are derived from primitive endoderm and propagate indefinitely in culture, also express typical markers of extra-embryonic endoderm derivatives. Therefore, as XEN cells are progenitor of visceral endoderm cells, they share key features of visceral endoderm cells, I employed the XEN differentiation by Gata6 overexpression for better differentiation efficiency to mimic the *in vivo* visceral endoderm (Niakan et al., 2013). However, increased expression of Afp and decrease of Sox7 in differentiated XEN cells revealed its differentiation properties toward visceral endoderm cells (Artus et al., 2012; Kunath et al., 2005). Consistently, I did not detect Afp expression in XEN cells. Additionally, a clear expression of XEN specific genes (such as Sox7, cd38), common endoderm markers genes (such as Foxa2, Sox17) and some pluripotency related genes (such as Oct4, Dppa) reflect the feature of XEN cells as previously reported (Figure 2.6B)(Niakan et al., 2010; Sherwood et al., 2007; Zhang et al., 2018). Interestingly, we found strong expression of Dppa family members including Dppa2, Dppa3, Dppa4 and Dppa5a in XEN cells consistent with what was observed in early lineage specification in mouse embryos (Zhang et al., 2018). The emerging roles of Dppa family in preventing de novo methylation through Uhrf1 suggest a lower level of DNA methylation at IAPEz and LINE in XEN control cells than definitive endoderm control cells (Eckersley-Maslin et al., 2019; Li et al., 2018). The high expression of Sox7 and low expression of Gsc suggested the standard XEN properties without the presence of definitive endoderm cells (Kanai-Azuma et al., 2002).

As no transcription factors are reported to efficiently differentiate ES cells towards definitive endoderm cells, I employed definitive endoderm differentiation by chemical induction with Activin and Wnt3a to mimic the *in vivo* definitive endoderm (Cernilogar et al., 2019b; Hansson et al., 2009; Singh et al., 2012). The differentiated definitive endoderm cells

featured expression of common endoderm marker genes and definitive endoderm specific genes (such as Gsc and Foxa1).

Upon XEN cell differentiation, cells were transduced with lentivirus containing Gata6 overexpression construct on day1, the overexpression of Gata6 could drive the differentiation and express Sox17 as early as day3. Similarly, upon definitive endoderm differentiation, Sox17 was expressed as early as day3. The differentiation efficiency could reach as high as 40 % of the total population on day5. But I kept them under the differentiation condition for 7 days for a better deletion rate.

As is mentioned above, the activation of Sox17 was first detected on day3 in both XEN and DE cells. But residual Setdb1 was only detected in definitive endoderm cells. Probably, the residual Setdb1 transcript and protein in definitive endoderm cells were due to the limitation of chemical induction which resulted in heterozygous differentiated population and the Setdb1 transcript and protein were not fully degraded in late differentiated cells (Figure 2.5). In contrast to the lentivirus transduction plus puromycin selection on day3 resulted in a more homogeneous population in differentiated XEN cells, but no reporters can be used to distinguish the early and late differentiated definitive endoderm cells. As the definitive endoderm differentiation efficiency could reach as high as 40 % on day5, the majority of the differentiated cell should be depleted of Setdb1. The IAP-GAG staining in definitive endoderm cells revealed that the majority of differentiated definitive endoderm cells which are depleted of Setdb1 also kept IAPEz repressed (Figure 2.3).

An efficient transcription factor based definitive endoderm differentiation could be useful to clarify the H3K9me3 changes without contamination of late differentiated cells. On the other hand, the adjustment of chemical induction by adding Activin and retinoic acid for XEN differentiation could be done to mimic the definitive endoderm differentiation efficiency and timing for Sox17 expression. The similar rate of late differentiation in XEN differentiation and residual Setdb1 transcript and protein may result in a more comparable result.

Considering all the above, despite the difference between primitive endoderm and visceral endoderm, the *in vitro* differentiated XEN cells and definitive endoderm cells mimic the *in vivo* main features of visceral endoderm and definitive endoderm. Accordingly, the exclusive derepression of IAPEz *in vitro* differentiated XEN knockout cells reflected the phenotype in the *in vivo* system.

3.2 Transcriptional regulation of Setdb1 in two types of endoderm cells

Setdb1, a histone H3K9me3 methyltransferase, repress not only retrotransposable elements but also euchromatic genes including imprinted genes and developmental regulators (Bilodeau et al., 2009; Schultz et al., 2002; Yuan et al., 2009). The top up-regulated genes in Setdb1 knockout XEN cells were either known Setdb1 targets such as testis genes Gabrr1 and Tuba3a or known genes affected by derepression of ERVs in the vicinity such as Gm1110 and cd22 (Figure 2.7A). GO term enrichment analysis revealed terms related to meiosis (Figure 2.7C), similar to what was observed in PGCs (Liu et al., 2014). Interestingly, Dppa family members including dppa4 and dppa2 were up-regulated. Dppa2/4 overexpression were shown to facilitate chromatin decompaction via Parp1 (Hernandez et al., 2018), which may suggest the pathways involved in DNA demethylation through Parp1 in XEN knockout cells. The top up-regulated genes in Setdb1 knockout DE cells were also known to be regulated by Setdb1. For example, the imprinted gene H19, the testis gene Tex19.1, the ERV affected gene cd22 and interferon-induced gene Ifi2712a. However, GO term enrichment analysis showed terms related to cell differentiation and cardiac and heart development, similar to what was observed in mESC (Bilodeau et al., 2009). It was recently reported that SETDB1 maintained the high level of DNA methylation and low level of histone acetylation to shield chromatin from excessive CTCF binding at the boundaries of topologically associated domains, which implicates multiple gene regulation simultaneously. The increased insulation triggered by the excessive CTCF binding might explain why so many developmental-related genes undergo downregulation in the absence of Setdb1 (Jiang et al., 2017).

3.3 Requirement of Setdb1 for the establishment of H3K9me3

H3K9me3 are catalyzed by a family of SET-domain containing methyltransferases: Suv39h1/h2 and Setdb1. Endogenous retroviruses are marked with H3K9me3 mediated by Setdb1 in ESCs (Karimi et al., 2011; Matsui et al., 2010). Recently, intact ERVs are proven to be marked by Suv39h (Bulut-Karslioglu et al., 2014). These methyltransferases can also collaborate in a multimeric complex (Fritsch et al., 2010).

The minor change of H3K9me3 on ERVs in Setdb1 knockout DE cells suggest H3K9me3 can be compensated by other methyltransferases (Figure 2.11B). This is supported by the current findings that loss of either Setdb1 or Suv39h1/h2 leads to mild decrease of H3K9me3. But Setdb1/Suv39h1/Suv39h2 TKO leads to a strong decrease of H3K9me3 in livers (Nicetto et al., 2019). In contrast, the strong loss of H3K9me3 on ERVs in Setdb1 knockout XEN cells suggests that Setdb1 is a major methyltransferase in XEN cells (Fiure 2.11A).

3.4 Epigenetic control of repeats by H3K9me3 and DNA methylation

3.4.1 Chromatin silencing pathways involved in retroelements regulation

The accumulation of TEs in the host genome, although potentially dangerous for the genome integrity, serve as a pool of regulatory sequences and function as a substrate for evolution to shape the genomic architecture (Bourque et al., 2008; Frank and Feschotte, 2017). During early embryonic development, extensive DNA methylation changes and chromatin remodeling take place (Wu et al., 2016; Zhang et al., 2018). Due to the possibly harmful effects of the endogenous retroelements ability to transpose and integrate, cells developed an epigenetic regulatory system to control their activity in a balanced expression. DNA methylation and H3K9me3 are considered as predominant repressive marks control retroelements in differentiated cells and ESC, respectively. Moreover, H3K27me3, H4K20me3, active marks such as H3K4me3 and H3K27ac and other histone marks showed important control of retroelements under certain circumstance such as in the absence of DNA methylation and so forth.

This study compares the transcriptome feature upon Setdb1 deletion in XEN and definitive endoderm cells and also provides insight into the difference of retroelements regulation between early differentiated endoderm cells and ESC. A mild derepression of ERVK and ERV1 with minimal change of H3K9me3 in Setdb1 knockout definitive endoderm cells indicates a weak control of Setdb1 mediated H3K9me3 in differentiated cell (Figure 2.12B). This is consistent with the previously reported a remained repression in Setdb1 knockout NPC and MEFs (Bulut-Karslioglu et al., 2014; Matsui et al., 2010). However, they observed a lower level of H3K9me3 at ERV1 and ERVK in knockout MEF cells. This difference can be explained due to the fact that I used differentiated heterozygous knockout as control where they used wild type. As they have shown a Suv39h dependent H3K9me3 enrichment over intact and a subset of truncated ERVs, the incomplete loss of H3K9me3 could be due to the redundant H3K9me3 mechanisms mediated by Suv39h in definitive endoderm.

In contrast, ERVK including IAPs and ERV1 were strongly induced in Setdb1 knockout XEN cells associated with a strong decrease of H3K9me3 (Figure 2.12A). The varying ERVK and ERV1 expression from two types of endoderm cells raise the question which differences of the two types of endoderm cells lead to the dissimilar response upon Setdb1 deletion. I found several pluripotency related genes such as Klf4, Oct4 and Dppa family members still highly expressed in XEN cells (Figure 2.6B). PCA analysis showed XEN cells were closer to ESC compared with definitive endoderm cells (Figure 2.6A). One possible explanation is that the incomplete shut down of the pluripotency network may keep the ERVs under the control of H3K9me3 in XEN cells. Since these ERVs remain repressed in Dnmt TKO ESC but are

significantly induced in mESC depleted with Setdb1 or Trim28 (Karimi et al., 2011; Matsui et al., 2010; Rowe et al., 2010), Setdb1 seems to be the primary enzyme in silencing ERVs not only in ESCs but also in XEN cells. Interestingly, when I looked at DNA methylation at IAPEz, derepression was accompanied with hypomethylation specific at IAP-GAG region (Figure 2.15B). As the derepression of IAPEz in Dnmt1 knockout embryo and Dnmt3L knockout testis suggests a dominant role of DNA methylation in silencing (Bourc'his and Bestor, 2004; Walsh et al., 1998). Our data could therefore reveal an important role of the Setdb1 mediated H3K9me3 in silencing through DNA methylation.

Neither of these two types of endoderm knockout cells showed a dramatic induction of MERVL (Figure 2.8A, B). However, MERVL ERVs were induced in the absence of G9a and GLP which were not required for ERV1 and ERVK silencing. The ERVL induction in Trim28 and HP1α/β knockout ESC, independent of Setdb1, may be a consequence of indirect effect through G9a/GLP (Maksakova et al., 2013). Eed and Ring1B knockout ES cells showed derepression of MLV and IAP retroelements associated with a reduction of DNA methylation of IAP. This indicates that H3K27me3 and the polycomb system contribute to the regulation of a subset of LTR retroelements (Leeb et al., 2010). In line with previous observations, a recent study showed accumulation of H3K27me3 over the MERVL in the absence of DNA methylation suggests a role of H3K27me3 based repression. Moreover, they found ERVL silencing also strongly relied on Suv39h in ESC (Walter et al., 2016). Taken together, MERVL rely on the Suv39h but not Setdb1 mediated H3K9me3. H3K27me3 dependent control can be supplement to DNA methylation.

I found mild derepression of LINE1 elements such as L1Md_T associated with decrease of DNA methylation and minimal change in H3K9me3 in Setdb1 knockout XEN cells (Figure 2.12C). In contrast, LINE1 elements were tightly controlled in Setdb1 knockout definitive endoderm cells with no change of DNA methylation and H3K9me3 (Figure 2.12D). Up-regulation of LINE-1 coincides with DNA demethylation in mice early embryonic development, the link between DNA hypomethylation and transient up-regulation was not established (Fadloun et al., 2013; Molaro et al., 2014). Dnmt3L mutant testis showed strong LINE1 derepression suggesting the role of DNA methylation in LINE1 regulation in certain cell types (Bourc'his and Bestor, 2004). A latter study showed enrichment of Suv39h-dependent H3K9me3 over 5'UTR of LINE elements, and mild derepression in Suv39h dko mESC indicating the LINE1 repression depends on Suv39h (Bulut-Karslioglu et al., 2014). A recent study revealed an additional role of Setdb1 and polycomb complex (Eed) in controlling LINE1 repression, but only in the absence of DNA methylation under 2i condition. While, LINE1 expression was not changed in Setdb1 and Eed knockout ESC with a methylated genome

under serum/Lif condition (Walter et al., 2016). Together with our study, a global decrease of H3K9me3 at ERVs but not on LINEs in XEN knockout cells suggesting LINE1 regulation is independent of Setdb1 mediated H3K9me3 but dependent on DNA methylation and Suv39h mediated H3K9me3.

3.4.2 A dominant role of DNA methylation through the crosstalk between H3K9me3 and DNA methylation in ERV regulation

Various studies demonstrated the link between histone H3K9 methylation and DNA methylation as introduced before (Chapter 1.4.3). Since the promoter activity of 5' LTR has been tested by LTR-luciferase assay (Dewannieux et al., 2004) Moreover, in previous studies, UTR regions of mouse IAP retrotransposons have been proved to silence neighboring promoters in lentiviral reporter assays (Rowe et al., 2010). Accordingly, most of the studies focused on the IAP LTR region but found no dramatic decrease of DNA methylation upon loss of Setdb1 (Dodge et al., 2004; Matsui et al., 2010). Our lab showed that GAG2.22 (the SHIN, short heterochromatin inducing, sequence), a 160 bp sequence of mouse IAP retrotransposons, is sufficient to trigger silencing of the neighboring constitutively active promoters like the PGK and the EF1α promoter (Sadic et al., 2015). The findings suggest an important role of IAP GAG in silencing. Moreover, when I looked at the distribution of H3K9me3, it is more enriched at IAP GAG region than IAP LTR region (Figure 2.14A).

Therefore, I not only focused on IAP LTR but also of the IAP GAG region. The unchanged DNA methylation level of both IAP GAG and IAP LTR was accompanied with no change of H3K9me3 in definitive endoderm knockout cells indicating that the Setb1 protein is dispensable for DNA methylation maintenance (Figure 2.5C, 2.14A, 2.15B). Nevertheless, the mild decrease of H3K9me3 accompanied with maintained DNA methylation still able to repress IAPEz. This is contradictory with the previous observations that Setdb1 interacts with Dnmt3a for proper gene silencing (Li et al., 2006). Of note, the decrease of DNA methylation at IAP GAG in XEN knockout cells suggests that the DNA methylation of a specific region IAP GAG is dependent on the level of H3K9me3 (Figure 2.14A, 2.15B). Although the maintenance of DNA methylation at IAP GAG is impaired by the loss of H3K9me3 is unprecedented, it has been recognized that H3K9me3 is critical for DNA methylation maintenance (Rose and Klose, 2014; Zhao et al., 2016).

Since the loss of DNA methylation at promoter region enables transcription factor binding and gene transcription activation (Lorincz et al., 2004), I postulated the IAP derepression was caused by the decrease of DNA methylation at IAP GAG which impairs the heterochromatin

formation to trigger silencing in XEN knockout cells. Alternatively, IAP derepression could result from an overall decrease of H3K9me3 in XEN knockout cells. The pathways involved in ERV silencing in definitive endoderm cells remain unknown. ERVs may either repressed by DNA methylation as previous observations in somatic tissue (Li et al., 2019; Walsh et al., 1998), or by H3K9me3 mediated by Suv39 as previous observation in ESC (Bulut-Karslioglu et al., 2014). Analyzing the IAP expression in Dnmt1 knockout cells will further reveal whether loss of DNA methylation up-regulates IAP and if DNA methylation and H3K9me3 are reciprocally affected.

The IAP expression analysis of Dnmt1 knockout cells through the evaluation of mean fluorescence intensity showed strong induction of IAP in both XEN and definitive endoderm knockout cells. A comparable IAP expression in Dnmt1 knockout XEN cells and Setdb1 knockout XEN cells indicates that the loss of DNA methylation results in ERV derepression without knowing the H3K9me3 level in XEN cells (data not shown). Moreover, the induction of IAP in definitive endoderm knockout cells suggests a dominant role of DNA methylation in silencing ERVs in definitive endoderm cells (Figure 2.16). Of note, the Dnmt1 knockout cells, which were differentiated for 7 days but negative for Sox17, also showed increased expression of IAP (Figure 2.16A). This finding is supported by the study of Dnmt1 loss of function wherein IAP was only activated in Dnmt1 knockout cells upon differentiation which is negative in Oct4 expression (Hutnick et al., 2010). These data revealed that DNA methylation become important in IAP repression as soon as the ES cells exit pluripotency.

Previous studies have shown that H3K9me3 is enriched at hypomethylated region in breast cancer (Hon et al., 2012), but DNMT1 is required for maintenance of the H3K9me2/me3 in human HCT-116 colon cancer cells (Espada et al., 2004). However, I found that the depletion of Dnmt1 did result in a reduction of H3K9me3 at imprinted genes but not result in a reduction of H3K9me3 at IAP elements in differentiated endoderm and pluripotent cells (Figure 2.17). The latter result is in line with the previous observations that the level of H3K9me3 is not changed at ERVs in Dnmt TKO mESC and reversion from primed ESC to naïve ESC (Karimi et al., 2011; Walter et al., 2016).

Together, these data support the hypothesis that the loss of DNA methylation without disturbing H3K9me3 at IAPs results in derepression and further suggest a dominant role of DNA methylation in ERV silencing in both XEN and definitive endoderm cells. Together with the data from Setdb1 knockout XEN cells, the derepression of IAPs was a result of specific loss of DNA methylation at IAP GAG region.

3.5 Conclusions and prospects

Deletion of Setdb1 during endoderm differentiation results in a strong ERV derepression selectively in visceral endoderm knockout cells suggesting a different feature of visceral endoderm cells compare with definitive endoderm cells. This finding has elucidated a new feature to distinguish two similar types of endoderm cells (Nowotschin et al., 2019).

Secondly, the strong derepression of ERVs in Setdb1 ko visceral endoderm cells with a dramatic decrease of H3K9me3 and DNA methylation demonstrate the suppressive role of H3K9me3 through DNA methylation in ERV regulation. However, the minor ERV derepression associated with the less affected H3K9me3 and DNA methylation in Setdb1 mutant definitive endoderm cells revealed redundant cell type-specific H3K9me3 pathways. The low level of H3K9me3 could be maintained by redundant methyltransferases. This is in line with the findings that H3K9me3 is only strongly decreased upon loss of Suv39h1/h2/Setdb1 (Nicetto et al., 2019).

Thirdly, the loss of DNA methylation does not affect H3K9me3 level on ERVs, but results in ERV derepression in both Dnmt1 mutant visceral endoderm and definitive endoderm cells.

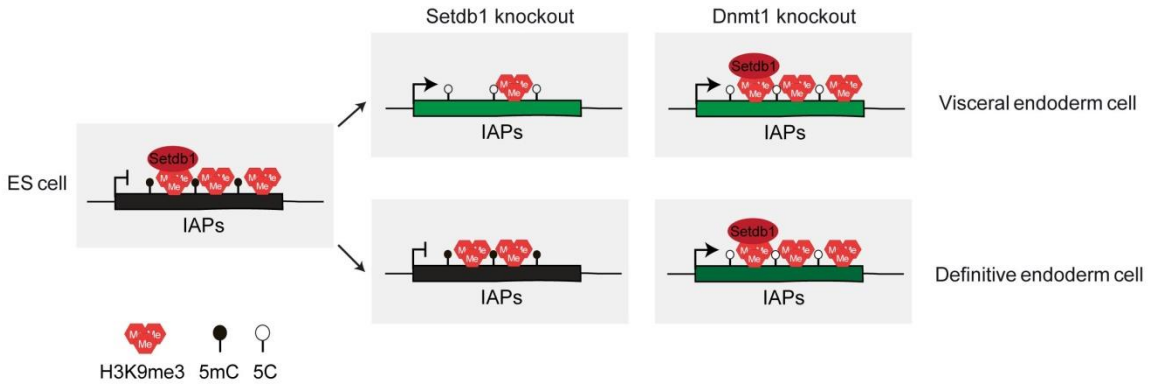

Figure 3 Model for ERV regulation in endoderm cells

Schematic depicts a dominant role of DNA methylation over H3K9me3 in ERV silencing during endoderm differentiation. Depletion of Setdb1 leads a less H3K9me3, thus impairs ERV repression in visceral endoderm differentiation but not for definitive endoderm differentiation. In contrast, depletion of Dnmt1 impairs ERV repression in both visceral endoderm and definitive endoderm differentiation although H3K9me3 is maintained.

This work provides a new feature to distinguish visceral endoderm from definitive endoderm, however, the cause of the different redundancies of H3K9me3 pathways in the two types of endoderm cells remain unclear. The difference in pluripotency-related and endoderm specific gene expression could be potentially helpful towards a better understanding of these two types of endoderm cells. The analysis of H3K9me3 levels on ERVs in triple knockout of

Setdb1/Suv39h1/Suv39h2 in visceral endoderm versus definitive endoderm would also help us to better understand these two types of endoderm cells.

Furthermore, based on the different IAP expression response to Setdb1 deletion in visceral endoderm and definitive endoderm, specific deletion of Setdb1 in endodermal derivatives such as liver could advance the knowledge of the contribution of visceral endoderm to embryonic endoderm organs and the different function of visceral endoderm descendants within endodermal organs.

Transposable elements are regulated by context-specific histone modification not only repressive marks but also active marks (He et al., 2019). The re-silencing of activated of IAP and LINE1 from the parental genome after fertilization is due to the loss of activating marks rather than the acquisition of conventional heterochromatic marks (Fadloun et al., 2013). The transposable silencing could be compensated by other histone marks such as H3K27me3 upon loss of DNA methylation in ES cells. Additionally, H3K27me3, which is usually considered dispensable in silencing retroelements, is critical in retroelements silencing upon loss of DNA methylation and Suv39h mediated H3K9me3 (Walter et al., 2016). Thus, studying the histone modification and DNA methylation interplay and combinational knockout of relevant proteins could unravel the redundant pathways involved in retroelements regulation.

In summary, the data of this work support a dominant role of DNA methylation in ERV silencing upon endoderm development. Moreover, Setdb1 mediated H3K9me3 control ERV expression through DNA methylation in visceral endoderm cells. Additionally, redundant H3K9me3 pathways were indicated in definitive endoderm cells. Besides that, further studies examining interplay of epigenetic modifications would give rise to a more specific understanding of retroelements regulation.

4. Material & Methods

4.1 Materials

4.1.1Tissue culture reagents

Name	Company
Dulbecco's Modified Eagle's Medium - high glucose	Sigma-Aldrich
Fetal Bovine Serum	Sigma-Aldrich
MEM Non-essential Amino Acid solution(100×)	Sigma-Aldrich
Penicillin-Streptomycin	Sigma-Aldrich
LIF	Homemade
Advanced DMEM/F-12	life technologies
Advanced RPMI 1640 Medium	life technologies
CTS GlutaMAX-I Supplement	life technologies
1 m HEPES Buffer Solution	life technologies
Insulin-Transferrin-Selenium-Ethanolamine (ITS - X) (100X)	life technologies
2-Mercaptoethanol	life technologies
Cytidine free base cell	Sigma-Aldrich
AlbuMAX II Lipid-Reich BSA	life technologies
Recombinant Mouse Wnt-3a Protein	R&D Systems = Biotechne
Recombinant Human/Mouse/Rat Activin A	R&D Systems = Biotechne
Trypsin(EDTA), 0.05 %	Thermo Fisher Scientific
DMSO	Sigma
Poly-D-Lysine	Sigma

4.1.2 Cell lines

Line	Type	Organism	generation	Plasmid
E584-4	wt pMEF	Mus musculus	-	
B70-1	Setdb1 con ES	Mus musculus	-	
B63-4	Setdb1 cko ES	Mus musculus	-	
B70-1	Setdb1 con XEN	Mus musculus	transduction	GS1579
B63-4	Setdb1 cko XEN	Mus musculus	transduction	GS1579
B70-1	Setdb1 con DE	Mus musculus	Chemical induction	
B63-4	Setdb1 cko DE	Mus musculus	Chemical induction	
293T	HEK	Homo sapiens	-	
J1	Wt ES	Mus musculus	-	
Dnmt1-ko	Dnmt1 ko ES	Mus musculus	-	

4.1.3 Kits

Name	Company
RNA Clean & Concentrator-25	Zymo research
SMART-Seq v4 Ultra Low Input RNA Kit for Sequencing	Clontech
MicroPlex Library Preparation Kit v2	Diagenode
Ultra II DNA Library prep kit for Illumina	NEB
DNEasy Blood and Tissue Kit	Qiagen
EpiTect Bisulfite Kit	Qiagen
Qiagen MinElute PCR purification Kit	Qiagen
Foxp3/Transcription Factor Staining Buffer Set	eBioscience

4.1.4 Antibodies

4.1.4.1 Primary antibodies

Antigen (species)	ID	Company	Purpose	Dilution
a-Tubulin(mouse)	220	Sigma Aldrich	Western blot	1:1000
GFP(Chicken)	284	Aves	Immunofluorescence intracellular staining	1:1000

H3K9me3(Rabbit)	249	Active Motif	ChIP-seq	3ug
IAP-GAG(Rabbit)	-	From Bryan R. Cullen	Immunofluorescence intracellular staining	1:1000
Setdb1(Rabbit)	074	Santa Cruz	Western blot	1:1000
Sox17(Goat)	291	Neuromics	Immunofluorescence intracellular staining	1:1000

4.1.4.2 Secondary antibodies

Antigen (species)	ID	Company	Purpose	Dilution
Donkey anti rabbit Alexa647	#6.3	Jackson	intracellular staining	1:500
Donkey anti Goat Alexa488	#9	Molecular Probes	intracellular staining	1:1000
Donkey anti rabbit Alexa 555	#17.2	Molecular Probes	Immunofluorescence	1:1000
Donkey anti Chicken Alexa488	#7.2	Jackson	Immunofluorescence	1:500

4.1.5 Primers and plasmids

4.1.5.1 RT-qPCR Primers

Name	Sequence 5´-3´
Gapdh-F	TCAAGAAGGTGGTGAAGCAG
Gapdh-R	GTTGAAGTCGCAGGAGACAA
Hprt-F	ATGAGCGCAAGTTGAATCTG
Hprt-R	CAGATGGCCACAGGACTAGA
Setdb1-exon4-F	AGCAGAACTCCAAAAGACCAGAAGC
Setdb1-exon4-R	TCTTGCCCAGAATCCGCATG
Sox17-F	GCTAGGCAAGTCTTGGAAGG
Sox17-R	CTTGTAGTTGGGGTGGTCCT
IAP-5'UTR-F	CGGGTCGCGGTAATAAAGGT
IAP-5'UTR-R	ACTCTCGTTCCCCAGCTGAA

4.1.5.2 Bisulfite sequencing primers

Name	Sequence 5´-3´	Reference
IAP-Gag-F	AGGTTAGTTTGTTGATTGGTTTTAG	(Sadic et al. 2015)
IAP-Gag-R	AATCAACAAAATAAACTCCCTAACC	
Illumina IAP-GAG-F	TACACGACGCTCTTCCGATCTAGGTTAGTTTGTTGATTGGTTTTAG	
Illumina IAP-GAG-R	CAGACGTGTGCTCTTCCGATCTAATCAACAAAATAAACTCCCTAACC	
LINE-1-F	GTTAGAGGATTTGATAGTTTTTGGAATAGG	(Tommasi et al. 2012)
LINE-1-R	CCAAAACAAAACCTTTCTCAAACACTATAT	
Illumina Line- F	TACACGACGCTCTTCCGATCTGTTAGAGGATTTGATAGTTTTTGGAATAGG	
Illumina Line- R	CAGACGTGTGCTCTTCCGATCTCCAAAACAAAACCTTTCTCAAACACTATAT	
IAP-LTR-F	GGTTTTGGAATGAGGGATTTT	(Rowe et al. 2013)
IAP-LTR-R	CTCTACTCCATATACTCTACCTTC	
Illumina IAP-LTR-F	TACACGACGCTCTTCCGATCTGGTTTTGGAATGAGGGATTTT	
Illumina IAP-LTR-R	CAGACGTGTGCTCTTCCGATCTCTCTACTCCATATACTCTACCTTC	
illumina P5 primer	AATGATACGGCGACCACCGAGAT	
illumina P7 primer	CAAGCAGAAGACGGCATACGA	

4.1.5.3 ChIP-qPCR Primers

Name	Sequence 5´-3´	Reference
Gapdh-F	CCATCCCACGGCTCTGCAC	
Gapdh-R	GCAAGGCTTCCGTGCTCTCG	
Polrmt-F	TCAGCAAACTCCAATAGCGCAC	
Polrmt-R	TTGCCGCACAACATGGACTT	
H19-F	AGCTTTGAGTACCCCAGGTTCA	
H19-R	GCCTCTGCTTTTATGGCTATGG	
IAP-LTR-F	GCTCCTGAAGATGTAAGCAATAAAG	

IAP-LTR-R	CTTCCTTGCGCCAGTCCCGAG	(Maksakova et al. 2013)
IAP-global-F	CGGGTCGCGGTAATAAAGGT	
IAP-global-R	ACTCTCGTTCCCCAGCTGAA	(Sadic et al. 2015)
IAP-GAG-F	CACGCTCCGGTAGAATACTTACAAAT	
IAP-GAG-R	CCTGTCTAACTGCACCAAGGTAAAAT	(Sharif et al. 2016)

4.1.5.4 Plasmids

Name	ID	Marker	Resistance	Vector purpose
psPAX2	GS183	None	Ampicillin	packaging lentivirus
pLP-ecoenv	GS811	puromycin	Ampicillin	packaging lentivirus
pLenti6/EF1a-GATA6-IRES-Puro	GS1579	puromycin	Ampicillin	stable expression

4.1.6 High-throughput sequencing libraries

sample name	ID	Experiment	Sequencing	Index
ES_B63-4-1st	GS364	RNAseq	50 bp SE	ATCACGTT
ES_B70-1-1st	GS365	RNAseq	50 bp SE	CGATGTTT
ES_B63-4-2nd	GS366	RNAseq	50 bp SE	TTAGGCAT
ES_B70-1-2nd	GS367	RNAseq	50 bp SE	TGACCACT
XEN_63-4-1st	GS368	RNAseq	50 bp SE	ATCACGTT
XEN_70-1-1st	GS369	RNAseq	50 bp SE	CGATGTTT
XEN_63-4-2nd	GS370	RNAseq	50 bp SE	TTAGGCAT
XEN_70-1-2nd	GS371	RNAseq	50 bp SE	TGACCACT
DE_63-4-1st	GS372	RNAseq	50 bp SE	ACAGTGGT
DE_70-1-1st	GS373	RNAseq	50 bp SE	GCCAATGT
DE_63-4-2nd	GS374	RNAseq	50 bp SE	CAGATCTG
DE_70-1-2nd	GS375	RNAseq	50 bp SE	ACTTGATG
DE_63-4-3rd	GS376	RNAseq	50 bp SE	GATCAGCG
DE_70-1-3rd	GS377	RNAseq	50 bp SE	TAGCTTGT
ES_B63-4-1st_H3K9me3	GS500	ChIP-seq	50 bp SE	CGATGT
ES_B70-1-1st_H3K9me3	GS501	ChIP-seq	50 bp SE	TTAGGC
ES_B63-4-2nd_H3K9me3	GS502	ChIP-seq	50 bp SE	ACTTGA
ES_B70-1-2nd_H3K9me3	GS503	ChIP-seq	50 bp SE	GATCAG
XEN_63-4-1st_H3K9me3	GS504	ChIP-seq	50 bp SE	TGACCA

XEN_70-1-1st_H3K9me3	GS505	ChIP-seq	50 bp SE	ACAGTG
XEN_63-4-2nd_H3K9me3	GS506	ChIP-seq	50 bp SE	TAGCTT
XEN_70-1-2nd_H3K9me3	GS507	ChIP-seq	50 bp SE	GGCTAC
DE_63-4-1st_H3K9me3	GS508	ChIP-seq	50 bp SE	ACAGTG
DE_70-1-1st_H3K9me3	GS509	ChIP-seq	50 bp SE	GCCAAT
DE_63-4-2nd_H3K9me3	GS510	ChIP-seq	50 bp SE	CTTGTA
DE_70-1-2nd_H3K9me3	GS511	ChIP-seq	50 bp SE	ATCACG
ES_B63-4-1st-IAP-GAG	GS448	Bisulfite-seq	300bp PE	AGTCAA
ES_B70-1-1st-IAP-GAG	GS449	Bisulfite-seq	300bp PE	AGTTCC
ES_B63-4-2nd-IAP-GAG	GS450	Bisulfite-seq	300bp PE	ATGTCA
ES_B70-1-2nd-IAP-GAG	GS820	Bisulfite-seq	300bp PE	GTCCGC
XEN_63-4-1st-IAP-GAG	GS452	Bisulfite-seq	300bp PE	GTCCGC
XEN_70-1-1st-IAP-GAG	GS453	Bisulfite-seq	300bp PE	GTGAAA
XEN_63-4-2nd-IAP-GAG	GS454	Bisulfite-seq	300bp PE	GTGGCC
XEN_70-1-2nd-IAP-GAG	GS455	Bisulfite-seq	300bp PE	GTTTCG
DE_63-4-1st-IAP-GAG	GS456	Bisulfite-seq	300bp PE	CGTACG
DE_70-1-1st-IAP-GAG	GS457	Bisulfite-seq	300bp PE	GAGTGG
DE_63-4-2nd-IAP-GAG	GS458	Bisulfite-seq	300bp PE	ACTGAT
DE_70-1-2nd-IAP-GAG	GS459	Bisulfite-seq	300bp PE	ATTCCT
ES_B63-4-1st-LINE	GS460	Bisulfite-seq	250bp PE	AGTCAA
ES_B70-1-1st-LINE	GS461	Bisulfite-seq	250bp PE	AGTTCC
ES_B63-4-2nd-LINE	GS462	Bisulfite-seq	250bp PE	ATGTCA
ES_B70-1-2nd-LINE	GS463	Bisulfite-seq	250bp PE	CCGTCC
XEN_63-4-1st-LINE	GS464	Bisulfite-seq	250bp PE	GTCCGC
XEN_70-1-1st-LINE	GS465	Bisulfite-seq	250bp PE	GTGAAA
XEN_63-4-2nd-LINE	GS466	Bisulfite-seq	250bp PE	GTGGCC
XEN_70-1-2nd-LINE	GS467	Bisulfite-seq	250bp PE	GTTTCG
DE_63-4-1st-LINE	GS468	Bisulfite-seq	250bp PE	CGTACG
DE_70-1-1st-LINE	GS469	Bisulfite-seq	250bp PE	GAGTGG
DE_63-4-2nd-LINE	GS470	Bisulfite-seq	250bp PE	ACTGAT
DE_70-1-2nd-LINE	GS471	Bisulfite-seq	250bp PE	ATTCCT
ES_B63-4-1st-IAP-LTR	GS478	Bisulfite-seq	250bp PE	AGTCAA
ES_B70-1-1st-IAP-LTR	GS479	Bisulfite-seq	250bp PE	AGTTCC
ES_B63-4-2nd-IAP-LTR	GS480	Bisulfite-seq	250bp PE	ATGTCA
ES_B70-1-2nd-IAP-LTR	GS481	Bisulfite-seq	250bp PE	CCGTCC
XEN_63-4-1st-IAP-LTR	GS482	Bisulfite-seq	250bp PE	GTCCGC

XEN_70-1-1st-IAP-LTR	GS483	Bisulfite-seq	250bp PE	GTGAAA
XEN_63-4-2nd-IAP-LTR	GS484	Bisulfite-seq	250bp PE	GTGGCC
XEN_70-1-2nd-IAP-LTR	GS485	Bisulfite-seq	250bp PE	GTTTCG
DE_63-4-1st-IAP-LTR	GS486	Bisulfite-seq	250bp PE	CGTACG
DE_70-1-1st-IAP-LTR	GS487	Bisulfite-seq	250bp PE	GAGTGG
DE_63-4-2nd-IAP-LTR	GS488	Bisulfite-seq	250bp PE	ACTGAT
DE_70-1-2nd-IAP-LTR	GS489	Bisulfite-seq	250bp PE	ATTCCT

4.2 Methods

4.2.1 Cell culture

B63-4/B70-1 mESCs (Setdb1$^{flox/flox}$; Sox17$^{2A\text{-}iCre/+}$) were thawed on gamma-irradiated feeders and maintained undifferentiated in ES medium based on DMEM (D6429, Sigma) containing 15 % FCS (F7542 Sigma), mLIF (self-made), 5 ml non-essential amino acids (M7145, Sigma), 5 ml Penicillin/Streptomycin (P4333; Sigma), and 1 ml 2-mercaptoethanol (Gibco, 31350-010).

In vitro differentiation of the mESCs towards definitive endoderm was carried out in monolayer on FCS coated dishes. The cells were two times pre-plated to deplete mouse embryo fibroblast feeder cells (MEF). On the day of differentiation, 0.1 million of mESCs were seeded on gelatine coated a 6-well plate directly in endoderm differentiation medium (EDM) consisting of 500 ml Advanced DMEM / F-12 (1x) (Gibco/LifeTechnologies; 12634-10- 500 ml), 500 ml Advanced RPMI 1640 (1x) (Gibco/LifeTechnologies; 12633-012- 500 ml), 22 ml GlutaMAXTM – I CTSTM (Gibco/LifeTechnologies; 12860-01- 100 ml), 200 µl AlbuMAX 100mg/ml (Gibco/LifeTechnologies; 11021-029 100g, 22 ml HEPES 1M (Gibco/LifeTechnologies; 15630-056- 100 ml), 70 µl Cytidine 150 mg/ml (SIGMA; C4654-5G), 0,9 ml ß-Mercaptoethanol 50mM (Gibco/LifeTechnologies; 31350-10- 20 ml), 12 ml Pen/Strep (10000U/ml) (Gibco/LifeTechnologies; 10378016 – 100 ml), 1 ml Insulin-Transferin-Selenium Ethanolamine (Gibco/LifeTechnologies; 51500-056-10 ml), supplemented with 2 ng/ml of murine Wnt3a (1324 WN-CF, R&D systems) and 10 ng/ml of Activin A (338-AC, R&D systems). Freshly prepared EDM supplemented with Wnt3a and Activin A was added every day. Cells were collected on day7 for FACS isolation (Cernilogar et al., 2019a).

In vitro differentiation of the mESCs towards extraembryonic endoderm was carried out in monolayer on 1 % gelatin coated dishes. The cells were carry on mouse embryo fibroblast feeder cells (MEF). On the day of differentiation, 0.2 million of mESCs were seeded on a gelatine coated 6-well plate directly in ES medium and then were transduced with ES medium containing 8 µg/ml polybrene and virus containing a lentiviral overexpression construct for (#1582 pLenti6/EF1a-GATA6-IRES-Puro) and centrifugation at 1000g for 1 hour at 34 degrees on the next day. Two days after transduction, cells were selected for GATA6 overexpression with 1

µg/ml puromycin. Five days after transduction, the ES medium was replaced with XEN medium consisting of Advanced RPMI 1640 (1x) (Gibco/LifeTechnologies; 12633-012- 500 ml), supplemented with 15 % FCS, 0.1 mM β-mercaptoethanol and 1 % penicillin-streptomycin. Cells were collected on day7 for FACS isolation.

4.2.2 Virus production for transduction

5*10^6 of 293T cells were seeded onto 10cm dishes and transfected by calcium phosphate transfection mix containing Cacl2 solution, HBS, packaging plasmids and overexpression construct. Change the fresh medium 6 hours after the transfection. Virus was collected 30 hours post transfection.

4.2.3 Immunofluorescence microscopy

The medium was aspirated and 7 days differentiated cells were carefully washed once in 1 mL of 1x PBS. Cells were fixed with 500 µL of 3.7 % formaldehyde (Carl Roth) in 1x PBS for 10 min at RT, followed with two times of wash in 1 mL of 1x PBS for 5 min and permeabilized with 500 µL of 3 mM sodium citrate tribasic dehydrate (Merck), 0.1 % v/v Triton X-100. Permeabilized cells were washed twice in 1 mL of washing solution 1x PBS and twice in washing solution containing 1x PBS, 0.1 % v/v Tween 20, 0.2 % w/v BSA for 5 min. The blocking was performed with 300 µL of blocking solution containing 1x PBS, 0.1 % v/v Tween 20, 2.5 % w/v BSA for 30 min. The primary antibody incubation was performed overnight at 4 °C with 200 µL of blocking solution containing the primary Ab in the dark. The plate was warmed to RT for 30 min on the next day and stained cells were washed three times with 1 mL of washing solution for 10 min. The secondary antibody incubation was performed with blocking solution containing secondary Ab and 10 % normal goat serum (Dianova-Jackson Immuno Research) at RT for 1 h in the dark. After washing three times in 1x PBS, 0.1 % Tween 20 for 10 min, cells were imbedded in Vectashield with DAPI (Vector Laboratories). The immunofluorescent staining was examined with Axiovert 200 M inverted microscope for transmitted light and epifluorescence (Carl Zeiss Microscopy) with the help of the AxioVision Special Edition Software (Carl Zeiss Microscopy).

4.2.4 Fluorescence Activated Cell Sorting

For RNA-seq, ChIP-seq and Bisulfite amplicon sequencing, *in vitro* cultured cells after trypsin treatment were resuspended in PBS with 0.2 % FCS before FACS collection. Cells from *in vitro* culture are sorted into 0.2 % FCS in PBS, then pellet for following step. For ChIP-seq cells, after FACS collection, were fixed for 10min at room temperature with 1 % Formaldehyde and quenched with 0.125 M final concentration glycine. For ChIP-qPCR cells, after FACS collection, were fixed for 30min at 4 degree with 1* Foxp3 fixation/permeabilization buffer (life technologies; 00552300) and washed with PBS. FACS was performed with a FACSAria instrument (BD Biosciences). Data were analyzed with FlowJo software.

4.2.5 Protein extract

Whole cell proteins extracts were prepared by resuspending 1 million cell pellets in 40 ul of freshly prepared lysis buffer containing 50 mM Tris/HCl pH 7.5, 2 % w/v SDS, 1 % v/v Triton X-100, 1 mM PMSF, 0.5x Roche Complete Protease Inhibitor Cocktail. Samples were vortexed for 10 s at max speed and boiled for 10 min at 95 °C. After incubation with 1 ul of Benzonase +2.5mM Mgcl2 at 37°C for 15 min, protein extracts were mixed with 12 µl 4x Laemmli-Sample buffer (Roth) and boiled again for 5min at 95 °C. The boiled protein extracts are ready to load.

4.2.6 Quantification of RNA levels

PCR was carried out with the Fast SYBR Green Master Mix (Applied Biosystems) in a LightCycler480 (Roche) according to the Fast SYBR Green Master Mix-protocol. Primers were evaluated for generating a single PCR product and for linear amplification in a wide range of DNA template dilutions. Every PCR-reaction was performed in a total volume of 10 µl in duplicates, triplicates or quadruplicates in a 384-well LightCycler plate (Sarstedt). Two independent control genes (Gapdh and Hprt) were used as reference genes for qRT-PCR experiments and geometric mean of reference Ct values was used as normalization as described by others (Vandesompele et al., 2002). For qRT-PCR of repetitive regions like IAP elements,

negative control samples that were not treated with reverse transcriptase were used to control for genomic DNA background. Ct-values were generated by the LightCycler480-Software (Roche) using the 2nd derivative max function and fold changes were calculated using the 2 –ΔΔC method.

4.2.7 Western blot

The boiled protein extracts were separated through SERVAGel TG PRiME 4-12 % precast SDS Page (SERVA Electrophoresis) in running buffer containing 25 mM Tris, 200 mM glycine, 1 % (m/v) SDS at RT for 1 h and 25 mA per gel. They were blotted onto methanol activated-PVDF membranes in a wet-blotting chamber (Bio-Rad Laboratories) containing blotting buffer 50 mM Tris, 40 mM glycine, 10 % v/v methanol, 5 µM SDS for 1.5 h at 4 °C and 400 mA. The blotting was performed at 400 mA under 4°C for 1.5 hours. Membranes were blocked with 2.5 % w/v BSA and 2.5 % w/v milk in 1x PBS at RT for 1 h under mild agitation. Primary Antibody incubation was performed for 16 hours in blocking buffer at 4°C. After that, they were washed 3 times with PBST buffer 1x PBS, 0.1 % v/v Tween 20 for 20 min. Incubation with secondary Ab was performed in a dilution of 1:3000 in blocking buffer at RT for 1.5 h. The probed membranes were washed 3 times in PBST for 20 min. Based on the detection method, Immobilon Western Chemiluminescent HRP Substrate (Merck Millipore) was used for ECL method and IRDye 800CW Secondary Antibodies for LI-cor method. Chemioluminescence was detected in by ChemiDoc MP Imaging System with the Image Lab Software using ECL Western blot detection reagent (Amersham Biosciences) or by Li-Cor Odyssey Imaging System with the Image studio software.

4.2.8 RNA-Sequencing

Total RNA from three independent biological replicates of day0 and day7 cells was isolated using the RNA Clean & Concentrator kit (Zymo Research) including digestion of remaining genomic DNA according to producer´s guidelines. The Agilent 2100 Bioanalyzer was used to assess RNA integrity and only high-quality RNA (RIN > 8) was further processed for cDNA synthesis with SMART-Seq v4 Ultra Low Input RNA Kit (Clontech cat. 634888) according to the manufacturer´s instruction. cDNA

was fragmented to an average size of 200-500 bp in a Covaris S220 device (temperature 4°C; peak incident power 175; duty cycle 10 %; cycles per burst 200) for 5 min. Fragmented cDNA was used as input for library preparation with MicroPlex Library Preparation Kit v2 (Diagenode, cat. C05010012) and processed according to the manufacturer´s instruction. Libraries were quality controlled with Agilent DNA kit (Agilent Technologies) by bioanalyzer analysis. Before the bioanalyzer analysis, sample concentration was measured using Qubit. Deep sequencing was performed on Illumina's HiSeq 1500 sequencer at the Laboratory for Functional Genome Analysis (LAFUGA) within the Gene Center (LMU Munich) according to the standard Illumina protocol for 50bp single-end reads (Cernilogar et al., 2019a).

4.2.9 Chromatin immunoprecipitation of histone modifications

0.5 million FACS-sorted cells were cross-linked under mild agitation for 10 min at RT with 1 % formaldehyde (Thermo Fischer Scientific) in ES medium. Fixation was quenched under mild agitation for 5 min at RT with 125 mM of 2.5 M glycine in 1x PBS. Cells were washed twice with 1x PBS 10 % v/v FCS followed with 3 min centrifugation at 400 g. Cell pellets were lysed in 100 ul Buffer-B-0.5 (50 mM Tris-HCl, pH 8.0, 10 mM EDTA, 0.5 % SDS, 1x protease inhibitors -Roche) and sonicated in a microtube (Covaris; 520045) using a Covaris S220 device until most of the DNA fragments were 200-500 base pairs long (settings: temperature 4°C, duty cycle 2 %, peak incident power 105 Watts, cycles per burst 200). After shearing, lysates were centrifuged for 10min at 4°C, 12000 g and supernatant diluted with 400 ul of Buffer-A (10 mM Tris-HCl, pH 7.5, 1 mM EDTA, 0.5 mM EGTA,1 % Triton X-100, 0.1 % SDS, 0.1 % Na-deoxycholate, 140 mM NaCl, 1x protease inhibitors-Roche). 150 ul of sonicated chromatin was then incubated 4h at 4°C on a rotating wheel with 3 ug of H3K9me3 (Active Motif S.A.; 39161) antibody conjugated to 10 ul of magnetic Dynabeads Protein G (Thermo Fischer Scientific). Beads were washed four times with Buffer-A (10 mM Tris-HCl, pH 7.5, 1 mM EDTA, 0.5 mM EGTA,1 % Triton X-100, 0.1 % SDS, 0.1 % Na-deoxycholate, 140 mM NaCl, 1x protease inhibitors-Roche) and once with Buffer-C (10 mM Tris-HCl, pH 8.0, 10 mM EDTA). Beads were re-suspended in 70 µl elution buffer (10 mM Tris-HCl, pH 8.0, 10 mM EDTA, 1 % SDS) with 2µl RNase A (10mg/ml) (Thermo Fischer Scientific) and incubated for 30 min at 37 °C. Proteins were digested with 2µl Proteinase K (20 mg/ml) (Thermo Fischer

Scientific) for 1 h at 55 °C and 900 rpm. Crosslink reversal of immunoprecipitated DNA was carried out overnight at 65 °C and 900 rpm. Supernatant was transferred to a new tube. Another 30 ul of elution buffer was added to the beads for 1 min and eluates were combined and incubated with another 1 ul of Proteinase K for 1 h at 55◦C. Finally, DNA was isolated and purified with SPRI AMPure XP beads at a sample-to-beads ratio 1:2 according to the manufacturer's instructions (Cernilogar et al., 2019a).

4.2.10 ChIP-sequencing

Purified DNA was used as input for library preparation with Ultra II DNA Library prep kit for Illumina (Biolabs, cat. E7645S) and processed according to the manufacturer´s instruction. Libraries were quality controlled with Agilent DNA kit (Agilent Technologies) by bioanalyzer analysis. Before the bioanalyzer analysis, sample concentration was measured using Qubit. Deep sequencing was performed on Illumina's HiSeq 1500 sequencer at the Laboratory for Functional Genome Analysis (LAFUGA) within the Gene Center (LMU Munich) according to the standard Illumina protocol for 50bp single-end reads.

4.2.11 Bisulfite sequencing

Genomic DNA was prepared using the DNEasy Blood and Tissue Kit (Qiagen) and was bisulfite converted using the EpiTect Bisulfite Kit (Qiagen) according to the manufacturer's instruction. Jumpstart Taq polymerase (Sigma Aldrich) was used to amplify the IAP GAG region, IAP LTR region and a 200bp region of LINE-1. PCR primers for bisulfite-converted DNA were modified by adding illummina adaptors for library preparation based on previous studies (Rowe et al., 2013a; Sadic et al., 2015; Tommasi et al., 2012). The gel-purified amplicon were indexed and double stranded by amplified with index primers/universal PCR primers and illunina P5/P7 primers. Before amplification, the DNA was purified with SPRI AMPure XP beads (sample-to-beads ratio 1:0.8). Libraries were checked for quality control and correct fragment length with Agilent DNA kit (Agilent Technologies) by bioanalyzer analysis and concentrations were measured with Qubit dsDNA HS Assay Kit (Life Technologies).

Final sequencing was carried out on a MiSeq sequencer (2x300 bp and 2 x 250bp paired end) with v3 chemistry (Illumina).

4.2.12 Intracellular Staining

ES cells and 7 days differentiated cells after trypsin treatment were resuspended in 500ul of PBS containing 2ul of zombie aqua (biolegend, cat no.423101). Samples were incubated at RT for 15min in the dark. After the centrifugation at 400g at RT for 5min with additional 2ml of PBS, samples were votexed to completely dissociate the pellet. Fixation/Permeabilization was performed by adding 1ml of Foxp3 fixation/permeabilization buffer and pulse vortex. After 30min incubation at 4°C in the dark, samples were washed with 2ml of 1X permeabilization buffer and centrifuged for 5min at 400g and RT. The pellet was resuspended in 100 ul of 1X permeabilization buffer after a second wash and incubated with recommended amount of primary antibody for at least 30 minutes at RT in the dark. After wash with 2ml of 1X permeabilization and centrifugation, the pellet was resuspended in 100 ul of 1X permeabilization buffer and incubated with recommended amount of secondary antibody for 60min at RT in the dark. After two time wash with 2ml of 1X permeabilization buffer, cells were resuspended in 300µl of FACS buffer and ready to load on the FACS Aria instrument.

4.2.13 Flow cytometry analysis of the intracellular stained IAP expression

ES and differentiated cells were analyzed by flow cytometry using FACS Aria instrument (BD Biosciences) with the BD FACSDiva Software. Data were further processed using the FlowJo v10 Software. FITC-A channel (Sox17) was used to distinguish the differentiated cell from the undifferentiated cells. The fold change of mean fluorescence intensity of cells were calculated by dividing the intensity values of APC-A channel (IAP-GAG) from differentiated cells by the intensity values of APC-A channel(IAP-GAG) from the undifferentiated ES cells.

4.2.14 Chromatin immunoprecipitation of histone modifications

0.5 million FACS-sorted cross-linked cells fixed by 1* Foxp3 fixation/permeabilization buffer for 30min at 4°C were used followed the protocol of 4.2.9.

4.2.15 Bioinfomatic analysis of RNA-seq

RNA-seq single end reads were aligned to the mouse genome version mm10 using STAR (Dobin et al., 2013) with default options "--runThreadN 32 --quantMode TranscriptomeSAM GeneCounts --outSAMtype BAM SortedByCoordinate". Read counts for all genes and repeats were normalized using DESeq2 (Love et al., 2014). Significantly changed genes were determined through pairwise comparisons using the DESeq2 results function (adjusted p-value <0.01). The expression levels of different repeat classes was assessed using Homer through analyzeRepeats.pl with the repeats function. The repeat definitions were loaded from UCSC. Significantly changed ERV families were determined through pairwise comparisons using the DESeq2 results function (log2 fold change threshold=1, adjusted p-value <0.01). PCA analyses were done using the plotPCA function of the DESeq2 package. Bargraphs showing expression data for selected genes were plotted using ggplot2 with RSEM-normalized data (TPM = Transcript Per Million). Heatmap with differentially expressed ERV families was plotted with pheatmap using rlog-normalized expression values. Genes in the vicinity of solitoray ERVs were identified using GREAT.

4.2.16 Bioinfomatic analysis of ChIP-seq

ChIP-seq single end reads were aligned to the mouse genome mm10 using Bowtie with options “-q -n 2 --best --chunkmbs 2000 -p 32 -S”. The H3K9me3 enrichment of different repeat classes was assessed using Homer through analyzeRepeats.pl with the repeats function. The repeat definitions were loaded from UCSC. Correlation of expression and H3K9me3 changes for ERVs were plotted by log2foldchange of H3K9me3 enrichment over input versus log2foldchange of expression. Cumulative read coverage across IAP elements was calculated using coverageBed and normalized to the library size. Coverage profiles were plotted using ggplot2.

4.2.17 Bioinfomatic analysis of bisulfite sequencing

Bisulfite sequencing paired end reads were aligned using CLC Genomics Workbench. Methylation analysis of sequencing data was performed using QUMA: quantification tool for methylation analysis (Kumaki et al., 2008).

5. Abbreviations

5mC	5-methyl cytosine
5hmC	5-hydroxy methyl cytosine
aa	amino acid(s)
Ab	antibody(ies)
AML	acute myeloid leukemia
bp	base pair(s)
cDNA	complementary DNA
ChIP	chromatin immunoprecipitation
ChIP-qPCR	chromatin immunoprecipitation followed by quantitative PCR
ChIP-Seq	chromatin immunoprecipitation followed by high throughput sequencing
cKO	conditional knockout
CpG	cytosine nucleotide followed by a guanine in the 5’ to 3’ direction
DAPI	4',6-diamidino-2-phenylindole
ddH_2O	double-distilled water
DE	definitive endoderm
dKO	double knockout
DNA	deoxyribonucleic acid
DNAme	deoxyribonucleic acid methylation
Dnmt	DNA methytransferase
DNMTi	DNA methyltransferase inhibitors
dpc	days post coitum
E	Embryonic Day
EDM	endoderm differentiation medium
EGFP	enhanced green fluorescent protein
EGFP+	EGFP-positive
Epi	epiblast
ERV	Endogeneous retroviral elements
FACS	fluorescence-activated cell sorting/counting
FITC channel	fluorescein isothiocyanate channel (FACS channel detecting green fluorescence)

GAG	group-specific antigen
GO	gene ontology
H3K9me2/3	Histone 3 Lysine 9 -, di- or tri- methylation
H3K9MT	Histone 3 Lysine 9 methyltransferase(s)
HEK	human embryonic kidney cell line 293 transformed with the large-T-antigen of SV40 virus
HKMT	Histone lysine methyltransferase(s)
IAP	Internal A-type Particle
ICM	inner cell mass
IP	immunoprecipitation
IRES	internal ribosome entry site
kb	kilobases
Kap1	KRAB-associated protein 1 (alternative name for Trim28)
KO	knockout
LIF	leukemia inhibitor factor
LINEs	long interspersed elements
LTR	long terminal repeat (a big subclass of retrotransposons) or regulatory sequence element actually flanking the retrotransposon sequence
MBD	methyl-CpG binding domain
MEF	mouse embryonic fibroblast(s)
mESC	mouse embryonic stem cell(s)
MFI	mean fluorescence intensity
MLV	Murine leukemia viruses
mRNA	messenger ribonucleic acid
Oct-4	octamer-binding transcription factor 4 (Pou5f1)
ORF	open reading frame
p	flox allele
PCA	principal component analysis
PGCs	primordial germ cells
PrE	primitive endoderm
PTM	post-translational modifications
puroR	puromycin resistance

qPCR	quantitative polymerase chain reaction
rpm	rotations per minute
RNA	ribonucleic acid
RNA-Seq	RNA high throughput sequencing
rRNA	ribosomal RNA
RPKM	Reads Per Kilobase of transcript per Million mapped reads
RT	room temperature
RT-qPCR	reverse transcription quantitative polymerase chain reaction
shRNA	short hairpin ribonucleic acid(s)
RNA-Seq	ribonucleic acid-sequencing
SAM	S-adenosyl-L-methyonine
Setdb1	SET domain bifurcated 1 (also ESET)
SRA	SET and RING finger associated domain
TE	transposable element(s)
TINATs	Treatment-induced non-annotated TSSs
TKO	triple knockout
TRD	transcriptional repression domain
Trim28	Tripartite motif containing 28 (also known as Kap1, Tif1β)
TSS	transcription start site(s)
TTD	Tandem tudor domain
Uhrf1	Ubiquitin-like, containing PHD and RING finger domains, 1
VE	visceral endoderm
VL30	Murine retroviruslike elements
WB	Western blot
XEN	Extraembryonic endoderm stem cells

6. Acknowledgements

First of all, I would like to express my gratitude to supervisor Prof. Dr. Gunnar Schotta for giving me the opportunity to join his group and work on an interest project. During the last years, I have been grateful for your support and supervision of my thesis.

Special thanks go to Dr. Rui Fan for initiating the interesting project and being a helpful supporter when I started my PhD life. I would like to thank Dr. Filippo Cernilogar for the help of NGS experiments. I would also like to thank Maryam Kazerani and Lisa Richter for cell sorting.

I would like to thank all Schotta lab members as well as the whole Molecular Biology Department for scientific discussions and nice working atmosphere. I would like to thank Sophia Groh, Irina Shcherbakova and Helena Moreno for input and technical support.

I also want to sincerely thank Dr. Elizabeth Schroeder-Reiter from the IRTG Graduate Program for being more than a coordinator and excellent assistance during the PhD.

I would like to thank my friends especially Dr. Weihua Qin for her awesome friendship and support.

Thanks to my parents for always supporting me to pursue my dreams. I would like to thank my wife Shanqi Han, who gave me strong support during my Ph.D. life.

7. Curriculum Vitae

The CV is not accessible in the public version.

8. Appendix

Table 8.1 Deregulated genes in Setdb1^{END} XEN cells

gene_id	Log BaseMean	log2 FoldChange
Gabrr1	6.510126	8.460568
Gm1110	5.886285	8.025945
Cd22	7.527945	7.970298
Plb1	8.216506	7.969666
Mctp1	6.878955	7.73121
Pnliprp2	7.044962	7.647599
Tuba3a	8.634943	7.441105
Tuba3b	5.49374	7.39905
Nlrp4c	6.466601	7.262362
Slc44a5	5.129696	7.014653
Zfp558	8.857359	6.81113
Dpep1	4.112936	6.771291
Slc22a13	6.315237	6.723266
BC051019	7.245934	6.717613
Tsga8	5.671184	6.249988
Slc38a11	3.281255	6.153185
Olfr1372-ps1	4.615274	6.063751
Bglap3	5.32699	5.956125
Asb12	3.103519	5.86823
Cd28	7.732398	5.825519
Megf11	6.909267	5.727183
Serpinb1c	3.972012	5.708467
St8sia6	5.256771	5.621887
Dpep3	4.702053	5.238378
Slc22a13b-ps	6.216491	5.113427
Emilin2	8.784642	5.084722
Gm5635	3.459267	5.061284
Zar1	6.491413	5.032551
Tmem158	9.009727	5.027732
4930428D18Rik	3.698208	4.93326
Btbd18	6.084091	4.902047
Wdr17	4.170609	4.879123
Neurog1	3.764423	4.840022
Slc47a1	4.874174	4.828101
Tex101	3.757657	4.822229
Angptl6	7.487172	4.806123
Ccdc172	3.563015	4.79893
Tgm3	4.033505	4.632836
Acaa1b	7.490888	4.625707
Cldn10	5.634787	4.597224
St6gal2	3.273014	4.597191
Gria4	4.820521	4.594281
Duoxa2	4.180067	4.584209
1700029P11Rik	6.588456	4.578655
Fkbp6	5.639763	4.546414
5330417C22Rik	3.748209	4.528125
Ptchd3	2.635315	4.508899
Ulbp1	5.673541	4.35695
Gm6682	5.602007	4.304566
F5	7.838094	4.303661
C130060K24Rik	3.055495	4.293825
Cyp2t4	1.87625	4.264858
Agmat	2.830745	4.224756
Sbspon	3.454912	4.223352
Gm4349	3.820998	4.211767
Gstp2	6.518899	4.180307
Gpat2	6.197806	4.135653
Pla2g5	6.892732	4.119789
Fam19a1	3.311025	4.108936
Gm5476	2.399501	4.107247

Tmem215	4.492064	4.085297
Tomm20l	2.722586	4.084538
Kcnf1	7.379888	4.017511
Mag	2.251539	4.004883
Gucy1b3	4.016681	4.004668
Nr2f1	2.273031	3.978837
C530008M17Rik	7.688844	3.977348
Reg1	5.501421	3.94568
A230065H16Rik	2.146065	3.944304
C630028M04Rik	3.287886	3.917726
Ceacam10	2.959097	3.894299
Rdm1	9.770175	3.880592
Rsph4a	4.668375	3.873911
H19	9.80087	3.856769
Tex12	2.826261	3.838582
Akr1c21	3.889805	3.829972
Zfp600	5.274137	3.82946
Gm5868	4.964684	3.823908
Gm4961	6.753517	3.816571
Fzd1	7.561247	3.811427
Rassf4	7.933539	3.79075
Gc	6.358678	3.789734
Il6	3.563113	3.736676
Pilrb2	7.932003	3.711426
Snrpn	3.082373	3.66516
Rbm44	6.342515	3.6613
Fibcd1	2.622591	3.6606
Nr3c2	5.258876	3.639688
Lat	6.027455	3.630217
2410088K16Rik	4.477523	3.622703
Rragd	10.24635	3.616744
Topaz1	2.541002	3.614751
AU022751	4.619082	3.611787
Ltk	6.003761	3.605257

Sycp3	7.799269	3.600049
Slc25a21	4.906424	3.595686
C330024D21Rik	5.186158	3.572795
Tmem87a	9.116247	3.543718
Padi3	7.678675	3.539281
Tmem74	2.757048	3.536428
Mov10l1	6.930207	3.51094
Tdrd9	2.653528	3.491409
Gareml	6.738721	3.489111
Duox2	2.445599	3.486834
Cxcl14	5.878123	3.483452
Tmprss12	4.814281	3.478456
Cox7b2	3.820285	3.477559
Tnfaip8l3	3.828848	3.468889
Sycp1	6.705508	3.463138
Adamts20	4.018046	3.447103
Cd209d	4.973439	3.441106
Cd6	4.509041	3.398312
Prr16	3.597868	3.392068
Eya2	7.761659	3.38726
Syde2	9.91632	3.381814
Speer7-ps1	3.093157	3.367691
Plbd1	8.628656	3.366438
Tex11	6.853695	3.346067
Lmo1	3.786878	3.312819
Col26a1	4.222488	3.310797
Slc25a31	5.491343	3.295501
Grin2c	4.937075	3.276256
Gpr150	3.300809	3.237607
Pnlip	3.520131	3.231609
Reg2	6.328716	3.212169
2810474O19Rik	12.17082	3.210707
Mael	6.853885	3.203252
Bin2	8.323656	3.198052

Tm6sf1	7.878529	3.186904
Apoh	2.813942	3.185601
Rhbdl2	3.436641	3.183451
4933416C03Rik	2.750037	3.174101
Them5	4.531133	3.170551
Zfp872	5.318542	3.17031
Acot1	6.141416	3.170151
Sectm1a	4.940506	3.16968
Tcfl5	8.17951	3.131577
Tescl	3.375262	3.118989
Sec1	6.746552	3.113026
Scml2	5.779996	3.106978
Gm10324	3.558809	3.08033
Pxt1	3.950234	3.078023
Dock2	4.356022	3.076293
BC052688	7.319661	3.048672
Scn3a	5.846371	3.045098
Adcy1	6.152459	3.040577
Grm4	5.38513	3.040276
Kcnk12	4.933961	3.034438
Zfp534	6.733398	3.026051
Entpd3	5.455075	3.02315
Nuggc	3.607179	3.021644
Tmem56	4.271305	3.019705
2310040G24Rik	4.124346	3.009108
2410076I21Rik	5.401243	2.998991
M1ap	6.152847	2.993372
Csrnp2	9.17048	2.992767
Tmem117	3.146036	2.98567
Gm10336	6.49557	2.977749
Plekhg4	4.776004	2.977387
H60b	5.021622	2.971609
Rln3	6.475977	2.966953
Clca4	5.627302	2.957046

Tbxa2r	4.72994	2.934671
Sidt1	5.231353	2.933332
Abo	3.550456	2.931104
Mtus2	5.639502	2.929932
Fut9	7.568385	2.926247
Ccnb1ip1	4.955917	2.916286
Gpm6a	5.929967	2.915853
BC068157	7.190861	2.91279
Tlx1	6.48547	2.89815
Zfp37	9.918421	2.897072
Slc2a10	6.896528	2.895087
2410141K09Rik	4.695354	2.889465
Best3	3.155335	2.876168
Sh3gl3	6.792751	2.867079
Hormad1	5.552793	2.865197
Gm13034	3.409828	2.834758
Gm13247	7.740004	2.824952
1810041L15Rik	5.164008	2.808893
Ano4	4.619459	2.792595
4933406J08Rik	3.278313	2.785287
Prkar2b	7.023217	2.7559
Defb36	6.566727	2.754546
Cd79a	4.105324	2.753696
Pnma5	6.932394	2.752099
Rtn4r	7.658951	2.750301
Akr1c13	8.40823	2.749989
Ankrd6	8.575718	2.738504
Stk31	7.260929	2.725678
Acyp2	4.970859	2.720653
Rasgrf2	5.451474	2.709745
Tfpi2	4.515954	2.7044
Fhit	4.987435	2.678791
Sema4a	6.844783	2.661423
4930433N12Rik	2.992631	2.661213

Sycp2	3.80225	2.652164
Ksr2	3.567714	2.652074
Mest	11.90381	2.648941
Tmem176a	5.541925	2.634677
Runx3	4.917828	2.632964
Ccdc85a	6.521863	2.631676
Mfn1	11.46796	2.625214
3830403N18Rik	5.190224	2.625131
BC021767	4.260087	2.616382
Prr19	6.443074	2.614855
Gm128	4.98102	2.609743
Pirt	4.670681	2.603283
H2-T23	7.57377	2.594814
Slc2a12	4.688465	2.594228
Amigo2	6.609966	2.59191
Serpinb6b	5.056118	2.588683
Fam159b	8.280349	2.580722
Pcdhga12	5.457851	2.578964
D1Pas1	7.194966	2.56572
Sec14l4	9.094591	2.55849
Klhdc7a	4.968718	2.540223
Catsperg1	4.293111	2.539757
Tktl2	4.187983	2.539192
Apobec2	8.435539	2.538697
Pkd1l2	7.095831	2.536288
Elovl2	6.796592	2.532259
Prrt3	5.035533	2.515413
H2-Oa	4.997436	2.507097
Pcolce2	7.796295	2.50047
Gm13154	8.157881	2.485039
Adm2	5.231246	2.479224
Tex19.1	10.56265	2.475568
Dmrtb1	5.283958	2.46806
Zfp709	6.324243	2.461156

Nalcn	4.03693	2.458509
Gm2382	5.36414	2.446709
Ube2l6	7.662847	2.440249
Ctsh	12.60331	2.438727
AI662270	8.64803	2.438083
Itga4	4.441657	2.436593
Cox4i2	4.788061	2.432289
Dhrs7	10.57015	2.414724
Nkx2-2	3.797784	2.41418
Fbxl7	5.255642	2.413669
Hsd17b1	4.597562	2.407674
Satb1	7.310945	2.403947
AW551984	6.038479	2.398587
Zfp385b	4.811166	2.39321
Tmprss11a	6.701585	2.392187
Wbp2nl	3.470088	2.383305
Gal3st3	5.888046	2.37761
C1rl	4.263038	2.359543
Cd38	9.739199	2.350277
Ubash3a	4.616817	2.344762
Osgin2	9.620441	2.342535
H1fx	8.46688	2.335783
Cyct	5.174267	2.334005
Pcsk9	9.537577	2.32598
Ncald	4.108249	2.32497
Tdrd12	9.264058	2.321781
Gfra1	6.540689	2.309608
Fuom	5.879747	2.301567
Stc2	8.366657	2.300459
Hdc	5.963242	2.29889
Gm13051	4.489155	2.291487
1700001L05Rik	7.635204	2.290981
Tex19.2	4.42959	2.289465
Foxa3	9.822692	2.280407

Wdr95	3.459778	2.266298
Psmb8	5.389834	2.260334
BC026585	6.434792	2.25922
Trim14	4.383683	2.242635
Inpp5d	9.411252	2.238393
Adad2	6.627121	2.227889
Got1l1	8.474988	2.226624
2410012M07Rik	5.2649	2.222041
Cilp2	6.98226	2.217627
Camk2b	6.861836	2.214267
H2-Eb1	3.956034	2.211348
Ccne2	10.14174	2.208825
Fsd1l	7.404443	2.194841
Dnah6	5.15847	2.18387
Smarca5-ps	4.183267	2.170208
2410089E03Rik	9.00187	2.166475
Chrnb4	6.779039	2.157679
Kcnk6	8.266789	2.157347
Ankrd46	11.18988	2.146536
Tas1r1	5.2946	2.145849
Fetub	5.433619	2.14143
Sox30	4.429104	2.139446
Fahd2a	7.657371	2.139108
Vegfc	5.627038	2.138695
Cdh4	6.686623	2.112344
Cpne8	7.358995	2.104345
Trim47	6.073263	2.103144
Tbx4	5.209959	2.096012
Rarres1	7.219236	2.092582
Pde3b	7.527699	2.089918
Sohlh2	6.37956	2.086332
Mfap2	7.923094	2.083483
Hbb-bh1	3.488904	2.079674
Batf3	4.273606	2.073631

Nhlrc1	3.566453	2.065553
Ly6a	6.762121	2.049227
Crlf2	9.012684	2.045451
Grb14	8.404711	2.045013
Abca1	9.258935	2.044754
Taf7l	6.329323	2.037254
Gpx7	7.059585	2.037142
Aoah	7.61993	2.036692
Mnd1	6.847824	2.035287
Nat8l	4.628585	2.034657
Nxnl2	4.29482	2.031595
Nell1	5.952167	2.027598
Tmem229a	3.684449	2.009862
Ttll9	3.733643	2.006022
Oasl2	5.890492	1.995444
Kcnb1	5.088234	1.994566
Morc1	8.823353	1.992419
Dlk1	9.479463	1.990681
Gm2381	6.188683	1.986526
Gm13242	6.226435	1.964092
Gnmt	5.779876	1.963703
Ddx4	9.327093	1.962074
Kcns3	8.331879	1.954416
Syce1	6.753921	1.953503
Acy3	6.561981	1.950455
EU599041	7.197201	1.941669
9430083A17Rik	5.359028	1.931733
Col9a3	8.951766	1.909144
Mcf2l	9.399227	1.904018
Mrc1	5.628309	1.902563
Zfp951	6.849478	1.901793
Zfp599	8.595041	1.900483
Mtr	10.29922	1.897342
Cnga3	5.632883	1.894951

Dock4	6.57521	1.893744
Aldh1l2	6.139535	1.886353
Urah	7.115743	1.885702
Cyp20a1	9.697377	1.880852
Jmy	7.38467	1.878381
Nfil3	7.779484	1.877554
Hdgfrp3	6.661301	1.87639
Piwil2	8.416625	1.865589
Lrrc3b	5.268476	1.859401
Cd8a	8.81254	1.856064
Atp10d	10.29289	1.839052
Zfp575	5.616182	1.830243
Fam109b	6.228014	1.829496
Slc7a4	6.11245	1.826399
Dnd1	6.817275	1.815487
Rab3ip	9.996104	1.815289
Npas3	4.390725	1.809035
Herc3	8.496823	1.802104
Rab26	5.520417	1.799129
Fmr1nb	8.987975	1.797
Slc41a2	7.629702	1.789183
Ripk3	7.893045	1.78725
Ube2e2	8.118172	1.784501
Atp12a	6.098287	1.784111
Ntf3	5.110561	1.777958
Spg20	10.75347	1.774029
Lipo1	7.152782	1.765876
Dppa4	9.413207	1.764505
Dnajb3	5.306631	1.760379
Gdf15	5.822537	1.755279
Mmp12	5.490927	1.752199
Slc29a4	7.941658	1.749835
Adora2b	6.253011	1.738519
Nkx6-1	6.241984	1.737418

2410004B18Rik	9.690972	1.735178
Stox1	5.083846	1.729771
Zfp418	6.605975	1.729363
Pnldc1	7.754942	1.726323
She	5.364818	1.719003
Gpc3	13.24918	1.717498
Gm13152	6.992086	1.697586
9130019O22Rik	6.4023	1.696384
H2-Ab1	7.111731	1.696179
Plekhn1	6.757328	1.693123
Emilin1	7.716228	1.6906
Clip4	6.434965	1.690504
Zp3	6.516197	1.687496
Sesn1	9.016701	1.687466
Map7d2	6.805315	1.687423
Pnpla3	6.970326	1.684492
Efna5	8.856386	1.682037
Tmem30b	8.666646	1.679033
Nmral1	7.621601	1.677246
Atf7ip2	6.463854	1.664498
Dnajc22	8.574949	1.664375
Itga8	5.232906	1.659446
Gm1673	5.83454	1.657629
Nipal1	4.303642	1.652473
Ahsg	4.411191	1.648194
Tenm3	8.881197	1.644789
Kirrel2	7.721709	1.643972
Csf2ra	7.924113	1.642753
2210016F16Rik	8.873834	1.641518
Iqcg	7.081574	1.635001
Ccdc36	5.951626	1.633356
Sptbn2	8.304115	1.633281
Comp	5.220008	1.629305
Evpl	7.169376	1.628355

Unc93b1	6.887409	1.619576
Farp2	5.384624	1.617628
Eng	9.213156	1.60528
Acad12	6.817364	1.601557
Pcsk6	7.72872	1.601129
Plch1	7.567095	1.588404
Dock11	9.222112	1.586603
Il3ra	7.664171	1.580252
Moxd1	6.607312	1.580023
Maea	11.63213	1.576899
Dppa2	8.494173	1.573901
Rpp25	9.475879	1.56367
Hck	7.611708	1.559297
Nefm	5.565539	1.558768
Adamts15	8.319525	1.554703
Tap2	6.626522	1.551431
Osbpl10	6.961736	1.54356
Ccdc112	7.921699	1.542263
Endog	7.284809	1.532527
Cables1	6.704041	1.528877
Col11a1	8.423894	1.528332
Smarcd3	7.962781	1.523741
Tnnt1	11.2072	1.523522
Zfp936	7.485868	1.513228
Sowahb	7.958236	1.507644
Stard3nl	10.56849	1.502083
Eci2	9.704402	1.498441
Tekt2	5.893724	1.491685
Cap2	5.967747	1.490705
Usp14	12.78168	1.487167
Slc6a9	8.162707	1.48444
Pls1	8.757767	1.479609
2810429I04Rik	5.517398	1.472069
Patz1	10.44038	1.471603
9030624G23Rik	6.570498	1.471456
Akr1c12	7.208818	1.46594
Slx4	10.25951	1.464914
Zyg11a	5.662492	1.460782
Tspyl3	5.648234	1.459364
Ccdc66	8.926532	1.458051
Degs1	12.6704	1.45639
Ppp1r14a	7.22111	1.455514
Peli3	6.422181	1.452947
Tmem38b	8.189627	1.449826
Cox6c	11.53748	1.449055
Ly6e	11.70836	1.444027
Gm7120	5.841761	1.441812
Car13	7.630902	1.436983
Fam221a	6.433998	1.43457
Zfp677	6.344814	1.430881
Qpct	7.187903	1.429653
R3hdml	6.626821	1.427686
Bhlha15	5.955765	1.420653
2700081O15Rik	7.100961	1.414216
Cyba	10.2948	1.411876
Prdm6	7.502397	1.410609
2610305D13Rik	10.36679	1.407524
Itm2c	11.72481	1.405416
A930004D18Rik	5.383553	1.403019
Ccdc126	8.337808	1.396809
Espn	10.06941	1.391901
Mrpl15	11.93667	1.386215
Slc16a2	7.136134	1.381154
Ptgis	8.709213	1.380404
St6galnac2	8.719833	1.379254
4930539E08Rik	5.6703	1.376787
Tmem185b	8.707858	1.370872
Csrp2	11.61662	1.369942

Dmc1	6.60566	1.366507
Acacb	8.690555	1.364805
Iqcd	5.558068	1.364584
Zfp873	7.573023	1.363609
Garem	7.84113	1.363002
Ppp2r3d	6.841127	1.359432
Zfp809	9.251754	1.347139
Il6st	10.66995	1.346944
Yy2	8.118665	1.339196
Car8	7.707961	1.338935
Pear1	5.894731	1.324661
Cul9	6.727343	1.321232
Rasal2	7.320155	1.320579
Sarm1	6.219889	1.320327
Aldh1l1	8.535254	1.316603
Arxes1	7.110105	1.315566
Nt5m	7.799448	1.314439
Apoc1	7.280424	1.308909
Fam129a	10.06574	1.308515
Id1	10.536	1.306722
Zfp747	7.722056	1.303707
Fancl	9.282598	1.303192
Spin1	10.71293	1.301422
Airn	5.754933	1.295107
Masp1	7.895559	1.294224
Slc4a4	5.700071	1.293231
Tarsl2	6.812157	1.291019
Gm10033	7.748071	1.288143
Lypla1	12.14649	1.278788
Ssbp2	7.346937	1.275621
Osbpl3	8.216997	1.27117
Mbd1	8.960706	1.268514
Homer2	7.240583	1.263259
Ankdd1b	7.766909	1.259377

B3galnt1	9.064309	1.253094
Tpd52l1	7.336777	1.249599
Trak1	9.423145	1.240254
Tmem17	6.541041	1.232502
Pfkp	11.44072	1.228094
Gatad1	9.777274	1.226719
Ece1	9.687169	1.220939
Ror2	9.048292	1.216708
Stbd1	7.63691	1.211188
Klc3	8.516555	1.202665
Fam134b	10.89438	1.19706
Mettl20	7.46612	1.196736
Prodh	7.922547	1.192296
Msantd3	8.988812	1.186862
Rnf17	10.26721	1.186578
Gm3604	7.909566	1.184035
Snx22	6.589721	1.181626
Ptpn18	6.192275	1.181087
Gulo	6.04937	1.161279
Ang	7.665478	1.157156
Epcam	12.12957	1.152497
Shisa2	10.73646	1.137581
Amn	9.14414	1.133293
Prkch	9.848183	1.131762
Commd4	11.14105	1.131416
Gpx3	12.87481	1.130773
Parp16	8.145518	1.130035
Nsmaf	9.819617	1.129562
Nadk2	9.268742	1.129557
Syne2	9.063736	1.129036
Epm2aip1	8.77455	1.128344
Oplah	10.72165	1.125729
Ccdc106	6.08402	1.122934
Cgnl1	9.02589	1.118128

Timd2	7.829676	1.114228
Dctd	10.363	1.111412
Ppargc1b	7.240189	1.11017
Zfp109	7.505063	1.107982
Trim24	10.34567	1.1056
Cwc27	10.2562	1.10412
Epb4.1l4a	9.354545	1.103248
Hmox2	9.292675	1.102988
Arxes2	8.594116	1.102784
Zfp612	7.547996	1.101507
Pxdc1	8.073384	1.096172
2810025M15Rik	9.370669	1.095803
Slc9b1	7.126121	1.093859
Sord	11.89812	1.091629
Fam78a	6.27026	1.091362
Tspan13	10.0353	1.085749
Rhoq	8.786568	1.07926
Abca3	9.075433	1.074624
Hpse	6.871334	1.073946
Trpm2	6.385642	1.068312
Id3	11.87068	1.06311
4930526I15Rik	7.482099	1.057803
Mical1	10.30262	1.056067
Hecw2	6.31581	1.055058
Rfc5	11.69977	1.052918
Triml2	9.743411	1.052325
E2f6	10.16637	1.042094
Lrrc8d	10.29172	1.040059
Tmem121	7.741935	1.039284
Arnt	10.99866	1.037045
Tcp11	6.871365	1.035974
5730507C01Rik	7.645543	1.03541
Ifitm2	10.99065	1.032883
Rab10os	7.910538	1.030197

P2rx4	10.23505	1.024039
Bckdhb	8.758007	1.023326
Drg1	12.56073	1.020412
Aplp1	10.76579	1.02041
Lxn	9.958299	1.0204
Alyref2	6.06849	1.015369
Actr3b	7.804855	1.011489
Zfp958	9.301339	1.006406
Klhl22	9.937114	1.006389
Dennd5b	8.24835	1.004347
Btbd6	8.247045	1.003835
Angptl4	7.666587	1.003334
Sp3os	6.811235	1.000639
Sntb1	7.239295	0.986485
Gstp1	11.59637	0.984604
Hsbp1	12.16913	0.979604
Uqcc2	10.49922	0.977554
Kif15	10.38054	0.976074
Thoc7	10.94094	0.973938
Slc1a4	9.993748	0.972431
Sptbn4	7.433666	0.971003
Optn	8.406901	0.969541
Lmbr1	7.256842	0.968783
Trp53inp1	11.59362	0.962669
Twsg1	11.61543	0.960595
Ndn	8.436354	0.957833
Creb3l1	10.21466	0.957674
Ell2	10.67454	0.952206
Jam2	8.460901	0.95023
Sgk3	9.123633	0.949266
Nod1	8.703184	0.947464
Ahcy	7.632113	0.942004
H2afx	11.44961	0.941926
Atf7ip	11.12662	0.928738

Slc38a4	12.31964	0.927936
Nfxl1	11.33184	0.927909
Cln5	10.10358	0.927324
Scamp5	10.34889	0.922634
Zfp654	8.393691	0.922079
Slc17a5	8.76341	0.921455
Pdpn	11.28814	0.919322
Nudt2	9.126904	0.917379
Asns	13.03534	0.916028
Yif1b	11.36347	0.908048
Apoe	14.50732	0.907477
Nxf7	8.791874	0.906263
2610524H06Rik	8.834604	0.902361
Zc3hav1	8.204071	0.901769
Tyms	11.05544	0.89956
Cd55	11.78621	0.895068
Osgepl1	9.088306	0.89413
Tgif2	8.790509	0.893346
1700030C10Rik	7.882149	0.892226
Klf10	11.22092	0.890732
Alkbh3	8.732557	0.886968
Spint1	11.36647	0.885097
Pcnt	10.95007	0.883686
Tfcp2	8.473445	0.88328
Psmg4	8.172522	0.880396
Cxxc5	9.373507	0.876043
Nxt2	7.434666	0.865777
Cblc	7.894455	0.865009
Dtnb	9.365211	0.864376
Gramd1b	8.735763	0.862761
Map10	6.671888	0.854178
Ldoc1l	8.564269	0.847613
Odf2l	8.781895	0.847045
Cdk19	7.834275	0.846542

Msh6	13.14145	0.845073
Xxylt1	10.08382	0.841415
8030462N17Rik	7.667967	0.829398
Pxmp2	7.030012	0.82616
Ermp1	9.986234	0.820125
Snapc1	9.572945	0.816824
Zfp808	7.615697	0.816803
Adat3	8.22931	0.813553
Cenpm	9.037065	0.813031
Gpr160	7.217641	0.810357
Sesn3	7.856679	0.808347
Zfp639	9.542546	0.806102
Msantd2	8.562978	0.805673
Ethe1	9.038661	0.803449
Arsk	7.004733	0.801524
Idnk	8.510353	0.798277
Ralgps2	10.01125	0.797292
Reck	8.936914	0.795964
Cox16	8.686275	0.79584
Glb1	11.18532	0.781292
Thg1l	7.640508	0.780525
Caprin2	8.547624	0.774619
Nck2	8.428505	0.773594
Shkbp1	10.34331	0.771125
Ppm1n	7.055914	0.765497
Panx1	8.300767	0.764374
Lrig3	10.28848	0.764128
Cggbp1	11.0404	0.762474
Gm13157	7.745174	0.758273
Cbx7	11.33399	0.754229
1110059G10Rik	7.711947	0.750752
Bex4	9.091655	0.749638
Chchd5	8.942963	0.73866
Colec12	9.027468	0.738598

Dscc1	8.660069	0.737914
Srek1ip1	8.471416	0.736185
Ska1	9.611684	0.736123
Mcm3ap	11.13759	0.727806
Plekhf2	11.10832	0.726819
Tcf12	10.00408	0.72609
Amn1	8.442726	0.725288
Marveld2	9.521345	0.724371
Nol11	11.40529	0.723384
Anapc7	10.19515	0.716836
Sh3glb2	10.04307	0.716024
Slc1a5	11.30633	0.704914
Itpkc	8.906358	0.704353
Tram1	12.54085	0.704331
Snx16	8.956641	0.701905
Hadh	11.55693	0.69995
Dnajc1	8.474844	0.692623
Uap1l1	10.28895	0.687138
Isoc1	9.947034	0.683275
Zfp707	8.151006	0.681633
Ormdl1	9.486386	0.681035
Tra2a	10.07168	0.677586
Papolg	9.456176	0.67674
Kdm6a	10.74931	0.67455
Coa7	9.666608	0.664729
1700021F05Rik	9.061678	0.664511
Kif21a	8.872793	0.651996
Reep3	9.445783	0.648919
Zmynd8	10.69238	0.644759
Tbc1d22a	9.097087	0.642732
Rhbdf2	11.13337	0.639132
Ccdc91	9.108912	0.638672
Rfc3	9.966004	0.638278
Fdft1	11.13717	0.63768

Srebf2	12.39219	0.635625
Acer3	9.106484	0.633292
Mfap3	10.70859	0.62864
Slc6a8	9.337894	0.626734
Ghitm	13.49613	0.622903
Pepd	11.06581	0.621526
Pdcl	10.58948	0.621307
1500011B03Rik	8.426201	0.620841
Asnsd1	10.78774	0.611535
Mta3	10.48128	0.607423
Pald1	10.77075	0.601629
Pick1	9.923841	0.587453
Rnf113a2	8.573554	0.582073
Ears2	8.53651	0.581524
Vcp	11.85674	0.569987
0610031J06Rik	11.78864	0.567061
Suv420h1	9.544301	0.564951
H2afj	9.941789	0.555332
Ubxn6	9.691324	0.54909
Ercc4	9.026015	0.547951
Pitrm1	12.07322	0.539283
B3glct	9.663501	0.538172
Dhx16	11.96944	0.537748
Slc35f2	9.696381	0.537561
Gpbp1l1	9.516326	0.523019
Taf1c	9.702289	0.522268
Dnmt3a	12.043	0.518383
Prmt5	12.53516	0.515753
Slc35f6	10.46972	0.512594
Ap3d1	11.74596	0.510036
Eef1g	10.55953	0.492402
Eif1ax	11.06015	0.488607
Ctps2	9.793737	0.483127
Gsr	11.64826	0.481626

Srfbp1	10.10109	0.47119
Msto1	10.67758	0.45923
Mina	9.652318	0.450892
Ube2q1	10.23941	0.446884
Trap1	11.69631	0.430647
Fam114a2	11.04949	0.42981
Mul1	9.259481	0.42875
Cul5	10.81092	0.381732
Mphosph8	10.22078	-0.35216
Bap1	11.97132	-0.35859
Actr1a	11.76344	-0.36122
Cops8	11.20042	-0.37877
Cdc25c	9.526241	-0.40444
Stambp	8.365306	-0.41143
Tmco3	9.777408	-0.42671
Rpap2	9.018552	-0.44333
Tm9sf1	10.92792	-0.45898
Acat2	10.79822	-0.47936
Pxk	10.03908	-0.48491
Pnn	11.14884	-0.49104
Slc25a17	10.41349	-0.49194
Ap3m1	10.21128	-0.50044
Zfp319	8.510687	-0.50298
Tmem263	10.28482	-0.50782
Rspry1	9.788907	-0.51871
Sufu	9.639346	-0.52155
Irak1	9.943491	-0.52286
Haus5	9.742353	-0.52298
Ipo4	11.58071	-0.52446
Tex264	10.43832	-0.52504
Cab39l	10.10121	-0.52872
Rdh11	9.548784	-0.53569
Katnb1	10.46724	-0.53824
Erlin1	9.464938	-0.54236
Smg9	9.3226	-0.54254
Mdp1	9.94475	-0.54306
Skp2	10.70023	-0.54451
Gorab	8.542826	-0.54539
Ctps	11.53363	-0.55051
Elf1	8.978981	-0.55105
Mavs	8.947978	-0.55195
Ccnd3	11.93182	-0.55287
Slc19a1	9.325387	-0.55499
Daglb	8.532304	-0.55968
Rrm2	13.2287	-0.56685
Smtn	10.87872	-0.56777
Ogfod1	9.114305	-0.56966
Chd1l	9.791044	-0.5718
Haus7	10.46553	-0.57183
Rpusd1	8.619196	-0.58163
Zcchc7	8.597633	-0.58393
Ergic1	11.33567	-0.5862
Zfp422	8.930195	-0.5876
Tspyl2	9.130751	-0.58795
Trabd	10.05912	-0.59014
Lrch1	8.21862	-0.59254
Usp40	9.125381	-0.59473
Tsr2	8.84627	-0.60399
4930427A07Rik	10.56492	-0.60806
Fam92a	8.728507	-0.60896
Cisd1	10.42724	-0.60938
Pctp	8.565211	-0.61286
Gramd3	9.554951	-0.61562
Tmem132a	10.37172	-0.61643
Rassf1	10.15718	-0.62176
Scoc	7.607342	-0.62199
Tagln2	13.03304	-0.62526
Cdc42se2	12.2504	-0.62686

Fgfr1op	10.72761	-0.6283
Pask	9.664005	-0.63225
Slc41a1	9.17505	-0.6338
Cnpy4	9.066353	-0.63678
Camk2d	8.978849	-0.63688
Rhobtb2	8.237841	-0.63723
Gfod2	9.07584	-0.64264
E2f8	9.748237	-0.6455
Dcaf11	10.66913	-0.64592
Msn	11.44294	-0.65137
Rad51ap1	9.56251	-0.65764
Gpsm1	8.895978	-0.66005
Tubgcp4	9.171161	-0.66012
Nnt	10.02988	-0.66149
Rusc1	8.966321	-0.66312
Tcf7l1	10.32382	-0.6644
Tdrd3	8.920986	-0.66545
4933411K20Rik	8.196996	-0.66722
Wdr1	12.67265	-0.66772
Tmem161a	10.3801	-0.67116
Pttg1	9.936681	-0.67193
Gramd1a	10.34574	-0.67413
Ccdc32	8.138217	-0.67857
Nsdhl	9.461015	-0.67996
Wdhd1	10.71158	-0.67998
Abhd6	8.601177	-0.68498
Tfdp1	11.56378	-0.69317
Tmem159	7.952947	-0.69357
Wdr41	8.504848	-0.69436
Sap18	8.322296	-0.69695
Diap3	8.994518	-0.69951
Ubac2	10.18618	-0.7073
Gja1	13.5932	-0.71328
Agpat5	12.20812	-0.71427

Rpa1	11.98813	-0.71472
Dnajc10	12.29638	-0.71487
Bin3	9.205038	-0.71589
G6pc3	9.951771	-0.7194
Gab1	13.00127	-0.71991
Fam64a	10.14164	-0.73048
Uchl3	10.20149	-0.73177
Marcksl1	12.43077	-0.7332
Phgdh	10.68009	-0.74258
Tmem147	10.24021	-0.74518
Ccdc137	8.980159	-0.74574
Cdkn2d	8.888228	-0.7471
Gpr180	10.05735	-0.7486
1700030K09Rik	8.051869	-0.74867
4930503L19Rik	8.496117	-0.74894
Phf20	9.722877	-0.75971
Senp7	7.269038	-0.76151
Pcbp4	12.09111	-0.76486
Alg12	8.704387	-0.7649
Tirap	8.930742	-0.76699
Hspb11	7.391241	-0.76834
Arntl	9.338541	-0.76935
Pdlim7	11.53199	-0.77419
Dclre1a	8.697471	-0.77837
Tmem219	7.178487	-0.77842
Pea15a	11.13554	-0.78236
Fbxw5	9.883224	-0.78245
Cd82	7.376557	-0.78384
Tes	10.22585	-0.79033
Stard5	8.52794	-0.79103
Slc25a24	9.049558	-0.79214
Mob3a	10.56876	-0.7983
Bora	9.746098	-0.80068
Mtrf1	8.025724	-0.81043

Mtmr6	9.821949	-0.81386
Ift122	8.779519	-0.81442
Rnd3	10.60273	-0.81739
Lzts2	10.6639	-0.81744
Rap2c	8.990502	-0.83086
1110051M20Rik	7.894083	-0.83881
Madd	7.60959	-0.8401
Cyb5b	12.21109	-0.84529
Arf2	9.448771	-0.84636
Papss1	10.08604	-0.84796
Cald1	10.80911	-0.84859
Rpgrip1l	7.31622	-0.84886
Rtn2	7.779709	-0.85921
Galnt7	9.434723	-0.85962
Speg	8.344958	-0.86143
Palld	10.54448	-0.86293
Gcnt4	6.68878	-0.86964
Gm2a	9.035816	-0.87223
Ids	8.608484	-0.8751
Dync2li1	7.484143	-0.87856
Lca5	8.080401	-0.88973
Ypel2	8.866243	-0.89165
Ggh	7.325039	-0.89403
Upp1	11.81927	-0.89561
Baiap2l1	9.301269	-0.89672
Clasp1	10.75815	-0.89754
Arid3a	9.540113	-0.89853
Mpp2	8.661171	-0.90206
Smyd4	8.110399	-0.90355
Mtm1	7.119417	-0.90432
Pex26	8.527312	-0.91276
Zfp473	9.415062	-0.91519
Pex11g	7.061188	-0.91739
Stx1a	7.462412	-0.91747

Tuft1	10.00753	-0.9202
Ap1g2	9.205207	-0.9212
Tctn2	8.587326	-0.9269
Porcn	9.484813	-0.9309
Zfp358	9.615263	-0.93113
Bcap29	8.672853	-0.93541
Kctd21	6.840758	-0.93662
Armcx2	9.19673	-0.93783
Dsg2	10.12263	-0.93802
Kifc3	9.213124	-0.93987
Cdh6	7.964436	-0.94313
Adamts9	8.273039	-0.95424
Thnsl1	8.800925	-0.95552
Hdac10	8.483758	-0.96135
Kcnk5	9.738106	-0.96318
Tbc1d19	9.054061	-0.96367
Wls	10.43883	-0.9692
Sdccag8	7.416302	-0.97486
Slc2a1	14.61466	-0.97769
Rhoa	11.4711	-0.97857
Aph1b	6.139872	-0.9809
Tcf19	8.05769	-0.98779
Nfkb2	9.226219	-0.98787
Rap1gap	7.88234	-0.98965
Slc22a17	9.16385	-0.99284
Chchd6	8.748597	-0.99577
Ift88	6.972491	-0.99691
Mks1	7.751858	-0.99852
Cd99l2	7.59284	-0.9994
Reep6	10.85134	-1.00901
Ipo5	13.38068	-1.01164
Slc44a3	9.177018	-1.0182
Timp3	10.8485	-1.01981
Ets2	9.184543	-1.02034

4931428F04Rik	8.017647	-1.02197
Ipp	8.355165	-1.02247
Fzd7	10.52551	-1.02447
Tmem43	10.78244	-1.02532
Vcl	11.7475	-1.0269
Ttc8	7.95461	-1.02706
Rabl2	8.530047	-1.02726
Slc44a2	10.81879	-1.02775
Pxmp4	7.859535	-1.0305
Gm4980	8.270346	-1.03087
Efcab7	7.185861	-1.03155
Asf1b	10.01738	-1.03436
D8Ertd82e	9.838487	-1.03449
Nr2c1	8.411891	-1.03599
Ramp2	7.883539	-1.04418
Sh3pxd2b	8.401235	-1.04631
Cited2	10.68291	-1.06371
Tmem109	10.1625	-1.06428
Ampd2	11.16288	-1.06792
2610015P09Rik	7.353786	-1.06877
Dhrs1	9.370828	-1.07065
Zfp579	6.610228	-1.0718
Selm	9.387532	-1.07654
Dcun1d4	9.736469	-1.07919
Slc7a8	9.937276	-1.09031
Cdk14	8.407366	-1.09314
Fblim1	11.82649	-1.09567
Mipol1	7.957566	-1.09652
Rgs19	9.563885	-1.10012
Nr4a1	9.191628	-1.10026
Tapbp	10.36261	-1.10656
Rnf219	8.576225	-1.11407
Ppp1r18	9.077885	-1.12161
5730559C18Rik	8.892276	-1.12831
Slc39a4	10.95844	-1.1289
Slc35e4	7.738961	-1.13011
Mdk	12.38455	-1.13447
Tmsb10	11.42786	-1.14521
Il1rap	5.871825	-1.15241
Ankle1	7.838215	-1.16151
Galnt11	8.485561	-1.16891
Tgfb1	8.562381	-1.17046
Myadm	12.36121	-1.17435
Itprip	7.897169	-1.17765
Abhd8	9.275985	-1.18043
Khk	6.311246	-1.18079
Ptges3l	5.890073	-1.18102
Sgk1	13.02941	-1.18594
Tfcp2l1	11.13894	-1.18905
Thtpa	7.638295	-1.19164
Pitpnm1	8.451732	-1.19201
Ccdc102a	7.90402	-1.20814
Msrb3	5.984673	-1.21005
2610318N02Rik	8.280532	-1.21057
Lgals1	10.34858	-1.21158
Hmgn5	8.189152	-1.21161
Nphp1	7.944846	-1.21442
Mob3c	6.085771	-1.21867
Prss35	8.895186	-1.2372
Tcl1	9.006846	-1.23961
Mapk11	7.378951	-1.25447
Kif24	7.965761	-1.25515
Gdpd1	9.387915	-1.25959
Enox2	7.346068	-1.26519
Abhd14b	7.271514	-1.27127
Igf2	12.67976	-1.27957
Kcnk1	10.12089	-1.29326
Epas1	10.96072	-1.30032

Trim68	6.371912	-1.30919
C8g	5.962092	-1.32304
Zc4h2	7.7067	-1.32444
Ankrd37	8.561768	-1.32599
Mxd3	7.159828	-1.33472
Wdr19	8.121624	-1.33676
Fggy	7.373203	-1.34005
Setdb1	10.57137	-1.34578
Syngr1	8.538281	-1.34738
Eml1	8.994878	-1.3494
Rrad	6.432434	-1.35611
Lrrn4	8.373146	-1.36176
Ccdc28b	7.46219	-1.36586
Cdca7l	8.835117	-1.37293
Tspan2	7.484593	-1.3803
Gng7	6.069002	-1.38191
Otub2	7.74143	-1.38833
Gstt3	8.060274	-1.39187
Pdrg1	10.10269	-1.39901
Tmc4	8.702798	-1.41897
Opn3	6.851816	-1.41905
Oscp1	6.508463	-1.42526
Dusp18	7.262194	-1.42666
Gatsl2	8.39414	-1.43048
Zfp286	5.547316	-1.43254
Itgb3bp	7.215183	-1.4371
Kalrn	7.215739	-1.44925
Spink3	12.66077	-1.47625
Enpp5	8.267595	-1.48576
Tnnc1	7.25421	-1.48904
Cd248	6.063089	-1.50544
Gstm7	5.286667	-1.5169
Uggt2	7.684125	-1.53116
Anxa6	10.97561	-1.53327

Kit	11.54559	-1.54736
Adamts1	8.783685	-1.55198
Irf2	6.028708	-1.55204
Ap3m2	7.225801	-1.56024
Nuak2	9.241929	-1.57949
Flna	13.28549	-1.58115
Car4	14.13332	-1.59092
Acsl6	5.903491	-1.59832
Raph1	8.299493	-1.60996
Fndc4	10.41283	-1.64394
Armcx3	5.536133	-1.65062
Apobec3	10.35209	-1.65921
Trim21	6.499734	-1.6676
St3gal4	7.075883	-1.68299
9530053A07Rik	4.811414	-1.69439
Ccnd2	9.824835	-1.70504
Dzip1l	7.13019	-1.74408
Tgfb2	7.242907	-1.76227
Wnk4	7.501381	-1.77576
Tmem108	7.075127	-1.78027
Tcf7l2	11.67012	-1.78106
Abat	5.893068	-1.87088
4933402E13Rik	6.569233	-1.87455
Cnn2	12.39465	-1.90643
Sh3bgrl	8.298422	-1.90778
Fut10	7.826725	-1.92965
Lrguk	4.424625	-1.93529
Tgfb1i1	8.420546	-1.95713
2810417H13Rik	9.658394	-1.98332
Ctgf	11.69966	-2.01149
Ccdc122	4.098416	-2.02973
Fkbp14	6.253032	-2.22391
Awat2	3.831097	-2.25148
Nxpe4	4.961206	-2.2983

Cd44	7.094047	-2.33678
Myl9	8.922092	-2.34787
Fam65b	4.536006	-2.3831
Hhip	6.71977	-2.38614
Drp2	6.782246	-2.49052
Tmem181b-ps	4.818119	-2.52363
Ptger3	3.629504	-2.68897

D730005E14Rik	4.131895	-2.83828
Ppp1r16b	7.242943	-3.00033
Wdfy1	10.18047	-3.67305
A2m	7.16927	-4.1605
Fn3krp	6.33349	-4.47686
Maml2	6.636041	-5.39002

Table 8.2 Deregulated genes in Setdb1^{END} DE cells

gene_id	Log baseMean	log2 FoldChange
H19	9.80087	7.260715
Ifi27l2a	7.454501	6.764082
Fmr1nb	8.987975	6.601552
Cd22	7.527945	6.49036
C330024D21Rik	5.186158	5.09344
Naip6	2.856722	5.0005
Ifi27l2b	7.386471	4.965766
Triml2	9.743411	4.956244
2010005H15Rik	4.487082	4.791796
Triml1	8.378377	4.753122
Naip5	3.579179	4.411213
Btn1a1	4.800979	4.398412
Slfn2	7.45434	4.374511
Rdh1	6.588094	4.345882
Fam19a4	6.037623	4.295547
Elmod1	4.999514	4.259183
Trpm1	3.611924	4.258796
Cdh9	2.721902	4.13509
Ttc29	2.903058	4.127007
Trap1a	10.3504	4.093454
4922502N22Rik	2.257871	4.072722
Slc2a13	2.140272	3.909099

Foxd3	5.363127	3.81452
Tex19.1	10.56265	3.752912
Rdh9	5.585348	3.680062
D6Ertd474e	2.623155	3.641955
Bcl11a	4.775226	3.566579
Dnaic1	4.779682	3.548811
Tsga8	5.671184	3.543215
Ptprb	5.85575	3.53439
Adra1a	2.557544	3.516684
Kcnu1	6.091603	3.502642
Nefh	7.263528	3.501525
Kcnk12	4.933961	3.473373
Tmem87a	9.116247	3.470615
Gm5868	4.964684	3.468213
Crybb1	1.890983	3.362138
Gm6682	5.602007	3.35537
Bglap3	5.32699	3.335105
AI662270	8.64803	3.324502
Agt	6.681525	3.300174
St8sia6	5.256771	3.29812
Rho	3.808702	3.269875
H2-M10.6	5.556956	3.269285
Akr1c12	7.208818	3.254438
Tmprss12	4.814281	3.230116

2410088K16Rik	4.477523	3.221274
9430021M05Rik	3.357559	3.211822
Gdf2	4.666394	3.15713
Zar1	6.491413	3.125115
Rims4	3.930734	3.118639
Igfbp7	6.205154	3.115817
EU599041	7.197201	3.104443
Gm13152	6.992086	3.086456
Mup6	4.982739	3.068982
Kirrel2	7.721709	3.064983
Timd2	7.829676	3.064533
Mogat1	5.245303	3.043424
Pou5f1	12.42141	2.983915
Slc35d3	3.358656	2.974078
Cyp2c65	3.304933	2.944741
Prr19	6.443074	2.936587
Rbp3	6.94005	2.932429
Nefl	9.477641	2.903729
Ackr4	6.551373	2.896349
Akr1c13	8.40823	2.875162
Ly6a	6.762121	2.856548
Fam84a	8.749158	2.846427
Defb36	6.566727	2.816757
Mrap	4.811752	2.810774
Cacna2d4	4.645028	2.804875
Capn9	3.35477	2.79444
Tnni3	9.341619	2.785001
Msc	5.73043	2.771544
Mapk10	3.649363	2.749554
Stxbp5l	6.343157	2.735079
Bcmo1	7.757164	2.711229
Hsd17b6	4.659212	2.710025
Slc45a1	5.252917	2.705765
Penk	8.023976	2.688217

C920025E04Rik	3.149817	2.680275
Gtsf1l	8.341642	2.661721
Mtmr10	9.958264	2.651791
Cib2	5.703331	2.648949
Sh3gl3	6.792751	2.635679
Osr1	3.65955	2.627893
Slc5a4b	4.558603	2.624771
C8b	4.094209	2.623976
Pcnxl2	4.731004	2.589768
E330020D12Rik	6.722748	2.586259
Syt4	4.329288	2.580945
Maged2	12.58567	2.556255
Hbb-bh1	3.488904	2.532573
Wnt2	4.399207	2.500042
Kng2	3.176417	2.498163
Gypc	4.723326	2.491553
Abcc8	7.440804	2.477964
Cd8a	8.81254	2.470352
Lrtm2	4.603038	2.45818
Trim31	6.029148	2.446937
Pnlip	3.520131	2.438815
Gm2373	9.503805	2.430268
Pgam2	7.500858	2.409199
Kcne3	4.056108	2.408976
Pdlim4	8.80942	2.407134
Rgs8	10.92356	2.398685
Pga5	14.87907	2.393611
Spock3	4.287443	2.388037
Padi3	7.678675	2.386127
Ghrl	6.271001	2.384563
Btn2a2	6.121735	2.367039
Amica1	5.96282	2.349242
Gm7120	5.841761	2.346243
Chsy3	8.105741	2.332954

Nod1	8.703184	2.31647
Pmepa1	9.123164	2.280085
Rnf39	9.395215	2.278065
Ly6e	11.70836	2.258806
Dok2	9.819656	2.248671
Gm10638	3.897511	2.23203
Ankrd35	7.600651	2.230069
Nefm	5.565539	2.210326
Dhrs7	10.57015	2.206679
Kcnh6	3.646932	2.19263
Rnf125	6.356646	2.185394
Creb3l3	6.069103	2.182387
Tmem158	9.009727	2.171701
Gfi1	5.338673	2.157924
Gstp1	11.59637	2.153634
Enho	6.620773	2.129185
Prr15l	7.184092	2.12611
Tcfl5	8.17951	2.124075
Zfp345	6.332381	2.120918
Hs3st5	4.676889	2.111043
Rasd2	7.131536	2.101128
Ngf	5.226524	2.098388
Lgals9	9.25601	2.088108
Fam134b	10.89438	2.079087
Gm973	4.238812	2.078782
Barhl2	4.819261	2.077642
Nkx6-1	6.241984	2.059115
Pcp4l1	5.944047	2.053448
Pkd1l2	7.095831	2.047571
Tnfaip2	5.86232	2.047104
Ulbp1	5.673541	2.035271
2510049J12Rik	7.270151	2.029994
Edn3	6.961539	2.019264
Pla2g5	6.892732	2.014035

Fam159b	8.280349	2.012655
4930552P12Rik	5.357357	2.002044
Crlf2	9.012684	2.000109
Ggct	8.505608	1.995142
Tspan5	10.59728	1.985667
Gm11744	4.455511	1.978662
Ppp1r14d	3.878749	1.971883
Col23a1	8.503473	1.951094
Sema5b	8.739517	1.949279
Nckap1l	8.661847	1.949177
Gchfr	5.156743	1.945072
Oaf	8.471431	1.943883
Proc	8.840521	1.940147
Abhd3	5.68767	1.938617
Fam151a	5.916139	1.937202
Ambp	6.814972	1.934742
Rtn4r	7.658951	1.91749
Ugt8a	5.644437	1.902012
Prph	7.248313	1.900876
Sez6l	4.692998	1.890715
Ube2ql1	8.303794	1.887296
Stmn3	5.314956	1.886104
5730507C01Rik	7.645543	1.884554
Fbxl7	5.255642	1.883824
Fuom	5.879747	1.877277
Apoa1	12.19495	1.873917
Brinp2	4.551686	1.871341
Cd59b	5.948584	1.870558
Nqo1	8.706406	1.858741
Aldh1l1	8.535254	1.84245
Ang	7.665478	1.830013
Folr1	11.24266	1.823791
Pde4d	7.960454	1.815398
Slc25a21	4.906424	1.808448

Tspan17	7.708768	1.795248
Rasgrf2	5.451474	1.790318
Ptprt	6.497549	1.786059
Abcg4	5.815487	1.783495
Cngb1	5.097847	1.780563
Tnfaip8l3	3.828848	1.776995
Acsm1	5.085846	1.771106
Ntn4	5.75474	1.755215
Ccdc154	5.24186	1.749648
2410003L11Rik	7.799928	1.747097
Crispld1	7.14104	1.743888
Tcf21	4.409031	1.735828
Gm2694	9.166294	1.735559
Fam81a	6.364962	1.731153
Dact2	7.547012	1.724601
Ephx4	6.243971	1.70977
Acad12	6.817364	1.702761
Itpka	5.682911	1.698917
Ffar4	7.440884	1.692264
Nrg4	5.36525	1.684299
Eepd1	7.603861	1.680529
Lypd6b	7.989617	1.67898
Gna15	7.862177	1.659885
Nell1	5.952167	1.656876
Fcgr3	6.953161	1.654092
Stat4	7.466765	1.652364
Kcns3	8.331879	1.635824
Aldh1b1	6.957524	1.635092
Sepp1	12.01055	1.635061
Cbln4	8.542979	1.63032
Oxct1	9.427227	1.629828
S1pr3	6.79915	1.629805
Slc25a29	6.181351	1.629353
Vat1l	4.618664	1.626096

Slc38a5	10.01676	1.612357
Hcn1	4.371065	1.610273
Glipr1	8.774276	1.605787
Ccdc65	4.354184	1.586027
Anxa9	6.420427	1.573577
H2-T23	7.57377	1.571214
Slc5a5	8.214507	1.567213
Mreg	10.32779	1.565163
Tmem238	6.391529	1.540599
Pycard	8.347135	1.535721
Slc41a2	7.629702	1.532695
Utf1	11.93314	1.527651
1010001N08Rik	5.736567	1.520247
Tubb3	9.885153	1.506964
Lhfp	8.048288	1.505988
Stard10	10.24187	1.503428
Cdkn2b	7.881211	1.498244
Slc18a1	7.323472	1.495516
Cyp2s1	9.744428	1.493276
P4ha3	5.224415	1.491828
Igsf11	5.159976	1.485658
Abtb2	8.986967	1.485
Ggt1	6.930556	1.478973
Ctsc	12.93257	1.476595
1700086O06Rik	5.082278	1.476582
Tcn2	12.04058	1.464884
Cacna2d3	8.786012	1.464796
Cyp2u1	4.916555	1.462132
Pgbd5	4.927377	1.459298
Zfp385b	4.811166	1.44834
Akr1c19	8.910081	1.443163
Bcl3	8.500109	1.441172
Fzd8	10.07661	1.433904
Abat	5.893068	1.43151

Vsig10l	5.611097	1.431271
Cbln1	8.66025	1.427142
Hnf1a	6.708229	1.425197
Bcl2l14	6.460957	1.416684
Kcnmb4	7.165113	1.412895
Sfrp1	12.57008	1.407239
2310009B15Rik	5.869486	1.404236
Cacnb4	5.117814	1.40421
Tst	6.870596	1.399634
B3gnt3	9.077895	1.398728
Lxn	9.958299	1.393009
1700030C10Rik	7.882149	1.3929
Ntm	7.542617	1.387933
Ticam1	7.77992	1.382836
Gm5595	7.889794	1.381654
Dlgap3	8.176222	1.380553
Trim32	10.56157	1.377785
Car7	5.346999	1.359639
Gpm6b	7.96882	1.356348
Ptger4	5.790279	1.354705
St3gal3	8.275216	1.354134
Cystm1	9.244631	1.352051
Tmem86b	6.246566	1.351632
Rfx2	7.558971	1.34913
Rbp4	12.56872	1.344542
L1td1	10.0761	1.343716
Hspb1	9.529564	1.340932
Dusp8	8.247146	1.322358
Neto2	7.00454	1.322213
2610305D13Rik	10.36679	1.318805
Slc35g2	8.292009	1.31791
Dnaja4	7.75967	1.315076
Ttc12	7.189008	1.314603
Tcp11	6.871365	1.308925

Rnase4	10.13656	1.304448
Paqr5	7.370483	1.303782
Sesn3	7.856679	1.299579
Enpp3	9.481728	1.298776
AI464131	9.433429	1.297144
Hdhd3	5.742456	1.295924
Sec14l2	10.611	1.295421
Pdia5	11.17064	1.293978
Ube2e2	8.118172	1.293614
AA414768	6.222897	1.292808
Mecom	6.55938	1.290386
Hipk2	8.901359	1.287089
Aes	11.53147	1.282928
Tacr1	6.28731	1.277908
Shisa9	5.647466	1.274075
Ell2	10.67454	1.272511
Tmem27	5.270486	1.272436
Atp10d	10.29289	1.267832
Tnfrsf21	10.69077	1.267143
Filip1l	6.684576	1.266829
Zfp58	8.126171	1.260784
L3mbtl3	8.979754	1.260459
Sap30l	8.723747	1.258379
Zfp42	11.27913	1.255519
Plxnd1	6.458733	1.252757
Stk32a	8.326284	1.25239
Fam210b	10.58092	1.250054
Dhrs11	9.175284	1.24661
Crip1	10.48762	1.245982
Arid3c	9.118409	1.245632
Cds1	8.31357	1.241316
Fbxo10	8.239579	1.237674
Nudt7	7.405073	1.236053
Lurap1l	8.615556	1.230316

Cox7a1	6.853251	1.228385
Pgap1	9.277983	1.226582
Serf1	8.160969	1.222654
Cdh4	6.686623	1.222613
Khdrbs3	7.284813	1.222594
Morn2	5.881154	1.222429
Mvb12b	8.343993	1.221206
9830147E19Rik	7.992524	1.217056
2310009A05Rik	7.224501	1.211324
Tle6	8.420247	1.207898
Blvrb	9.67463	1.205606
Tmem160	9.117822	1.195748
Pde9a	8.844871	1.195237
Birc3	7.01854	1.192314
Alkbh7	8.640137	1.190602
Snx18	10.82961	1.187616
Rab26	5.520417	1.183428
Zic5	5.929667	1.180563
Ctsh	12.60331	1.177751
Efna2	8.416341	1.177
Qpct	7.187903	1.176592
Tmem243	6.830713	1.176047
Jund	12.44856	1.16906
Map3k15	6.586405	1.167607
Otud3	7.002671	1.162662
Slc25a33	10.07744	1.159795
C1galt1c1	8.660283	1.158852
Hpcal1	9.733999	1.157497
Ahcy	7.632113	1.157313
Gsc	8.51182	1.155505
Derl3	7.040473	1.153145
Pde2a	7.438947	1.149967
Zfpm1	9.123427	1.149188
Uqcrb	10.18716	1.148342

LOC100503676	7.256248	1.145566
Ttc8	7.95461	1.144014
Rab6b	7.769166	1.139922
Ncam1	9.535538	1.139071
Ccdc85a	6.521863	1.138625
Map1lc3a	9.854906	1.136163
Gtf2ird2	6.774242	1.133251
Scamp5	10.34889	1.129212
Cited2	10.68291	1.127978
Phyh	10.03833	1.127198
Nfkbiz	7.615167	1.126002
Cd59a	10.5227	1.121289
Tmem98	9.180128	1.119259
Ak8	5.175894	1.116434
Calm1	14.16202	1.105859
Ethe1	9.038661	1.10362
Dmrta1	7.011797	1.102729
Ucp2	11.01997	1.102392
Espn	10.06941	1.101757
Hsbp1	12.16913	1.10058
Rap1gap	7.88234	1.099029
Idh1	12.08301	1.096569
Ankrd40	9.744467	1.09544
Cd38	9.739199	1.095382
Zfp672	7.264537	1.093033
Smagp	8.199568	1.091975
Fbxo6	9.949063	1.091019
8030462N17Rik	7.667967	1.090686
Fut8	9.864687	1.088196
Tex264	10.43832	1.085883
Acad10	8.072732	1.085551
Lipt2	6.638973	1.084323
Snta1	7.584812	1.084294
Trim62	6.525237	1.084144

Peli3	6.422181	1.08165
Fkbp1b	7.844134	1.077934
Btd	8.560977	1.076738
Rtn2	7.779709	1.074642
Dynlt1a	6.604802	1.074247
Cdc42ep3	7.337732	1.071025
Lgmn	12.90022	1.069735
Ppp1r14b	9.274822	1.069322
Gpx4	10.62572	1.065153
Hexb	10.22859	1.063477
2700089E24Rik	8.638591	1.061728
Shf	8.120356	1.057874
Trim26	11.3061	1.05637
Sord	11.89812	1.052903
Chchd10	11.61853	1.050379
Crtc3	7.439599	1.047327
Rab17	5.688344	1.045773
Tmem42	5.927995	1.044404
Sema6c	7.506725	1.042906
Gckr	9.532001	1.042335
Lipo1	7.152782	1.03904
Xxylt1	10.08382	1.033637
4930526I15Rik	7.482099	1.032392
Arhgap22	8.021683	1.029781
Vps37c	11.02579	1.028032
Commd4	11.14105	1.026077
Wnk3	9.278968	1.025827
Dbndd1	7.23147	1.01724
Cox6a1	12.31457	1.01515
Wsb2	9.964434	1.014908
Slc12a2	11.35281	1.014839
Mylpf	9.690429	1.010716
Kcnn1	8.954841	1.00963
Fam129a	10.06574	1.008695

Tulp1	8.756482	1.006262
Kcnk5	9.738106	1.005165
Dbndd2	6.923898	1.004046
Gcsh	12.60862	1.001539
Mpzl2	11.69222	0.998922
Sbk1	10.65962	0.99866
Rdh10	7.885421	0.997417
Gpr153	6.782482	0.9925
P2rx4	10.23505	0.989317
Rnf19b	9.64998	0.989263
Sp3os	6.811235	0.988525
Tprgl	10.63342	0.987722
Anxa4	10.52845	0.985316
Ccdc92	8.096952	0.984187
Chga	10.10842	0.981987
Pfkfb4	7.235386	0.980634
Dapk2	9.108489	0.980413
2610035D17Rik	6.600699	0.980357
Sppl2a	9.572008	0.979749
Rpp25	9.475879	0.97968
Atox1	11.43575	0.978498
Cib1	10.37502	0.97826
Pcsk9	9.537577	0.977028
Bdh1	8.529704	0.976516
Tox3	9.219169	0.974089
Cyb561d2	8.893134	0.973838
Ankrd9	6.813166	0.971567
Sec11c	8.800404	0.971367
Tnnt1	11.2072	0.970899
Crnde	7.68404	0.969585
Sec13	12.55691	0.967842
Tpgs1	8.978836	0.967494
Bloc1s1	8.972615	0.963358
Fth1	14.32666	0.960898

Ppapdc2	6.868695	0.960898
Rem2	8.104832	0.959536
Fam110b	7.812878	0.959119
Dab1	8.254153	0.952259
Alg14	8.787021	0.946633
Slc16a13	9.083418	0.945568
Creb3l1	10.21466	0.944355
Eps8l2	10.63137	0.941866
Dhrs4	9.658814	0.940281
Shb	8.649579	0.939882
Ldlrap1	10.39435	0.937632
Aplp2	13.51243	0.934916
Pld3	11.60944	0.934839
Samd3	7.784666	0.92687
Agfg1	11.47188	0.924477
Atg4d	9.600593	0.924073
Uros	8.342559	0.923912
Trp53inp2	9.964322	0.923769
Mvk	9.140223	0.923378
Mrpl20	10.79259	0.920553
2310039H08Rik	7.969313	0.920074
Fam96b	10.3844	0.917725
Foxa3	9.822692	0.914218
Gale	9.697146	0.914044
St6galnac2	8.719833	0.911691
Ctsl	14.44032	0.911627
Tuba1a	12.21882	0.911332
Ptger1	6.286994	0.911303
2810474O19Rik	12.17082	0.911178
Ovol2	9.142236	0.91013
Asap1	9.387435	0.909284
Mrpl33	9.971944	0.907801
Sephs2	11.66851	0.904059
Car4	14.13332	0.903959

1110001J03Rik	8.689487	0.903908
1110008P14Rik	8.802257	0.901295
Pink1	8.850657	0.899856
1700052K11Rik	6.648014	0.899146
Rnd2	7.303939	0.895722
Cox19	8.868113	0.894873
Coa6	8.487395	0.892489
Myeov2	9.630003	0.892268
Scly	8.29767	0.892129
Crat	8.964307	0.890968
Cdk2ap2	9.474455	0.889704
Cd55	11.78621	0.889665
Gabarap	11.73279	0.889448
Rhoc	10.98692	0.886988
Ubl5	10.61423	0.886681
Lamtor4	8.899709	0.885109
Uqcrq	11.32433	0.883504
Ccdc28a	7.070465	0.883257
Ppp1r11	10.04305	0.882488
Naa38	8.796322	0.882104
Ap5b1	7.188054	0.881745
Pigyl	9.325088	0.88141
Map1lc3b	11.57983	0.881072
Acat1	10.32724	0.880749
Map2k2	11.06296	0.880248
Iscu	8.737438	0.880115
Mesdc1	9.312338	0.877417
Gcat	11.1777	0.877275
Sec61b	9.960948	0.871643
Dirc2	9.557631	0.870609
Idh3a	12.063	0.869813
Rpp21	8.92997	0.865923
Mast1	6.975735	0.865496
Rxra	8.82653	0.864824

Ccdc23	8.749849	0.864085
Cdr2	8.972134	0.861537
Tmem256	10.43335	0.861456
Taf7	11.90882	0.861433
Ndufa3	10.43292	0.861424
Bag3	10.59701	0.859699
Prrg2	8.582404	0.859452
Syngr3	8.096472	0.859232
Ndufa12	9.169265	0.858681
Abhd17a	10.77678	0.858636
Pilra	8.993351	0.85738
Neil1	7.568939	0.854618
Spint1	11.36647	0.853702
Adipor1	12.39549	0.852865
Rwdd2a	6.740529	0.852796
Cdk5rap1	9.134249	0.852532
2610524H06Rik	8.834604	0.851695
Gucd1	10.44661	0.850617
Klc4	10.37051	0.849926
Tmem82	7.047569	0.849019
Pmm2	9.663778	0.848464
Sdhaf1	7.550986	0.847856
Slc44a3	9.177018	0.843982
Ndufb2	10.34576	0.843695
Tuba1c	10.57855	0.841381
Ino80b	7.83128	0.836201
Gemin7	9.633622	0.836078
Pbx3	7.706374	0.835666
Cltb	10.53507	0.835486
Hras	9.814016	0.832975
Tmem150a	10.60378	0.831751
2210016F16Rik	8.873834	0.830942
Adal	8.037098	0.830915
Ebp	10.2092	0.829191

Xbp1	11.78226	0.82906
Tusc2	9.511187	0.828127
Etfa	11.34336	0.826095
Ptdss1	11.41759	0.8254
Mrpl34	10.33128	0.825362
Slc25a10	9.912921	0.823542
9030624G23Rik	6.570498	0.823336
Aldh2	11.10989	0.823143
Pnrc1	10.38067	0.822882
Dapk3	9.848886	0.822091
Eme2	7.31005	0.822039
Scand1	8.862986	0.820746
Chchd7	8.544556	0.820114
Clcn2	10.14324	0.81884
Dpm2	9.442302	0.818552
Apoe	14.50732	0.815719
37316	8.91621	0.813272
Polm	8.070355	0.812215
Snx3	12.84743	0.810959
Vps26a	12.25775	0.809827
Cdk20	7.880334	0.804883
Dand5	6.651196	0.804284
Reep6	10.85134	0.804189
Selk	10.49303	0.802441
B3galt6	7.158167	0.801611
Msrb1	8.098224	0.801197
Smdt1	10.64049	0.79956
Nphp3	8.355058	0.791107
Slc27a4	8.469081	0.790219
Slc23a2	10.09121	0.788485
Acvr1	7.533095	0.786815
Dynll1	12.29685	0.785555
Tma7	9.056865	0.784094
Arl16	8.048479	0.780629

Bud31	10.04826	0.780424
Zfp809	9.251754	0.779959
Lpgat1	8.915465	0.777598
Casc4	9.34457	0.777471
Cdkn3	8.482393	0.776681
Pdlim1	10.93849	0.774044
Ndufb9	11.4465	0.773888
Znrd1	9.603518	0.772092
Dctn3	10.93738	0.771973
Hadhb	7.596319	0.771392
Cox4i1	13.47818	0.770883
Sirt7	8.635282	0.770607
Uqcr11	10.33103	0.770405
Hint1	12.3502	0.768884
Agtrap	10.65722	0.766094
Lrrc57	8.956292	0.765212
Gnptg	9.435127	0.764865
Atp5h	9.967933	0.764004
Ndrg2	8.426873	0.763207
Wars	12.41844	0.759204
Elovl7	9.519963	0.755616
Abcc10	8.451355	0.755042
Dxo	9.147789	0.754519
Tmem51	10.59101	0.752522
Rabac1	10.79614	0.752347
Saysd1	7.931551	0.751188
Mif	11.2663	0.750474
Spns1	11.4116	0.75008
Amacr	8.272984	0.74699
Manf	12.05884	0.746914
Galnt10	10.77011	0.746865
Ndufs8	10.89604	0.746398
Ikbip	9.796976	0.745582
Med29	8.363267	0.743706

Tango2	8.797033	0.743489
Mxi1	10.46989	0.741998
2010107E04Rik	10.52968	0.741362
Acaa1a	9.796774	0.740861
Slc35b1	10.90583	0.740614
Sec24d	11.48738	0.73999
Yipf3	10.24576	0.738638
Fam3c	10.49073	0.737198
Rit1	9.126662	0.735944
Man2b2	9.511745	0.733769
Smim13	8.018602	0.731528
Cox6b1	12.0536	0.730421
Sh3bgrl3	11.03149	0.730126
Tpst2	9.927803	0.72943
Tmem120b	8.312902	0.728618
Ten1	8.728625	0.726556
Ccdc84	7.358781	0.726448
Mien1	9.937303	0.721489
Bet1l	8.801808	0.716916
Atp1b1	10.79246	0.716842
Mesdc2	11.48863	0.715153
Tapt1	8.531847	0.715051
Rmnd5b	10.13367	0.714355
Med10	10.36839	0.712925
Tmem134	9.457832	0.71113
Atp6v0b	12.116	0.710503
Ppp2r5b	10.64874	0.707969
Sirt2	9.935164	0.70708
Kctd21	6.840758	0.705295
Sertad1	9.612145	0.705247
Ralgds	9.880608	0.704452
Mpc2	8.652816	0.70207
D8Ertd738e	11.00438	0.701031
Gskip	9.418682	0.699561

Pik3c3	10.19905	0.698862
Zc3hav1	8.204071	0.698574
Parp16	8.145518	0.696318
Ndufa4	11.87591	0.696138
Sys1	9.178249	0.695575
Cox8a	11.9305	0.695334
H2afj	9.941789	0.695236
Spsb2	7.731915	0.694984
Suds3	10.30686	0.694569
Agpat2	9.418772	0.694269
B9d1	7.913201	0.693435
Pafah2	9.09123	0.693223
Lrp10	11.17366	0.693015
Ndnl2	8.988245	0.692918
Tbc1d10a	9.910613	0.691984
Taldo1	12.25087	0.691568
Apba3	10.47766	0.690592
Ict1	9.959863	0.690105
Ano10	10.03112	0.689637
Bag1	11.13113	0.688872
Arrdc4	10.34617	0.686528
Tesk2	8.145697	0.685929
Abhd5	10.6116	0.685737
Fam83d	10.33223	0.683079
Ttpal	8.618704	0.682119
Lsr	12.04543	0.681686
Vcp	11.85674	0.68069
Dusp3	9.362111	0.680028
Anapc16	9.352811	0.680012
Nfyc	9.127094	0.678939
Cox6c	11.53748	0.678627
Cmpk1	10.49607	0.678617
Rab28	9.77492	0.677585
Reck	8.936914	0.676545

Dda1	11.4229	0.676493
BC004004	9.859352	0.676377
Dhcr24	10.30217	0.676156
Romo1	9.278604	0.675802
Mif4gd	9.874584	0.674088
Ubl3	10.19016	0.673551
Pacsin3	8.808271	0.673325
Gnpnat1	9.989699	0.673315
Trappc2l	9.484087	0.671646
Pex16	8.372344	0.671476
Tmco1	11.03466	0.671462
Pi4k2a	9.537118	0.671437
Edf1	10.91493	0.671342
Ppic	10.68283	0.668177
Gnas	13.57923	0.668124
Creld1	8.657889	0.667988
Pih1d1	9.660687	0.663581
Uqcr10	11.30178	0.66268
Dynlrb1	10.9049	0.66117
Ftl1	14.71586	0.660996
H3f3a	9.436838	0.657126
Zfp428	9.106552	0.656711
Cox5b	9.885577	0.654871
Bola3	8.360811	0.654761
Fbxo9	8.673425	0.652056
Rela	10.61564	0.651746
Arntl	9.338541	0.651565
Dpp7	9.12273	0.649979
Ndufb8	12.00761	0.649969
Adipor2	8.373991	0.647636
Wdr8	9.111997	0.647367
Dtd2	8.863396	0.646212
Timm10b	9.207689	0.645129
Dhcr7	10.17849	0.644293

Ufm1	10.04237	0.643595
Syap1	9.180319	0.640856
Dcbld1	11.32656	0.640274
Mad2l1bp	9.436938	0.640211
Lyrm2	8.449398	0.640032
Cyth3	9.839731	0.636468
Ap2s1	10.94438	0.635178
Zfp622	10.89244	0.635052
Eif1b	9.853417	0.634793
Ndufa11	10.93207	0.634488
Atg5	10.1552	0.631353
Cox5a	12.44888	0.630137
Dph3	10.13509	0.629156
St5	10.38802	0.628884
Rhoq	8.786568	0.626555
Bsdc1	10.00023	0.625014
B3gat3	10.19267	0.623391
Cd63	12.25055	0.622226
Stk38l	9.035369	0.620537
Nt5c	9.769518	0.62
Zdhhc12	10.35639	0.619956
Znrf1	9.448688	0.619073
Eif3f	10.72314	0.617931
Zdhhc2	9.146929	0.617246
Gramd1b	8.735763	0.616151
Gars	12.94502	0.61609
Ing2	9.035243	0.61552
Lpar6	10.0209	0.615107
Copz1	12.4703	0.613791
Atp6v0d1	11.80122	0.613313
Clta	11.48222	0.613113
Acot8	8.621277	0.612851
Dbnl	11.39415	0.610691
Lamtor1	10.58907	0.609014

Yif1a	10.5649	0.608748
Haus5	9.742353	0.608087
Clic1	13.11706	0.60768
Ptplb	9.486606	0.6072
Spint2	12.42806	0.60487
Polr2j	10.25981	0.604449
Nipsnap3b	10.753	0.602314
2310036O22Rik	10.97875	0.601016
Eapp	9.710081	0.59979
Arpc3	11.25244	0.599724
Ptms	9.768293	0.599689
Ppa2	9.839623	0.598907
Alg1	8.630027	0.597423
Ngfrap1	12.86988	0.596731
Drap1	10.13922	0.596533
Mlf2	13.12693	0.59556
Mknk2	10.43377	0.595494
Srd5a3	8.866434	0.593993
Vps28	10.80614	0.591821
Zdhhc9	10.30757	0.590359
Dedd2	8.685122	0.590268
Nagk	9.238702	0.588704
Ufc1	10.36664	0.588195
Scmh1	9.110711	0.585906
Psmd8	12.28708	0.581316
Dnlz	9.219764	0.581048
Znhit2	8.260254	0.580202
Bex2	10.39974	0.577539
Atp5d	12.48889	0.576804
Zfp213	8.665731	0.573655
Rab9	9.63676	0.572222
Frmd8	11.38122	0.569303
Ogfod2	7.958409	0.568595
H2afx	11.44961	0.567363

Gltp	10.98348	0.566456
Polr1d	10.17356	0.563783
Cuta	10.159	0.563197
Rnf10	12.14936	0.561361
Wbp1	9.598209	0.559707
Phpt1	9.707919	0.558677
Ezr	13.11584	0.556766
Pcyt2	10.36019	0.556534
Fkrp	8.619112	0.552583
Ccdc12	9.129414	0.55204
Higd2a	10.25255	0.551046
Pole4	10.01177	0.550456
Gba2	9.035895	0.549529
Gpatch1	9.68568	0.547896
Pik3cb	10.47418	0.54407
Pdcd2	9.382764	0.538006
Lyrm5	8.316491	0.532684
Tmbim4	10.18338	0.532129
Atp6ap1	12.17729	0.527634
Zfp707	8.151006	0.520461
Zfp511	8.829966	0.517642
Rusc1	8.966321	0.517278
Snap23	11.00863	0.515909
Zbtb7a	8.353533	0.513873
Mcee	8.245439	0.510704
Rmdn3	10.43192	0.510196
Srp14	10.65057	0.507933
Tmem147	10.24021	0.507338
Pmvk	9.928646	0.504598
Prmt2	9.783492	0.503161
Tex261	10.4078	0.49874
Epcam	12.12957	0.495177
Acadl	9.680781	0.494175
Kdelr2	11.44664	0.489171

Cpt2	10.21618	0.48472
Ric8	10.46294	0.483672
Mmp11	9.830975	0.482362
Mbd3	11.58241	0.479087
Sdf2	10.21217	0.477247
Acat2	10.79822	0.471209
Taf1c	9.702289	0.468734
Tmem50b	8.950346	0.466393
Zdhhc4	8.972261	0.454813
1700025G04Rik	8.7705	0.452479
Trim8	10.06101	0.446554
Atp6v1e1	11.89578	0.445503
Taf12	9.493285	0.434994
Tmco3	9.777408	0.430725
Hmg20b	9.891982	0.430268
Opa3	9.830792	0.425025
Sgsm3	9.690126	0.41979
Fdft1	11.13717	0.415755
Mul1	9.259481	0.414574
Napa	11.93656	0.402601
Anapc5	12.76217	0.374965
Rnps1	10.71198	-0.29477
Pisd	10.91213	-0.32824
Elp2	11.8033	-0.33574
Brd3	11.24789	-0.33593
Rbbp5	10.36915	-0.34142
Cct8	13.98161	-0.35831
Wdr75	11.33622	-0.36216
Ppp2r2a	11.51189	-0.3637
Supt20	10.60564	-0.37499
Smarcc1	12.21077	-0.38197
Tcerg1	11.77194	-0.38944
Krr1	10.73224	-0.39881
Spdl1	9.587062	-0.40249

Racgap1	11.84666	-0.4053
Tomm70a	12.05114	-0.41499
Zfp512	10.66291	-0.41817
Matr3	12.94398	-0.41821
Prune	10.12416	-0.41928
Usp10	12.92301	-0.42733
Fnbp4	10.46545	-0.43442
Tpx2	12.37404	-0.43498
Cct4	13.51407	-0.4374
Nkap	9.188777	-0.43779
Wdr77	11.92745	-0.43808
Mis18bp1	10.63291	-0.43968
Nop56	12.45386	-0.44035
Wdr43	12.33018	-0.44197
Ppid	11.56636	-0.44516
Adh5	12.58213	-0.44548
Coa5	10.70584	-0.44822
Nop14	10.76589	-0.45037
Mcm3	13.01523	-0.45175
Skiv2l2	12.18573	-0.4588
Eif4b	12.62885	-0.45917
Hspa9	13.89769	-0.45976
Elp3	11.47718	-0.45996
Pygb	10.91646	-0.46366
Gramd1a	10.34574	-0.46376
Nup133	12.00669	-0.46404
Rpap3	9.796946	-0.46486
Trit1	9.416768	-0.46577
Snx27	10.64907	-0.4667
Cep57	10.51955	-0.46874
Utp15	11.09795	-0.47015
Top2a	13.08562	-0.47061
Naa15	11.35493	-0.47202
Mybbp1a	13.59978	-0.47223

Pias1	10.41072	-0.47273
Hspd1	12.51133	-0.47432
Rrp15	10.48448	-0.48202
Fip1l1	11.17717	-0.48254
Pnn	11.14884	-0.48293
Slc9a1	9.042356	-0.48691
Bicd2	9.173755	-0.48962
Qrsl1	8.961832	-0.49249
Cenpe	11.49908	-0.49281
Mbd4	8.721893	-0.49391
Uri1	10.96543	-0.497
Nvl	10.80853	-0.49851
Trmt5	8.923479	-0.49969
Fgfr1op	10.72761	-0.50044
Pald1	10.77075	-0.50244
Mphosph8	10.22078	-0.50586
Dkc1	11.6676	-0.50672
Supt16	11.08596	-0.50838
Mtf2	11.49355	-0.50895
Fbxo21	10.99852	-0.51015
Zfp281	10.49062	-0.51364
Cdca2	11.07401	-0.51537
Naa16	10.127	-0.51718
4933411K20Rik	8.196996	-0.52717
Mavs	8.947978	-0.52908
Dtd1	9.288868	-0.52965
Got1	11.4692	-0.53064
Ankrd27	11.04633	-0.53131
Ogt	11.72295	-0.53177
Palb2	8.877263	-0.53195
Crkl	10.78582	-0.53288
Mms22l	10.20433	-0.53371
Luc7l	11.50749	-0.53411
Bbx	10.66167	-0.53486

Cldn12	9.691274	-0.53569
Dhx30	11.8029	-0.53578
Tmem237	8.768088	-0.53702
Mthfd1l	10.71653	-0.53735
Elac1	7.973643	-0.53855
Rtn4ip1	9.32977	-0.53948
Pgap2	9.212815	-0.53996
Opa1	10.86732	-0.54027
BC027231	8.562358	-0.54192
Gar1	10.60449	-0.54355
Alkbh8	9.171841	-0.54458
Aqr	11.61175	-0.54551
Champ1	11.16212	-0.5463
Pcnxl4	8.950159	-0.55053
Naa25	11.77186	-0.55269
Ttk	10.27104	-0.55369
Tubgcp4	9.171161	-0.55463
Agtpbp1	7.929322	-0.5587
Dph5	8.885241	-0.55877
Gart	13.24644	-0.56019
Sdad1	10.92718	-0.56092
Ska3	10.37967	-0.56106
Anp32e	12.30729	-0.56534
Tasp1	8.182643	-0.56541
Exo1	10.52672	-0.56892
Fam92a	8.728507	-0.56914
Rad50	10.22063	-0.57054
Appl1	10.47609	-0.57094
Rrp12	10.95157	-0.57278
Dnm1l	11.52316	-0.57385
Mios	10.09845	-0.5739
Ska2	9.238686	-0.57456
Smc5	11.11056	-0.57905
Cdc40	10.08445	-0.58128

Xpo5	11.45871	-0.5813
AI597479	9.690155	-0.58569
Arl6ip6	9.992222	-0.58664
Arl15	9.048417	-0.58811
Camk2d	8.978849	-0.5882
Soat1	12.33158	-0.59585
Stil	9.735302	-0.59704
Sgol2	10.23392	-0.5972
Nol10	10.51514	-0.59973
Atad1	11.08962	-0.6001
Adck2	7.828081	-0.60067
Usp37	10.26754	-0.60151
Ogfod1	9.114305	-0.60241
Sf3b3	13.64401	-0.60266
Rbbp7	13.83016	-0.60272
Sec61a2	10.58989	-0.60338
Ncapd3	11.0412	-0.60436
Mtap	10.9659	-0.60451
Slc39a10	10.88436	-0.60456
Gnl3	12.03202	-0.60508
Tbl2	10.83998	-0.60951
Zfp689	7.446656	-0.60988
Cep85	10.61506	-0.61052
Bag4	10.97076	-0.61087
Ddx21	11.57855	-0.61362
Tbc1d2b	9.47368	-0.61549
Elovl5	11.03676	-0.61597
Dclre1a	8.697471	-0.61759
Rtkn2	8.54416	-0.61888
Psrc1	11.34746	-0.61914
Wdr12	10.49692	-0.61929
Cdc7	10.21268	-0.62061
Cenpf	11.42586	-0.62286
Nat10	11.16786	-0.62384

Itsn1	10.13786	-0.62519
Enox2	7.346068	-0.62886
Haus6	10.26109	-0.62917
Pcyox1l	9.148372	-0.63231
Arl4a	9.078473	-0.63231
Sccpdh	11.03229	-0.63254
Zranb3	9.263396	-0.63326
Rcbtb1	10.90005	-0.63502
Lrch3	8.79117	-0.63503
Klhl22	9.937114	-0.63559
Srpk2	9.56927	-0.63773
Dcaf17	9.85211	-0.63965
Lca5	8.080401	-0.64023
Znhit6	9.53328	-0.64027
Phf21a	8.942798	-0.64195
Xpo7	11.91507	-0.64578
Arhgap33	7.658652	-0.64585
Serac1	8.485412	-0.64625
Acsl3	10.98058	-0.64689
Nup160	12.10094	-0.64828
Mre11a	10.15691	-0.64856
Anln	11.69464	-0.65053
Mzt1	10.04569	-0.65063
Brca1	10.58976	-0.65108
Zfp397	8.727404	-0.65233
Msn	11.44294	-0.65331
Tmem161a	10.3801	-0.65616
Fignl1	11.66022	-0.65645
Ctps	11.53363	-0.6593
Slc39a6	8.669002	-0.66015
Ktn1	11.52375	-0.66017
Tmem209	11.06338	-0.66093
Cep72	9.048185	-0.66322
Exoc4	10.88155	-0.6633

Phf20	9.722877	-0.66446
Ckap5	12.0295	-0.66446
Tsn	11.67507	-0.66484
Arhgap10	9.218323	-0.66576
Pold1	11.87042	-0.66607
Atp1b3	11.10843	-0.66962
Myo1c	12.3565	-0.67008
Trmt13	6.836762	-0.67035
Spag5	10.50858	-0.67202
Tcof1	12.20742	-0.67306
Bid	9.881498	-0.67465
Nol6	11.56766	-0.67489
Chek1	9.781665	-0.67626
Kdelc1	9.837737	-0.6775
Trim6	11.59125	-0.67757
Wdhd1	10.71158	-0.67769
Bub1b	12.21504	-0.67923
Atad5	9.723252	-0.67936
Pms1	9.331241	-0.68489
E2f7	9.600735	-0.68517
Anapc1	12.23879	-0.68663
Pprc1	12.30107	-0.69059
Bcl2l1	11.26094	-0.69401
Trub1	9.242998	-0.69591
Fam60a	8.116897	-0.69621
Ttll4	10.58573	-0.69695
Swap70	10.40497	-0.70072
Pdrg1	10.10269	-0.70139
Xpo1	13.2473	-0.70383
Crlf3	10.50433	-0.70401
Ddx11	9.597646	-0.70548
Nifk	11.43747	-0.70893
Tmem206	8.106417	-0.71178
Erbb2	9.720666	-0.71504

F2r	11.61054	-0.7151
Nup188	12.00156	-0.71543
Tmx4	7.825408	-0.71598
Slc25a37	7.121531	-0.71707
Mbtps2	7.853523	-0.71798
Rbak	7.600037	-0.7184
Kif15	10.38054	-0.71933
Ttf2	10.39431	-0.72068
Sh3rf1	9.53691	-0.72384
Acer3	9.106484	-0.72496
Sdc2	9.165181	-0.725
Plekho2	8.607337	-0.72558
Ift140	9.130014	-0.72593
Vprbp	11.08999	-0.72644
Hus1	9.550189	-0.72666
Prr11	8.05581	-0.72674
Bms1	11.50683	-0.72851
Polr3g	10.2197	-0.73201
Nthl1	8.278454	-0.73296
Pds5b	10.02572	-0.73341
Rif1	11.87654	-0.73436
Fanci	10.25898	-0.73575
Ung	8.89521	-0.737
Dgke	8.132811	-0.74591
Laptm4b	11.0817	-0.74724
Hnrnph3	7.920758	-0.74943
Cep170	8.882607	-0.75129
Mphosph9	8.546777	-0.75142
Ric8b	8.899267	-0.75268
Pfkm	9.5838	-0.75413
Sirpa	8.190061	-0.75431
Arhgef39	8.955399	-0.7557
Kif2a	7.899714	-0.75674
AI314180	10.03162	-0.75683

Smad5	9.045158	-0.75693
Polr1b	11.03725	-0.75746
Peo1	9.374726	-0.75914
Dcp1a	10.46103	-0.75927
Nup155	11.0015	-0.76131
Xrcc2	8.963624	-0.76362
Rttn	8.410985	-0.76416
Slc5a6	8.442613	-0.77849
2610015P09Rik	7.353786	-0.78335
Nsl1	9.466848	-0.78584
Serpine2	12.09761	-0.78652
Ninl	9.156617	-0.78667
Dhdh	6.631005	-0.78689
Fam178a	10.76824	-0.78882
Rrp1b	11.33689	-0.78898
Ect2	12.04014	-0.79303
Tm7sf3	10.15019	-0.79371
Fstl1	10.75859	-0.80057
Phtf2	9.737237	-0.80348
Yeats2	11.03553	-0.80842
Ccdc18	8.421665	-0.8101
Fam185a	7.991493	-0.81357
Galnt7	9.434723	-0.81725
Tbc1d31	9.315759	-0.81919
Ap1s2	8.030107	-0.82257
Plekha1	10.73902	-0.82291
Ppm1f	10.06892	-0.82552
Lrrc61	7.059165	-0.82594
Adat1	8.846121	-0.82595
Aasdh	8.956064	-0.82608
Mettl4	8.73965	-0.82633
Sugp2	9.472215	-0.82883
Ttc37	10.18047	-0.82895
Kntc1	10.6952	-0.83334

Rhbdf1	9.301837	-0.83369
Nfatc4	8.975622	-0.83421
Hyls1	8.096207	-0.8366
G2e3	10.79963	-0.83836
Pask	9.664005	-0.83962
Ppat	11.94302	-0.84134
Dyrk3	9.100614	-0.84238
Slc19a1	9.325387	-0.84284
Echdc1	6.437141	-0.84313
Hbegf	8.783802	-0.84837
Arap1	9.16909	-0.85148
Mgmt	7.992538	-0.85706
Sgms1	8.884554	-0.86038
Fxr1	10.80432	-0.86269
Gspt2	7.045152	-0.86406
Zfp280c	8.66685	-0.86847
Pdk3	9.568835	-0.8714
Wrb	9.859394	-0.87326
Poli	8.53362	-0.87591
Fam115a	9.487177	-0.87611
Fkbp10	9.587372	-0.87691
Lrp12	8.255125	-0.87708
Syngr1	8.538281	-0.87846
Cdh6	7.964436	-0.88053
Timm21	8.291435	-0.88262
Ncapd2	12.43438	-0.88273
Spata5l1	6.481756	-0.88293
Rhobtb3	8.772652	-0.8841
Adamts10	7.613768	-0.88465
Espl1	11.82216	-0.88745
Ccdc171	6.74681	-0.88975
Heatr1	11.92833	-0.89096
Slc38a1	11.47461	-0.89106
Zfp473	9.415062	-0.89403
Il6st	10.66995	-0.89445
4930503L19Rik	8.496117	-0.89587
Hdac11	7.067858	-0.89764
Igsf3	9.425945	-0.89816
Nnt	10.02988	-0.90214
Slc34a2	8.401672	-0.90468
Ppfibp2	9.858008	-0.90474
Zfp451	9.839322	-0.90555
Wdr19	8.121624	-0.90623
Rad51b	6.779135	-0.90782
Cpne3	9.45677	-0.90983
Fbxo17	7.145211	-0.9104
Zfp61	7.826061	-0.91139
Nek1	9.619139	-0.91248
Srgap2	9.862926	-0.91617
Sall1	11.10134	-0.91886
Qtrtd1	8.943379	-0.92006
Ticrr	10.05879	-0.92219
Lyrm9	7.182425	-0.9246
Gas2l3	9.3069	-0.92561
Usp28	11.08404	-0.92751
Bivm	8.641933	-0.92828
Frs2	10.46112	-0.92958
Bcap29	8.672853	-0.93385
Zfp72	6.29694	-0.93484
Eda2r	9.954147	-0.93827
Fam122b	8.747174	-0.94195
Nek4	8.520705	-0.94299
Trp53bp1	10.65201	-0.94315
Zfp937	5.971612	-0.94441
Aldh4a1	9.944564	-0.94508
Hpn	8.331022	-0.9453
Sfi1	7.783419	-0.94711
Pex26	8.527312	-0.94844

Usp54	9.02086	-0.94946
Elmod2	8.882987	-0.94995
Extl3	10.27173	-0.95058
Abi2	10.27325	-0.951
Dennd4b	7.489419	-0.95642
Zak	9.34272	-0.95715
Zfp275	8.279061	-0.96094
Tpm1	12.89416	-0.96453
Kif14	8.58933	-0.96759
Rasa3	8.319107	-0.96809
Tnfrsf10b	9.062622	-0.96818
Dctd	10.363	-0.9684
Litaf	11.0409	-0.96876
Arid3b	11.25531	-0.96887
Eif2ak2	7.597233	-0.97483
Mcm8	9.444528	-0.97493
Lrch1	8.21862	-0.97521
Pphln1	10.39311	-0.97754
Dtl	11.26897	-0.97969
Arhgap19	11.08511	-0.9828
Cep192	10.92868	-0.98302
Taf4b	8.623491	-0.98624
St6galnac4	7.230407	-0.98654
Nrbp2	7.128363	-0.98719
Ern1	6.467341	-0.99178
Add3	9.976674	-0.99383
Gyg	8.71299	-0.99404
Manba	10.66976	-0.99429
Sh3pxd2b	8.401235	-0.99695
Zcchc11	9.281111	-1.00582
Ccdc15	6.780759	-1.00652
Ulk4	5.770041	-1.00733
Col4a1	16.15989	-1.00791
Slc12a7	10.79869	-1.01088

Spry1	8.908079	-1.01114
Fam53b	7.631591	-1.01123
Tmem47	9.940252	-1.01421
Wdfy2	6.736595	-1.02089
Nabp1	10.10923	-1.02162
Zfp334	8.699797	-1.02332
Cdca7	11.38528	-1.02757
Hip1	10.81479	-1.02778
Mdm1	9.314287	-1.02828
Mpp6	9.465923	-1.03125
38961	7.619232	-1.03473
Pus7	10.23475	-1.03714
Bora	9.746098	-1.0446
Adrb3	8.230674	-1.04486
Gjb3	10.86572	-1.05153
Ahctf1	11.34656	-1.05209
Gyltl1b	9.310089	-1.05352
Mks1	7.751858	-1.05634
Net1	10.04432	-1.05892
Plagl2	8.244326	-1.06416
Kcnd1	5.914793	-1.06523
Sdc1	9.66562	-1.0683
Znrf3	6.633128	-1.06852
Abcc1	10.00404	-1.06937
Tap1	9.985608	-1.071
Wrn	8.741709	-1.07107
Cpxm1	9.140185	-1.07307
Mboat1	6.675593	-1.07773
Zfp354c	7.72539	-1.07907
Caprin2	8.547624	-1.08431
Spry2	8.058515	-1.08494
Ppp1r26	6.517877	-1.08716
2200002D01Rik	8.662278	-1.0878
Mrc2	7.262358	-1.08919

Phka1	7.906353	-1.09452
39692	8.418295	-1.09577
Piezo1	10.89501	-1.10019
Cald1	10.80911	-1.10487
Ephb3	10.71802	-1.10921
Ddx26b	9.066335	-1.10968
Atg4c	7.725794	-1.11549
Elavl2	7.60816	-1.11829
Rab27a	8.216661	-1.11867
Tns3	10.04827	-1.12101
Phf6	9.714826	-1.12341
Fancd2	10.06493	-1.12584
Slc29a2	7.970479	-1.12977
Zc3h8	7.885866	-1.13048
40422	7.07942	-1.13474
Dusp4	9.440699	-1.13654
Htra1	11.40016	-1.14233
Peak1	8.753014	-1.14659
Ift57	7.688339	-1.14992
Fam163a	6.487693	-1.1514
Klhl42	8.137155	-1.15152
Ankrd26	8.410709	-1.15154
Tuft1	10.00753	-1.15221
Zfp521	6.587786	-1.15541
Cdc14a	7.41077	-1.15555
Zdhhc17	8.476506	-1.15584
Cep112	6.250261	-1.16116
Fgfr3	9.669247	-1.16639
Osbpl1a	8.812412	-1.16891
Tmem38b	8.189627	-1.17025
Dennd5b	8.24835	-1.17088
Slc41a1	9.17505	-1.17496
Tbc1d32	7.167567	-1.17512
Iqgap2	9.40199	-1.17762
Tfrc	11.66068	-1.17871
Sertad4	6.791338	-1.17886
Fut10	7.826725	-1.17977
Myh10	11.33176	-1.18187
Sox13	8.062839	-1.18745
Sh3bp1	9.481321	-1.18794
Dmc1	6.60566	-1.19455
Adcy3	7.107681	-1.19556
Tmod2	6.84574	-1.19955
Zfand4	4.890402	-1.19978
B3galnt1	9.064309	-1.20858
Pbk	9.898651	-1.20935
B3gnt5	9.420797	-1.21025
Peg3	13.13978	-1.21751
Fhl1	11.2122	-1.21875
Gcnt4	6.68878	-1.22088
Fzd1	7.561247	-1.2239
Ankrd6	8.575718	-1.22514
Amotl2	12.71049	-1.22799
Adam19	10.6294	-1.24112
Pxylp1	7.424381	-1.24188
Ssbp2	7.346937	-1.24201
Zfp248	7.324603	-1.24397
Abhd2	6.563437	-1.24403
Apcdd1	5.419708	-1.24487
Lin28a	11.46193	-1.24675
Slc2a3	16.02701	-1.25165
Casr	6.897449	-1.25377
Pik3cd	8.984887	-1.25458
Ntf3	5.110561	-1.25579
Dse	11.43594	-1.25615
Dzip1l	7.13019	-1.25796
Slc7a6	11.92143	-1.2664
Smarca1	8.96994	-1.26846

Prkci	11.41612	-1.26966
Cers6	8.276309	-1.27962
1700030K09Rik	8.051869	-1.29175
Setdb1	10.57137	-1.29227
Plat	11.39447	-1.29506
Ust	7.660686	-1.30024
Angpt2	9.068353	-1.3006
Rnd3	10.60273	-1.30225
Igfbp4	8.032919	-1.30239
Braf	9.45866	-1.30863
Evc2	8.677286	-1.3115
Clasp1	10.75815	-1.31994
Thbs3	6.955115	-1.32455
Zc3hav1l	8.027159	-1.32576
Dusp22	8.136423	-1.327
Prkab2	8.694409	-1.32866
Mme	10.36966	-1.32923
Zik1	7.681827	-1.33091
Fam199x	8.733424	-1.33925
Cask	7.378778	-1.34146
Gpm6a	5.929967	-1.3533
Nid1	12.12857	-1.35739
Pld6	6.459935	-1.35764
Acsl5	9.140995	-1.35836
Itgb5	9.922735	-1.36015
Zfp449	8.836043	-1.36418
Vegfc	5.627038	-1.36469
Snai1	8.685869	-1.36618
Zfp454	5.544582	-1.36649
1810041L15Rik	5.164008	-1.3705
Kitl	6.770513	-1.37209
Peg12	5.106189	-1.37457
Lats2	8.55594	-1.37858
2900056M20Rik	7.196938	-1.38118
St6galnac3	7.188293	-1.38279
Wdr86	7.717558	-1.39133
Pabpc4l	5.121412	-1.3944
Ptprg	9.126622	-1.40019
Fam213a	11.05848	-1.40128
D630045J12Rik	7.391493	-1.40575
Ptpn14	10.00299	-1.40612
Sall2	8.032612	-1.41237
Rab11fip1	10.06402	-1.42017
Spred1	9.106555	-1.4222
Nrcam	8.187233	-1.42549
Igf2os	7.140692	-1.42591
Ihh	8.029732	-1.4274
Msx2	8.878853	-1.43037
Bdh2	6.434178	-1.44128
Pmaip1	11.13688	-1.44627
Adamts4	6.33773	-1.44823
Wipf3	6.040743	-1.4508
Fastkd1	7.300292	-1.4562
Moxd1	6.607312	-1.45745
Trpm6	7.493405	-1.45862
Hmga2	7.504556	-1.4596
Katnal1	6.881793	-1.46364
Kcp	6.332389	-1.47144
Irak4	6.483651	-1.47158
Akap2	12.1387	-1.47237
Hk2	11.19168	-1.47357
Matn1	6.637889	-1.48093
Nfkb1	7.7728	-1.48545
Spns2	8.206787	-1.49724
Cox4i2	4.788061	-1.51325
Pus7l	7.953278	-1.52201
Gli3	6.947169	-1.52784
Tram2	5.879996	-1.53271

Sulf1	9.379649	-1.53349
Mtr	10.29922	-1.53456
Ank2	7.499126	-1.53772
Susd1	5.885718	-1.54936
Bcam	10.83437	-1.55624
Pnck	4.725182	-1.55657
Stom	8.376346	-1.57188
Epb4.1l1	8.975507	-1.57567
8430419L09Rik	7.808145	-1.57662
Hspa12a	6.319687	-1.57836
Pcdhgc3	8.09705	-1.58111
Apob	10.12577	-1.58267
B4galt6	8.769913	-1.58312
Cpm	12.06406	-1.58403
Ikzf4	6.31576	-1.58453
Slc7a4	6.11245	-1.58756
Zfp185	8.401514	-1.59129
Mpp3	6.043055	-1.59659
Sv2a	6.639806	-1.60207
Fam78a	6.27026	-1.60214
Endod1	7.494846	-1.61288
Fzd4	6.242026	-1.61915
Phactr2	5.865898	-1.62418
A2m	7.16927	-1.62574
Six4	8.038119	-1.63473
Il15	4.158303	-1.63509
Dab2	14.09086	-1.65156
Prss35	8.895186	-1.65208
Ablim1	9.023917	-1.65737
Zcchc24	6.240047	-1.6594
Eno3	8.550347	-1.66258
Cul9	6.727343	-1.66397
Efnb2	8.730535	-1.66568
Shank3	5.299754	-1.6672

Msrb3	5.984673	-1.67129
Abcb1b	8.837882	-1.67147
Itga9	6.518879	-1.67584
Col8a2	7.125783	-1.67769
Fbln5	5.511003	-1.67991
Nrk	9.603687	-1.68095
Kazald1	4.698285	-1.68826
Fstl3	5.210965	-1.6885
Slc2a4	4.5868	-1.68891
Hspb8	8.373858	-1.69285
Mmd	6.888764	-1.69428
Frmd6	8.198118	-1.69548
Col4a2	14.55873	-1.69594
Napepld	7.499851	-1.69748
Igdcc3	6.609133	-1.70046
Ehbp1l1	8.279952	-1.7105
Rlbp1	5.863573	-1.71248
Gpc6	7.150894	-1.71308
Dpp4	11.03769	-1.71596
Nrg1	9.321341	-1.71624
Gnmt	5.779876	-1.71663
Kcng1	8.073083	-1.71683
Usp46	9.712245	-1.71897
Mgat4a	7.057542	-1.72204
St3gal5	6.58545	-1.72994
Pyy	8.143533	-1.73019
Stox2	5.986204	-1.73097
Masp1	7.895559	-1.73103
Usp29	4.991792	-1.737
Dmtn	8.980676	-1.74253
Cnksr2	5.972589	-1.76018
Boc	8.635475	-1.76147
Irx4	5.402532	-1.76552
Frmd4a	9.117535	-1.76747

Asic1	5.81553	-1.76782
Ccdc109b	4.638736	-1.76895
Gli2	8.142768	-1.77075
Adamts3	5.668543	-1.77342
Kirrel3	5.942358	-1.78286
Rgl1	8.486636	-1.8012
Hey2	5.186664	-1.80541
Ppm1j	8.345718	-1.80925
Lmo7	8.037403	-1.81232
Med12l	5.850392	-1.81248
Wls	10.43883	-1.82004
Mfap4	5.75933	-1.82011
Prkar2b	7.023217	-1.83489
Hs6st2	6.986493	-1.83505
Ptch1	8.269037	-1.8417
Rasl11b	6.902623	-1.84739
Afap1l1	7.596889	-1.8498
Tnfrsf19	6.820123	-1.86102
Neu3	6.402794	-1.86868
Batf	3.907399	-1.87311
Pknox2	7.408374	-1.87418
Fam65b	4.536006	-1.88369
Dock4	6.57521	-1.89264
Npr3	4.940287	-1.89292
Itpr1	9.018356	-1.89346
Lhx5	4.301129	-1.89643
Emilin1	7.716228	-1.90192
Igf1r	8.337142	-1.90416
Tenm3	8.881197	-1.90567
Ephx2	7.946482	-1.91049
Iqsec2	5.198348	-1.92344
Prss41	6.279912	-1.93246
Tspan18	6.129261	-1.9502
0610040J01Rik	4.829419	-1.95638
Csdc2	6.464863	-1.95767
Snai2	4.352059	-1.96112
Icam1	9.222567	-1.96844
Rgs22	3.666144	-1.97217
Frem2	7.375485	-1.97514
Hspg2	11.56543	-1.9829
Calcrl	4.878247	-1.98811
Rprm	5.562469	-1.98832
Has2	9.09752	-1.99014
Ikbke	6.633984	-2.00708
Uggt2	7.684125	-2.00718
Zeb2	6.427452	-2.00812
Eya1	6.520325	-2.01391
Pvt1	7.376545	-2.01591
Myl3	7.633234	-2.01892
Tap2	6.626522	-2.02483
D630045M09Rik	9.307799	-2.03668
Mocs1	8.264762	-2.04215
Capn6	10.77368	-2.04366
Gria3	6.221155	-2.04889
Neurl1b	4.836991	-2.06854
St8sia4	3.878759	-2.07235
C530008M17Rik	7.688844	-2.07266
Olfml2b	5.669267	-2.07271
Tmem119	5.607421	-2.07888
Des	8.117009	-2.08129
38231	5.88213	-2.0828
Frzb	8.817553	-2.08448
Fbn2	6.02517	-2.0859
Parp8	6.320516	-2.09105
Shroom4	5.869482	-2.0913
Apom	6.887669	-2.10147
Six3	5.082426	-2.10961
Thsd7a	7.220126	-2.13355

Tspyl3	5.648234	-2.15836
Chst8	5.216168	-2.15904
Rbms3	4.38466	-2.17311
Fam198b	9.838013	-2.18165
Procr	6.730082	-2.19178
Amer2	3.530023	-2.19781
Slc4a5	6.499532	-2.21389
Slc6a15	8.718083	-2.2152
Six1	6.701744	-2.21791
Psmb8	5.389834	-2.22591
Mn1	5.068612	-2.2304
Ldb3	5.314365	-2.23981
Irf5	5.25254	-2.24155
Lfng	6.612661	-2.24667
Crb2	7.699659	-2.24938
Tmem181b-ps	4.818119	-2.25034
Fgl1	3.849833	-2.2631
Nsg2	5.559603	-2.26755
Kif6	4.507169	-2.28775
Arsi	5.900553	-2.28821
Nexn	5.324028	-2.30071
Tex15	8.187926	-2.30953
Thbd	7.133667	-2.31561
Plekhg1	7.5522	-2.32805
Hhat	4.750621	-2.3465
Oas3	4.975582	-2.34901
Fam107a	4.564006	-2.38946
Meis1	8.036225	-2.3988
Calr3	5.358406	-2.40599
Kcns1	5.284373	-2.40737
Nfam1	4.767273	-2.41978
Hmgcll1	6.220534	-2.42612
Fam181b	5.167788	-2.43276
Nhsl2	6.967672	-2.43868

Ube2l6	7.662847	-2.44349
Sgpp1	6.832927	-2.44358
Tal2	5.747083	-2.44919
Otx1	5.066635	-2.45006
Tspan2	7.484593	-2.45547
Palm2	4.546189	-2.4773
AU015836	5.461191	-2.48045
Tchh	6.121333	-2.48199
Myh7b	6.218133	-2.48261
Nkx2-2	3.797784	-2.48586
Ccdc141	6.41837	-2.48829
Cxcl14	5.878123	-2.50754
Cpne5	5.728422	-2.5083
B4galnt2	7.41799	-2.52601
Slc36a2	3.101789	-2.53144
Wnt5a	7.690283	-2.54814
Bmp5	4.140231	-2.54973
Lifr	11.3319	-2.56281
Alpk3	6.258406	-2.57313
Dkk3	7.078629	-2.57578
Popdc2	4.54426	-2.59626
Six3os1	4.293023	-2.61056
Arhgef9	5.134367	-2.61239
Srd5a2	6.525041	-2.62517
Syde1	6.862147	-2.63498
Atp2a1	4.698333	-2.63511
Pgf	6.058579	-2.63872
Anxa8	8.040809	-2.6553
Dner	4.561065	-2.65991
Camk2a	4.956642	-2.67225
Tnnc1	7.25421	-2.70935
Flnc	9.408088	-2.71702
Shh	4.491094	-2.7469
Pmp22	8.762475	-2.7703

Bmp4	7.970695	-2.78121
Acvrl1	4.653516	-2.78727
Igfbp5	9.714044	-2.78982
4930506M07Rik	8.302047	-2.80231
4632428N05Rik	8.571754	-2.80592
Klk13	3.22382	-2.85953
Prtg	9.523019	-2.88003
Gad1	5.071044	-2.89527
Gm7694	3.996194	-2.89625
Vcam1	5.814962	-2.90278
Cd248	6.063089	-2.90318
Foxc2	3.474741	-2.91834
Dmrt3	5.234385	-2.97864
Gli1	8.070227	-2.99718
Paqr9	3.364286	-3.00215
Esam	7.706586	-3.00654
Gucy1b3	4.016681	-3.04196
Galnt14	3.051449	-3.06787
Ebf2	3.130474	-3.07403
Tek	9.92012	-3.09468
2510009E07Rik	3.850334	-3.1101
Fezf2	3.936512	-3.13624
Krt20	2.947343	-3.16332
Chrna6	3.617509	-3.16837
Tacstd2	6.15391	-3.17978
Tmem132c	5.051077	-3.21066
Adamts17	4.314204	-3.22761
Nkx2-9	7.029166	-3.25924
Ankrd1	7.280263	-3.2697
Cryab	11.16936	-3.27538
Hspb2	4.483165	-3.2809
Sema3a	4.736824	-3.30479
Kdr	7.597967	-3.32359
Klk14	2.812078	-3.32814

Akap5	7.282942	-3.3531
Irx1	2.30733	-3.35326
Foxf1	4.042609	-3.36162
Wdfy1	10.18047	-3.37087
Postn	5.335351	-3.39641
Tril	5.408262	-3.4391
Hapln3	2.894961	-3.45453
Lgi1	2.371271	-3.46855
Ptprm	7.368398	-3.48493
Serping1	8.920855	-3.49556
Scube1	5.785274	-3.49882
Lama1	15.13134	-3.60516
Mef2c	3.495401	-3.61026
Kctd1	4.59693	-3.61476
Lmx1a	4.686272	-3.62753
Slc7a10	2.658152	-3.62866
Ccnd2	9.824835	-3.66651
Usp18	6.814216	-3.66911
Rcsd1	7.117507	-3.73066
Plagl1	6.922123	-3.75803
Mgat3	6.149154	-3.80719
Prss22	2.431795	-3.85047
Myh7	7.765749	-3.8548
Vgll2	4.295038	-3.90886
Ppp1r16b	7.242943	-3.94252
Meis2	5.216507	-3.9991
Foxc1	5.794677	-4.00707
Limch1	7.133139	-4.01278
Nkx2-3	5.256865	-4.03084
Lbp	3.692511	-4.08191
Stard8	10.33431	-4.09212
Unc5c	2.649483	-4.0952
Jph2	4.105749	-4.10084
Pax6	4.986979	-4.2022

Myh6	4.903764	-4.47364
Il17re	3.362722	-4.49626
Bgn	7.6463	-4.50255
Foxe1	3.572398	-4.53777
Maml2	6.636041	-4.58866
Atoh8	3.24201	-4.59924
Nkx2-5	5.95495	-4.78783
Ctxn3	2.659403	-4.82203
Fn3krp	6.33349	-5.6868

Table 8.3 Deregulated ERVs in Setdb1^{END} XEN cells

RepeatID	logbaseMean	log2FoldChange	pvalue	padj
RLTR1F_Mm|LTR|ERVK	4.960689	5.080123	8.44E-23	2.77E-21
IAPLTR1a_Mm|LTR|ERVK	9.849496	4.999145	2.83E-131	8.36E-129
RLTR10C|LTR|ERVK	9.664767	4.730325	4.78E-130	9.40E-128
RLTR1B|LTR|ERV1	9.916956	4.711235	7.12E-105	1.05E-102
IAPEz-int|LTR|ERVK	14.05291	4.361231	1.80E-54	1.06E-52
RLTR1B-int|LTR|ERV1	12.30751	4.243785	1.39E-67	1.17E-65
RLTR10D2|LTR|ERVK	5.169707	4.208208	1.09E-19	3.40E-18
MMERVK10C-int|LTR|ERVK	11.47809	4.162188	9.08E-202	5.36E-199
IAPLTR2a2_Mm|LTR|ERVK	7.595302	4.057812	6.89E-66	5.08E-64
IAP-d-int|LTR|ERVK	7.684545	3.951239	8.90E-81	1.05E-78
IAPLTR1_Mm|LTR|ERVK	10.44735	3.914437	6.98E-61	4.58E-59
IAPLTR4_I|LTR|ERVK	3.6088	3.902746	1.27E-09	1.83E-08
MuRRS4-int|LTR|ERV1	8.105848	3.801289	7.15E-29	3.24E-27
IAPA_MM-int|LTR|ERVK	4.227117	3.761352	1.94E-11	3.36E-10
IAPLTR2_Mm|LTR|ERVK	7.514594	3.665783	3.89E-71	3.82E-69
RLTR10B2|LTR|ERVK	6.063311	3.578714	1.65E-25	6.48E-24
IAPEY5_I-int|LTR|ERVK	2.315788	3.455714	8.75E-05	0.000688
IAPEY3-int|LTR|ERVK	6.321548	3.433722	2.54E-14	5.35E-13
MMERGLN-int|LTR|ERV1	12.59941	3.370245	7.77E-40	3.82E-38
RLTR50A|LTR|ERVK	1.392989	3.266811	0.000354	0.00243
MMERVK10D3_I-int|LTR|ERVK	7.197821	3.192412	1.59E-51	8.51E-50
IAPLTR3-int|LTR|ERVK	5.38479	3.099264	1.56E-14	3.42E-13
RLTR44D|LTR|ERVK	2.913928	3.070896	7.34E-07	8.49E-06
MURVY-int|LTR|ERV1	3.450875	2.988458	8.13E-07	9.23E-06
RLTR19A2|LTR|ERVK	1.963214	2.874594	0.00159	0.009022
IAPLTR4|LTR|ERVK	3.928716	2.683046	2.31E-08	3.02E-07
IAPEy-int|LTR|ERVK	3.754317	2.553476	2.09E-05	0.000176
IAPEY2_LTR|LTR|ERVK	5.177496	2.532723	9.16E-10	1.39E-08
RLTR13C2|LTR|ERVK	6.507473	2.525152	1.95E-16	4.61E-15
RLTR10-int|LTR|ERVK	8.454231	2.524628	1.51E-14	3.42E-13
MMERGLN_LTR|LTR|ERV1	8.251965	2.43455	5.70E-23	1.98E-21
RLTR44B|LTR|ERVK	3.251987	2.298391	0.000222	0.001581
RMER16_Mm|LTR|ERVK	4.890553	2.265606	9.53E-11	1.52E-09
IAP1-MM_LTR|LTR|ERVK	4.550582	2.196468	1.09E-05	9.75E-05
IAPEY3C_LTR|LTR|ERVK	2.64168	2.15568	0.00078	0.004947
ETnERV-int|LTR|ERVK	7.640131	2.080777	4.32E-17	1.16E-15
RLTR1A2_MM|LTR|ERV1	7.3243	2.065585	5.21E-17	1.34E-15
RLTR6_Mm|LTR|ERV1	6.584547	2.06431	1.35E-13	2.65E-12
IAPEY4_I-int|LTR|ERVK	7.018162	2.044592	6.14E-14	1.25E-12
ERVB4_2-I_MM-int|LTR|ERVK	5.480323	1.94992	1.42E-09	2.00E-08

RMER3D-int|LTR|ERVK	7.261488	1.913466	3.72E-19	1.10E-17
ORR1F-int|LTR|ERVL-MaLR	4.446714	1.877181	1.00E-07	1.26E-06
RMER16-int|LTR|ERVK	8.588965	1.875726	2.23E-24	8.21E-23
RLTR26D_MM|LTR|ERVK	6.997299	1.866494	2.23E-17	6.28E-16
RLTR13B1|LTR|ERVK	5.570331	1.825778	2.59E-09	3.55E-08
MLTR12|LTR|ERV1	5.487265	1.794128	3.94E-11	6.46E-10
ORR1A1-int|LTR|ERVL-MaLR	8.576878	1.765328	5.58E-26	2.35E-24
RLTR45-int|LTR|ERVK	8.130562	1.754261	1.93E-16	4.61E-15
RLTR10F|LTR|ERVK	5.108398	1.734462	3.61E-06	3.68E-05
RLTR10D|LTR|ERVK	5.315502	1.71613	8.23E-09	1.10E-07
ORR1A0-int|LTR|ERVL-MaLR	6.792759	1.620354	3.09E-10	4.80E-09
RLTR30D2_MM|LTR|ERV1	6.365166	1.605435	9.17E-12	1.69E-10
RLTR13C3|LTR|ERVK	4.702976	1.537385	0.000132	0.000984
RLTR13B2|LTR|ERVK	3.913611	1.407987	0.001058	0.006372
ERVB4_1B-I_MM-int|LTR|ERVK	5.385165	1.364243	2.73E-06	2.82E-05
RMER17C-int|LTR|ERVK	6.25466	1.345371	1.32E-05	0.000114
LTR33B|LTR|ERVL	4.567475	1.342042	0.000104	0.000808
MLT1F|LTR|ERVL-MaLR	8.068393	1.333692	1.16E-09	1.72E-08
RLTR13D3|LTR|ERVK	4.419737	1.306622	0.000487	0.003227
BGLII|LTR|ERVK	7.113052	1.301038	1.03E-11	1.83E-10
ETnERV2-int|LTR|ERVK	7.479304	1.28926	2.73E-08	3.51E-07
RLTR45|LTR|ERVK	5.759951	1.28713	1.01E-06	1.09E-05
IAPLTR2a|LTR|ERVK	5.319585	1.276187	0.000587	0.003807
MTB_Mm-int|LTR|ERVL-MaLR	5.493968	1.269759	9.71E-06	8.82E-05
RLTR1D|LTR|ERV1	5.866913	1.261785	2.02E-05	0.000173
RLTR10|LTR|ERVK	7.353551	1.260651	2.14E-12	4.08E-11
ORR1C2-int|LTR|ERVL-MaLR	7.239086	1.255585	2.80E-11	4.72E-10
MMVL30-int|LTR|ERV1	8.207996	1.224601	6.91E-05	0.000558
IAPEY4_LTR|LTR|ERVK	5.579249	1.197707	0.000271	0.001903
RLTR53_Mm|LTR|ERVK	5.356736	1.128646	0.00108	0.006437
MERV1_I-int|LTR|ERV1	6.304955	1.118356	0.001038	0.006312
RLTR21|LTR|ERVK	9.744088	1.043554	3.86E-05	0.000316
IAPLTR2b|LTR|ERVK	6.110518	1.013515	8.55E-07	9.52E-06
MERVL-int|LTR|ERVL	7.577075	1.010632	0.000221	0.001581
LTR37-int|LTR|ERV1	7.002451	-1.04023	0.001668	0.009372
MTEa-int|LTR|ERVL-MaLR	7.533671	-1.13045	1.74E-07	2.14E-06
MER110A|LTR|ERV1	7.243132	-1.17501	0.000388	0.002631
MER50B|LTR|ERV1	7.972794	-1.26579	0.000153	0.001131
MER76|LTR|ERVL	4.324237	-1.31253	0.000349	0.002422
RLTR13B3|LTR|ERVK	5.346883	-1.40689	1.29E-05	0.000114
RLTR30D_RN|LTR|ERV1	5.795067	-1.76112	8.70E-05	0.000688

RLTR3_Mm|LTR|ERVK	4.16527	-1.82874	0.000744	0.004774

Table 8.4 Deregulated LINEs in Setdb1^{END} XEN cells

RepeatID	logbaseMean	log2FoldChange	pvalue	padj
L1Md_Gf|LINE|L1	6.439111	2.003291	1.22E-15	3.98E-14
L1Md_T|LINE|L1	12.94997	1.706154	2.72E-16	1.18E-14
L1Md_A|LINE|L1	10.82747	1.666215	5.82E-17	3.78E-15
L1ME3F|LINE|L1	4.615931	1.565317	1.21E-06	1.97E-05
L1_Mus2|LINE|L1	11.19369	1.323672	2.03E-12	5.27E-11
L1Md_F2|LINE|L1	12.04385	1.166034	5.04E-12	1.09E-10
L1MDa|LINE|L1	7.609234	1.116536	5.24E-10	9.74E-09

Table 8.5 Deregulated ERVs in Setdb1^{END} DE cells

RepeatID	logbaseMean	log2FoldChange	pvalue	padj
RLTR19D|LTR|ERVK	4.311627	2.5856	1.71E-06	7.15E-05
RLTR1B-int|LTR|ERV1	12.30751	2.406249	2.34E-22	6.35E-20
MuRRS-int|LTR|ERV1	6.791991	2.302639	7.58E-20	1.37E-17
LTRIS_Mm|LTR|ERV1	6.564521	2.202838	9.27E-19	1.26E-16
RLTR4_MM-int|LTR|ERV1	9.065868	2.186017	7.16E-10	6.47E-08
IAP1-MM_LTR|LTR|ERVK	4.550582	1.946674	3.52E-06	0.000112
RLTR30D_MM|LTR|ERV1	4.967259	1.937593	3.40E-09	2.63E-07
IAPEY2_LTR|LTR|ERVK	5.177496	1.784852	5.51E-06	0.000166
RLTR9F|LTR|ERVK	4.840468	1.641784	2.38E-06	9.20E-05
ERVB5_1-LTR_MM|LTR|ERVK	3.301962	1.612678	0.000466	0.007017
RLTR45|LTR|ERVK	5.759951	1.541948	2.32E-07	1.14E-05
ERVB7_2-LTR_MM|LTR|ERVK	6.578599	1.428419	1.38E-11	1.50E-09
MMERVK10C-int|LTR|ERVK	11.47809	1.397979	3.17E-23	1.72E-20
RLTR1D|LTR|ERV1	5.866913	1.282442	2.87E-06	0.000104
RLTR10-int|LTR|ERVK	8.454231	1.256876	0.000193	0.003486
RLTR4_Mm|LTR|ERV1	5.134911	1.249574	3.45E-05	0.000935
IAP-d-int|LTR|ERVK	7.684545	1.224034	9.01E-08	6.10E-06
MLT1I|LTR|ERVL-MaLR	6.685658	1.202139	1.92E-07	1.07E-05
RLTR13C2|LTR|ERVK	6.507473	1.14849	0.000504	0.00738
ERVB7_3-LTR_MM|LTR|ERVK	4.907835	1.101637	0.000113	0.002109
IAPEY4_LTR|LTR|ERVK	5.579249	1.065097	0.000102	0.002045
RLTR10C|LTR|ERVK	9.664767	1.0304	1.97E-07	1.07E-05
ETnERV2-int|LTR|ERVK	7.479304	1.004282	6.13E-07	2.77E-05
RLTR13B3|LTR|ERVK	5.346883	-1.40316	3.34E-06	0.000112

ERVB4_1-I_MM-int|LTR|ERVK	5.193469	-1.47947	0.000289	0.005055

9. References

Artus, J., Douvaras, P., Piliszek, A., Isern, J., Baron, M.H., and Hadjantonakis, A.K. (2012). BMP4 signaling directs primitive endoderm-derived XEN cells to an extraembryonic visceral endoderm identity. Dev Biol *361*, 245-262.

Bachman, K.E., Park, B.H., Rhee, I., Rajagopalan, H., Herman, J.G., Baylin, S.B., Kinzler, K.W., and Vogelstein, B. (2003). Histone modifications and silencing prior to DNA methylation of a tumor suppressor gene. Cancer Cell *3*, 89-95.

Bakshi, A., and Kim, J. (2014). Retrotransposon-based profiling of mammalian epigenomes: DNA methylation of IAP LTRs in embryonic stem, somatic and cancer cells. Genomics *104*, 538-544.

Bannert, N., and Kurth, R. (2006). The evolutionary dynamics of human endogenous retroviral families. Annu Rev Genomics Hum Genet *7*, 149-173.

Barbot, W., Dupressoir, A., Lazar, V., and Heidmann, T. (2002). Epigenetic regulation of an IAP retrotransposon in the aging mouse: progressive demethylation and de-silencing of the element by its repetitive induction. Nucleic Acids Res *30*, 2365-2373.

Becker, J.S., Nicetto, D., and Zaret, K.S. (2016). H3K9me3-Dependent Heterochromatin: Barrier to Cell Fate Changes. Trends Genet *32*, 29-41.

Bilodeau, S., Kagey, M.H., Frampton, G.M., Rahl, P.B., and Young, R.A. (2009). SetDB1 contributes to repression of genes encoding developmental regulators and maintenance of ES cell state. Genes Dev *23*, 2484-2489.

Bourc'his, D., and Bestor, T.H. (2004). Meiotic catastrophe and retrotransposon reactivation in male germ cells lacking Dnmt3L. Nature *431*, 96-99.

Bourque, G., Leong, B., Vega, V.B., Chen, X., Lee, Y.L., Srinivasan, K.G., Chew, J.L., Ruan, Y., Wei, C.L., Ng, H.H.*, et al.* (2008). Evolution of the mammalian transcription factor binding repertoire via transposable elements. Genome Res *18*, 1752-1762.

Brocks, D., Schmidt, C.R., Daskalakis, M., Jang, H.S., Shah, N.M., Li, D., Li, J., Zhang, B., Hou, Y., Laudato, S.*, et al.* (2017). DNMT and HDAC inhibitors induce cryptic transcription start sites encoded in long terminal repeats. Nat Genet *49*, 1052-1060.

Bulut-Karslioglu, A., De La Rosa-Velazquez, I.A., Ramirez, F., Barenboim, M., Onishi-Seebacher, M., Arand, J., Galan, C., Winter, G.E., Engist, B., Gerle, B.*, et al.* (2014). Suv39h-dependent H3K9me3 marks intact retrotransposons and silences LINE elements in mouse embryonic stem cells. Mol Cell *55*, 277-290.

Buzdin, A.A. (2004). Retroelements and formation of chimeric retrogenes. Cell Mol Life Sci *61*, 2046-2059.

Cernilogar, F.M., Hasenoder, S., Wang, Z., Scheibner, K., Burtscher, I., Sterr, M., Smialowski, P., Groh, S., Evenroed, I.M., Gilfillan, G.D*., et al.* (2019a). Pre-marked chromatin and transcription factor co-binding shape the pioneering activity of Foxa2. Nucleic Acids Res *47*, 9069-9086.

Cernilogar, F.M., Hasenoder, S., Wang, Z., Scheibner, K., Burtscher, I., Sterr, M., Smialowski, P., Groh, S., Evenroed, I.M., Gilfillan, G.D*., et al.* (2019b). Pre-marked chromatin and transcription factor co-binding shape the pioneering activity of Foxa2. Nucleic Acids Res.

Chazaud, C., Yamanaka, Y., Pawson, T., and Rossant, J. (2006). Early lineage segregation between epiblast and primitive endoderm in mouse blastocysts through the Grb2-MAPK pathway. Dev Cell *10*, 615-624.

Chiappinelli, K.B., Strissel, P.L., Desrichard, A., Li, H., Henke, C., Akman, B., Hein, A., Rote, N.S., Cope, L.M., Snyder, A*., et al.* (2015). Inhibiting DNA Methylation Causes an Interferon Response in Cancer via dsRNA Including Endogenous Retroviruses. Cell *162*, 974-986.

Collins, P.L., Kyle, K.E., Egawa, T., Shinkai, Y., and Oltz, E.M. (2015). The histone methyltransferase SETDB1 represses endogenous and exogenous retroviruses in B lymphocytes. Proc Natl Acad Sci U S A *112*, 8367-8372.

Collins, R.E., Tachibana, M., Tamaru, H., Smith, K.M., Jia, D., Zhang, X., Selker, E.U., Shinkai, Y., and Cheng, X. (2005). In vitro and in vivo analyses of a Phe/Tyr switch controlling product specificity of histone lysine methyltransferases. J Biol Chem *280*, 5563-5570.

Cuellar, T.L., Herzner, A.M., Zhang, X., Goyal, Y., Watanabe, C., Friedman, B.A., Janakiraman, V., Durinck, S., Stinson, J., Arnott, D*., et al.* (2017). Silencing of retrotransposons by SETDB1 inhibits the interferon response in acute myeloid leukemia. J Cell Biol *216*, 3535-3549.

Deniz, O., Frost, J.M., and Branco, M.R. (2019). Regulation of transposable elements by DNA modifications. Nat Rev Genet.

Dewannieux, M., Dupressoir, A., Harper, F., Pierron, G., and Heidmann, T. (2004). Identification of autonomous IAP LTR retrotransposons mobile in mammalian cells. Nat Genet *36*, 534-539.

Dobin, A., Davis, C.A., Schlesinger, F., Drenkow, J., Zaleski, C., Jha, S., Batut, P., Chaisson, M., and Gingeras, T.R. (2013). STAR: ultrafast universal RNA-seq aligner. Bioinformatics *29*, 15-21.

Dodge, J.E., Kang, Y.K., Beppu, H., Lei, H., and Li, E. (2004). Histone H3-K9 methyltransferase ESET is essential for early development. Mol Cell Biol *24*, 2478-2486.

Dong, K.B., Maksakova, I.A., Mohn, F., Leung, D., Appanah, R., Lee, S., Yang, H.W., Lam, L.L., Mager, D.L., Schubeler, D*., et al.* (2008). DNA methylation in ES cells requires the lysine methyltransferase G9a but not its catalytic activity. EMBO J *27*, 2691-2701.

Eckersley-Maslin, M., Alda-Catalinas, C., Blotenburg, M., Kreibich, E., Krueger, C., and Reik, W. (2019). Dppa2 and Dppa4 directly regulate the Dux-driven zygotic transcriptional program. Genes Dev *33*, 194-208.

Engert, S., Liao, W.P., Burtscher, I., and Lickert, H. (2009). Sox17-2A-iCre: a knock-in mouse line expressing Cre recombinase in endoderm and vascular endothelial cells. Genesis *47*, 603-610.

Espada, J., Ballestar, E., Fraga, M.F., Villar-Garea, A., Juarranz, A., Stockert, J.C., Robertson, K.D., Fuks, F., and Esteller, M. (2004). Human DNA methyltransferase 1 is required for maintenance of the histone H3 modification pattern. J Biol Chem *279*, 37175-37184.

Fadloun, A., Le Gras, S., Jost, B., Ziegler-Birling, C., Takahashi, H., Gorab, E., Carninci, P., and Torres-Padilla, M.E. (2013). Chromatin signatures and retrotransposon profiling in mouse embryos reveal regulation of LINE-1 by RNA. Nat Struct Mol Biol *20*, 332-338.

Frank, J.A., and Feschotte, C. (2017). Co-option of endogenous viral sequences for host cell function. Curr Opin Virol *25*, 81-89.

Friedli, M., and Trono, D. (2015). The developmental control of transposable elements and the evolution of higher species. Annu Rev Cell Dev Biol *31*, 429-451.

Fritsch, L., Robin, P., Mathieu, J.R., Souidi, M., Hinaux, H., Rougeulle, C., Harel-Bellan, A., Ameyar-Zazoua, M., and Ait-Si-Ali, S. (2010). A subset of the histone H3 lysine 9 methyltransferases Suv39h1, G9a, GLP, and SETDB1 participate in a multimeric complex. Mol Cell *37*, 46-56.

Fuentes, D.R., Swigut, T., and Wysocka, J. (2018). Systematic perturbation of retroviral LTRs reveals widespread long-range effects on human gene regulation. Elife *7*.

Fuks, F., Hurd, P.J., Deplus, R., and Kouzarides, T. (2003). The DNA methyltransferases associate with HP1 and the SUV39H1 histone methyltransferase. Nucleic Acids Res *31*, 2305-2312.

Garcia-Perez, J.L., Widmann, T.J., and Adams, I.R. (2016). The impact of transposable elements on mammalian development. Development *143*, 4101-4114.

Grapin-Botton, A. (2008). Endoderm specification. In StemBook (Cambridge (MA)).

Habibi, E., Brinkman, A.B., Arand, J., Kroeze, L.I., Kerstens, H.H., Matarese, F., Lepikhov, K., Gut, M., Brun-Heath, I., Hubner, N.C.*, et al.* (2013). Whole-genome bisulfite sequencing of two distinct interconvertible DNA methylomes of mouse embryonic stem cells. Cell Stem Cell *13*, 360-369.

Hajkova, P., Erhardt, S., Lane, N., Haaf, T., El-Maarri, O., Reik, W., Walter, J., and Surani, M.A. (2002). Epigenetic reprogramming in mouse primordial germ cells. Mech Dev *117*, 15-23.

Hansson, M., Olesen, D.R., Peterslund, J.M., Engberg, N., Kahn, M., Winzi, M., Klein, T., Maddox-Hyttel, P., and Serup, P. (2009). A late requirement for Wnt and FGF signaling during activin-induced formation of foregut endoderm from mouse embryonic stem cells. Dev Biol *330*, 286-304.

He, J., Fu, X., Zhang, M., He, F., Li, W., Abdul, M.M., Zhou, J., Sun, L., Chang, C., Li, Y.*, et al.* (2019). Transposable elements are regulated by context-specific patterns of chromatin marks in mouse embryonic stem cells. Nat Commun *10*, 34.

Hermann, A., Goyal, R., and Jeltsch, A. (2004). The Dnmt1 DNA-(cytosine-C5)-methyltransferase methylates DNA processively with high preference for hemimethylated target sites. J Biol Chem *279*, 48350-48359.

Hernandez, C., Wang, Z., Ramazanov, B., Tang, Y., Mehta, S., Dambrot, C., Lee, Y.W., Tessema, K., Kumar, I., Astudillo, M.*, et al.* (2018). Dppa2/4 Facilitate Epigenetic Remodeling during Reprogramming to Pluripotency. Cell Stem Cell *23*, 396-411 e398.

Hon, G.C., Hawkins, R.D., Caballero, O.L., Lo, C., Lister, R., Pelizzola, M., Valsesia, A., Ye, Z., Kuan, S., Edsall, L.E.*, et al.* (2012). Global DNA hypomethylation coupled to repressive chromatin domain formation and gene silencing in breast cancer. Genome Res *22*, 246-258.

Hutnick, L.K., Huang, X., Loo, T.C., Ma, Z., and Fan, G. (2010). Repression of retrotransposal elements in mouse embryonic stem cells is primarily mediated by a DNA methylation-independent mechanism. J Biol Chem *285*, 21082-21091.

Jern, P., and Coffin, J.M. (2008). Effects of retroviruses on host genome function. Annu Rev Genet *42*, 709-732.

Jiang, Y., Loh, Y.E., Rajarajan, P., Hirayama, T., Liao, W., Kassim, B.S., Javidfar, B., Hartley, B.J., Kleofas, L., Park, R.B.*, et al.* (2017). The methyltransferase SETDB1 regulates a large neuron-specific topological chromatin domain. Nat Genet *49*, 1239-1250.

Kanai-Azuma, M., Kanai, Y., Gad, J.M., Tajima, Y., Taya, C., Kurohmaru, M., Sanai, Y., Yonekawa, H., Yazaki, K., Tam, P.P.*, et al.* (2002). Depletion of definitive gut endoderm in Sox17-null mutant mice. Development *129*, 2367-2379.

Karimi, M.M., Goyal, P., Maksakova, I.A., Bilenky, M., Leung, D., Tang, J.X., Shinkai, Y., Mager, D.L., Jones, S., Hirst, M.*, et al.* (2011). DNA methylation and SETDB1/H3K9me3 regulate predominantly distinct sets of genes, retroelements, and chimeric transcripts in mESCs. Cell Stem Cell *8*, 676-687.

Kato, M., Takemoto, K., and Shinkai, Y. (2018). A somatic role for the histone methyltransferase Setdb1 in endogenous retrovirus silencing. Nat Commun *9*, 1683.

Kato, Y., Kaneda, M., Hata, K., Kumaki, K., Hisano, M., Kohara, Y., Okano, M., Li, E., Nozaki, M., and Sasaki, H. (2007). Role of the Dnmt3 family in de novo methylation of imprinted and repetitive sequences during male germ cell development in the mouse. Hum Mol Genet *16*, 2272-2280.

Kawamoto, S., Niwa, H., Tashiro, F., Sano, S., Kondoh, G., Takeda, J., Tabayashi, K., and Miyazaki, J. (2000). A novel reporter mouse strain that expresses enhanced green fluorescent protein upon Cre-mediated recombination. FEBS Lett *470*, 263-268.

Kidwell, M.G. (2002). Transposable elements and the evolution of genome size in eukaryotes. Genetica *115*, 49-63.

Koide, S., Oshima, M., Takubo, K., Yamazaki, S., Nitta, E., Saraya, A., Aoyama, K., Kato, Y., Miyagi, S., Nakajima-Takagi, Y.*, et al.* (2016). Setdb1 maintains hematopoietic stem and progenitor cells by restricting the ectopic activation of nonhematopoietic genes. Blood *128*, 638-649.

Kubicek, S., O'Sullivan, R.J., August, E.M., Hickey, E.R., Zhang, Q., Teodoro, M.L., Rea, S., Mechtler, K., Kowalski, J.A., Homon, C.A.*, et al.* (2007). Reversal of H3K9me2 by a small-molecule inhibitor for the G9a histone methyltransferase. Mol Cell *25*, 473-481.

Kubo, A., Shinozaki, K., Shannon, J.M., Kouskoff, V., Kennedy, M., Woo, S., Fehling, H.J., and Keller, G. (2004). Development of definitive endoderm from embryonic stem cells in culture. Development *131*, 1651-1662.

Kumaki, Y., Oda, M., and Okano, M. (2008). QUMA: quantification tool for methylation analysis. Nucleic Acids Res *36*, W170-175.

Kunath, T., Arnaud, D., Uy, G.D., Okamoto, I., Chureau, C., Yamanaka, Y., Heard, E., Gardner, R.L., Avner, P., and Rossant, J. (2005). Imprinted X-inactivation in extra-embryonic endoderm cell lines from mouse blastocysts. Development *132*, 1649-1661.

Kwon, G.S., Viotti, M., and Hadjantonakis, A.K. (2008). The endoderm of the mouse embryo arises by dynamic widespread intercalation of embryonic and extraembryonic lineages. Dev Cell *15*, 509-520.

Lamprecht, B., Walter, K., Kreher, S., Kumar, R., Hummel, M., Lenze, D., Kochert, K., Bouhlel, M.A., Richter, J., Soler, E.*, et al.* (2010). Derepression of an endogenous long terminal repeat activates the CSF1R proto-oncogene in human lymphoma. Nat Med *16*, 571-579, 571p following 579.

Lawson, K.A., Meneses, J.J., and Pedersen, R.A. (1991). Clonal analysis of epiblast fate during germ layer formation in the mouse embryo. Development *113*, 891-911.

Leeb, M., Pasini, D., Novatchkova, M., Jaritz, M., Helin, K., and Wutz, A. (2010). Polycomb complexes act redundantly to repress genomic repeats and genes. Genes Dev *24*, 265-276.

Lehnertz, B., Ueda, Y., Derijck, A.A., Braunschweig, U., Perez-Burgos, L., Kubicek, S., Chen, T., Li, E., Jenuwein, T., and Peters, A.H. (2003). Suv39h-mediated histone H3 lysine 9 methylation directs DNA methylation to major satellite repeats at pericentric heterochromatin. Curr Biol *13*, 1192-1200.

Leung, D., Du, T., Wagner, U., Xie, W., Lee, A.Y., Goyal, P., Li, Y., Szulwach, K.E., Jin, P., Lorincz, M.C.*, et al.* (2014). Regulation of DNA methylation turnover at LTR retrotransposons

and imprinted loci by the histone methyltransferase Setdb1. Proc Natl Acad Sci U S A *111*, 6690-6695.

Leung, D.C., Dong, K.B., Maksakova, I.A., Goyal, P., Appanah, R., Lee, S., Tachibana, M., Shinkai, Y., Lehnertz, B., Mager, D.L.*, et al.* (2011). Lysine methyltransferase G9a is required for de novo DNA methylation and the establishment, but not the maintenance, of proviral silencing. Proc Natl Acad Sci U S A *108*, 5718-5723.

Li, E., Bestor, T.H., and Jaenisch, R. (1992). Targeted mutation of the DNA methyltransferase gene results in embryonic lethality. Cell *69*, 915-926.

Li, H., Rauch, T., Chen, Z.X., Szabo, P.E., Riggs, A.D., and Pfeifer, G.P. (2006). The histone methyltransferase SETDB1 and the DNA methyltransferase DNMT3A interact directly and localize to promoters silenced in cancer cells. J Biol Chem *281*, 19489-19500.

Li, S.Y., Park, J., Guan, Y., Chung, K., Shrestha, R., Palmer, M.B., and Susztak, K. (2019). DNMT1 in Six2 Progenitor Cells Is Essential for Transposable Element Silencing and Kidney Development. J Am Soc Nephrol *30*, 594-609.

Li, Y., Zhang, Z., Chen, J., Liu, W., Lai, W., Liu, B., Li, X., Liu, L., Xu, S., Dong, Q.*, et al.* (2018). Stella safeguards the oocyte methylome by preventing de novo methylation mediated by DNMT1. Nature *564*, 136-140.

Li, Z., Dai, H., Martos, S.N., Xu, B., Gao, Y., Li, T., Zhu, G., Schones, D.E., and Wang, Z. (2015). Distinct roles of DNMT1-dependent and DNMT1-independent methylation patterns in the genome of mouse embryonic stem cells. Genome Biol *16*, 115.

Liang, G., Chan, M.F., Tomigahara, Y., Tsai, Y.C., Gonzales, F.A., Li, E., Laird, P.W., and Jones, P.A. (2002). Cooperativity between DNA methyltransferases in the maintenance methylation of repetitive elements. Mol Cell Biol *22*, 480-491.

Liu, S., Brind'Amour, J., Karimi, M.M., Shirane, K., Bogutz, A., Lefebvre, L., Sasaki, H., Shinkai, Y., and Lorincz, M.C. (2014). Setdb1 is required for germline development and silencing of H3K9me3-marked endogenous retroviruses in primordial germ cells. Genes Dev *28*, 2041-2055.

Liu, X., Gao, Q., Li, P., Zhao, Q., Zhang, J., Li, J., Koseki, H., and Wong, J. (2013). UHRF1 targets DNMT1 for DNA methylation through cooperative binding of hemi-methylated DNA and methylated H3K9. Nat Commun *4*, 1563.

Lock, F.E., Rebollo, R., Miceli-Royer, K., Gagnier, L., Kuah, S., Babaian, A., Sistiaga-Poveda, M., Lai, C.B., Nemirovsky, O., Serrano, I.*, et al.* (2014). Distinct isoform of FABP7 revealed by screening for retroelement-activated genes in diffuse large B-cell lymphoma. Proc Natl Acad Sci U S A *111*, E3534-3543.

Lorincz, M.C., Dickerson, D.R., Schmitt, M., and Groudine, M. (2004). Intragenic DNA methylation alters chromatin structure and elongation efficiency in mammalian cells. Nat Struct Mol Biol *11*, 1068-1075.

Love, M.I., Huber, W., and Anders, S. (2014). Moderated estimation of fold change and dispersion for RNA-seq data with DESeq2. Genome Biol *15*, 550.

Macfarlan, T.S., Gifford, W.D., Driscoll, S., Lettieri, K., Rowe, H.M., Bonanomi, D., Firth, A., Singer, O., Trono, D., and Pfaff, S.L. (2012). Embryonic stem cell potency fluctuates with endogenous retrovirus activity. Nature *487*, 57-63.

Maksakova, I.A., Romanish, M.T., Gagnier, L., Dunn, C.A., van de Lagemaat, L.N., and Mager, D.L. (2006). Retroviral elements and their hosts: insertional mutagenesis in the mouse germ line. PLoS Genet *2*, e2.

Maksakova, I.A., Thompson, P.J., Goyal, P., Jones, S.J., Singh, P.B., Karimi, M.M., and Lorincz, M.C. (2013). Distinct roles of KAP1, HP1 and G9a/GLP in silencing of the two-cell-specific retrotransposon MERVL in mouse ES cells. Epigenetics Chromatin *6*, 15.

Marx, V. (2012). Epigenetics: Reading the second genomic code. Nature *491*, 143-147.

Matsui, T., Leung, D., Miyashita, H., Maksakova, I.A., Miyachi, H., Kimura, H., Tachibana, M., Lorincz, M.C., and Shinkai, Y. (2010). Proviral silencing in embryonic stem cells requires the histone methyltransferase ESET. Nature *464*, 927-931.

Mikkelsen, T.S., Ku, M., Jaffe, D.B., Issac, B., Lieberman, E., Giannoukos, G., Alvarez, P., Brockman, W., Kim, T.K., Koche, R.P.*, et al.* (2007). Genome-wide maps of chromatin state in pluripotent and lineage-committed cells. Nature *448*, 553-560.

Molaro, A., Falciatori, I., Hodges, E., Aravin, A.A., Marran, K., Rafii, S., McCombie, W.R., Smith, A.D., and Hannon, G.J. (2014). Two waves of de novo methylation during mouse germ cell development. Genes Dev *28*, 1544-1549.

Mouse Genome Sequencing, C., Waterston, R.H., Lindblad-Toh, K., Birney, E., Rogers, J., Abril, J.F., Agarwal, P., Agarwala, R., Ainscough, R., Alexandersson, M.*, et al.* (2002). Initial sequencing and comparative analysis of the mouse genome. Nature *420*, 520-562.

Niakan, K.K., Ji, H., Maehr, R., Vokes, S.A., Rodolfa, K.T., Sherwood, R.I., Yamaki, M., Dimos, J.T., Chen, A.E., Melton, D.A.*, et al.* (2010). Sox17 promotes differentiation in mouse embryonic stem cells by directly regulating extraembryonic gene expression and indirectly antagonizing self-renewal. Genes Dev *24*, 312-326.

Niakan, K.K., Schrode, N., Cho, L.T., and Hadjantonakis, A.K. (2013). Derivation of extraembryonic endoderm stem (XEN) cells from mouse embryos and embryonic stem cells. Nat Protoc *8*, 1028-1041.

Nicetto, D., Donahue, G., Jain, T., Peng, T., Sidoli, S., Sheng, L., Montavon, T., Becker, J.S., Grindheim, J.M., Blahnik, K.*, et al.* (2019). H3K9me3-heterochromatin loss at protein-coding genes enables developmental lineage specification. Science *363*, 294-297.

Nowotschin, S., Setty, M., Kuo, Y.Y., Liu, V., Garg, V., Sharma, R., Simon, C.S., Saiz, N., Gardner, R., Boutet, S.C.*, et al.* (2019). The emergent landscape of the mouse gut endoderm at single-cell resolution. Nature *569*, 361-367.

Okano, M., Bell, D.W., Haber, D.A., and Li, E. (1999). DNA methyltransferases Dnmt3a and Dnmt3b are essential for de novo methylation and mammalian development. Cell *99*, 247-257.

Pasquarella, A., Ebert, A., Pereira de Almeida, G., Hinterberger, M., Kazerani, M., Nuber, A., Ellwart, J., Klein, L., Busslinger, M., and Schotta, G. (2016). Retrotransposon derepression leads to activation of the unfolded protein response and apoptosis in pro-B cells. Development *143*, 1788-1799.

Pastor, W.A., Stroud, H., Nee, K., Liu, W., Pezic, D., Manakov, S., Lee, S.A., Moissiard, G., Zamudio, N., Bourc'his, D.*, et al.* (2014). MORC1 represses transposable elements in the mouse male germline. Nat Commun *5*, 5795.

Peters, A.H., O'Carroll, D., Scherthan, H., Mechtler, K., Sauer, S., Schofer, C., Weipoltshammer, K., Pagani, M., Lachner, M., Kohlmaier, A.*, et al.* (2001). Loss of the Suv39h histone methyltransferases impairs mammalian heterochromatin and genome stability. Cell *107*, 323-337.

Rose, N.R., and Klose, R.J. (2014). Understanding the relationship between DNA methylation and histone lysine methylation. Biochim Biophys Acta *1839*, 1362-1372.

Rossant, J., and Tam, P.P. (2009). Blastocyst lineage formation, early embryonic asymmetries and axis patterning in the mouse. Development *136*, 701-713.

Rothbart, S.B., Krajewski, K., Nady, N., Tempel, W., Xue, S., Badeaux, A.I., Barsyte-Lovejoy, D., Martinez, J.Y., Bedford, M.T., Fuchs, S.M.*, et al.* (2012). Association of UHRF1 with methylated H3K9 directs the maintenance of DNA methylation. Nat Struct Mol Biol *19*, 1155-1160.

Roulois, D., Loo Yau, H., Singhania, R., Wang, Y., Danesh, A., Shen, S.Y., Han, H., Liang, G., Jones, P.A., Pugh, T.J.*, et al.* (2015). DNA-Demethylating Agents Target Colorectal Cancer Cells by Inducing Viral Mimicry by Endogenous Transcripts. Cell *162*, 961-973.

Rowe, H.M., Friedli, M., Offner, S., Verp, S., Mesnard, D., Marquis, J., Aktas, T., and Trono, D. (2013a). De novo DNA methylation of endogenous retroviruses is shaped by KRAB-ZFPs/KAP1 and ESET. Development *140*, 519-529.

Rowe, H.M., Jakobsson, J., Mesnard, D., Rougemont, J., Reynard, S., Aktas, T., Maillard, P.V., Layard-Liesching, H., Verp, S., Marquis, J.*, et al.* (2010). KAP1 controls endogenous retroviruses in embryonic stem cells. Nature *463*, 237-240.

Rowe, H.M., Kapopoulou, A., Corsinotti, A., Fasching, L., Macfarlan, T.S., Tarabay, Y., Viville, S., Jakobsson, J., Pfaff, S.L., and Trono, D. (2013b). TRIM28 repression of retrotransposon-based enhancers is necessary to preserve transcriptional dynamics in embryonic stem cells. Genome Res *23*, 452-461.

Sadic, D., Schmidt, K., Groh, S., Kondofersky, I., Ellwart, J., Fuchs, C., Theis, F.J., and Schotta, G. (2015). Atrx promotes heterochromatin formation at retrotransposons. EMBO Rep *16*, 836-850.

Sakaue, M., Ohta, H., Kumaki, Y., Oda, M., Sakaide, Y., Matsuoka, C., Yamagiwa, A., Niwa, H., Wakayama, T., and Okano, M. (2010). DNA methylation is dispensable for the growth and survival of the extraembryonic lineages. Curr Biol *20*, 1452-1457.

Saksouk, N., Simboeck, E., and Dejardin, J. (2015). Constitutive heterochromatin formation and transcription in mammals. Epigenetics Chromatin *8*, 3.

Schultz, D.C., Ayyanathan, K., Negorev, D., Maul, G.G., and Rauscher, F.J., 3rd (2002). SETDB1: a novel KAP-1-associated histone H3, lysine 9-specific methyltransferase that contributes to HP1-mediated silencing of euchromatic genes by KRAB zinc-finger proteins. Genes Dev *16*, 919-932.

Sharif, J., Endo, T.A., Nakayama, M., Karimi, M.M., Shimada, M., Katsuyama, K., Goyal, P., Brind'Amour, J., Sun, M.A., Sun, Z.*, et al.* (2016). Activation of Endogenous Retroviruses in Dnmt1(-/-) ESCs Involves Disruption of SETDB1-Mediated Repression by NP95 Binding to Hemimethylated DNA. Cell Stem Cell *19*, 81-94.

Sharif, J., Muto, M., Takebayashi, S., Suetake, I., Iwamatsu, A., Endo, T.A., Shinga, J., Mizutani-Koseki, Y., Toyoda, T., Okamura, K.*, et al.* (2007). The SRA protein Np95 mediates epigenetic inheritance by recruiting Dnmt1 to methylated DNA. Nature *450*, 908-912.

Sherwood, R.I., Jitianu, C., Cleaver, O., Shaywitz, D.A., Lamenzo, J.O., Chen, A.E., Golub, T.R., and Melton, D.A. (2007). Prospective isolation and global gene expression analysis of definitive and visceral endoderm. Dev Biol *304*, 541-555.

Shimosuga, K.I., Fukuda, K., Sasaki, H., and Ichiyanagi, K. (2017). Locus-specific hypomethylation of the mouse IAP retrotransposon is associated with transcription factor-binding sites. Mob DNA *8*, 20.

Singh, A.M., Reynolds, D., Cliff, T., Ohtsuka, S., Mattheyses, A.L., Sun, Y., Menendez, L., Kulik, M., and Dalton, S. (2012). Signaling network crosstalk in human pluripotent cells: a Smad2/3-regulated switch that controls the balance between self-renewal and differentiation. Cell Stem Cell *10*, 312-326.

Smith, Z.D., Chan, M.M., Mikkelsen, T.S., Gu, H., Gnirke, A., Regev, A., and Meissner, A. (2012). A unique regulatory phase of DNA methylation in the early mammalian embryo. Nature *484*, 339-344.

Srinivas, S. (2006). The anterior visceral endoderm-turning heads. Genesis *44*, 565-572.

Stocking, C., and Kozak, C.A. (2008). Murine endogenous retroviruses. Cell Mol Life Sci *65*, 3383-3398.

Tachibana, M., Sugimoto, K., Nozaki, M., Ueda, J., Ohta, T., Ohki, M., Fukuda, M., Takeda, N., Niida, H., Kato, H.*, et al.* (2002). G9a histone methyltransferase plays a dominant role in euchromatic histone H3 lysine 9 methylation and is essential for early embryogenesis. Genes Dev *16*, 1779-1791.

Takikita, S., Muro, R., Takai, T., Otsubo, T., Kawamura, Y.I., Dohi, T., Oda, H., Kitajima, M., Oshima, K., Hattori, M.*, et al.* (2016). A Histone Methyltransferase ESET Is Critical for T Cell Development. J Immunol *197*, 2269-2279.

Tamaru, H., and Selker, E.U. (2001). A histone H3 methyltransferase controls DNA methylation in Neurospora crassa. Nature *414*, 277-283.

Tamaru, H., Zhang, X., McMillen, D., Singh, P.B., Nakayama, J., Grewal, S.I., Allis, C.D., Cheng, X., and Selker, E.U. (2003). Trimethylated lysine 9 of histone H3 is a mark for DNA methylation in Neurospora crassa. Nat Genet *34*, 75-79.

Tan, S.L., Nishi, M., Ohtsuka, T., Matsui, T., Takemoto, K., Kamio-Miura, A., Aburatani, H., Shinkai, Y., and Kageyama, R. (2012). Essential roles of the histone methyltransferase ESET in the epigenetic control of neural progenitor cells during development. Development *139*, 3806-3816.

Todd, C.D., Deniz, O., Taylor, D., and Branco, M.R. (2019). Functional evaluation of transposable elements as enhancers in mouse embryonic and trophoblast stem cells. Elife *8*.

Tommasi, S., Zheng, A., Yoon, J.I., Li, A.X., Wu, X., and Besaratinia, A. (2012). Whole DNA methylome profiling in mice exposed to secondhand smoke. Epigenetics *7*, 1302-1314.

Trojer, P., and Reinberg, D. (2007). Facultative heterochromatin: is there a distinctive molecular signature? Mol Cell *28*, 1-13.

Tsumura, A., Hayakawa, T., Kumaki, Y., Takebayashi, S., Sakaue, M., Matsuoka, C., Shimotohno, K., Ishikawa, F., Li, E., Ueda, H.R.*, et al.* (2006). Maintenance of self-renewal ability of mouse embryonic stem cells in the absence of DNA methyltransferases Dnmt1, Dnmt3a and Dnmt3b. Genes Cells *11*, 805-814.

Vandesompele, J., De Preter, K., Pattyn, F., Poppe, B., Van Roy, N., De Paepe, A., and Speleman, F. (2002). Accurate normalization of real-time quantitative RT-PCR data by geometric averaging of multiple internal control genes. Genome Biol *3*, RESEARCH0034.

Viotti, M., Nowotschin, S., and Hadjantonakis, A.K. (2014). SOX17 links gut endoderm morphogenesis and germ layer segregation. Nat Cell Biol *16*, 1146-1156.

Walsh, C.P., Chaillet, J.R., and Bestor, T.H. (1998). Transcription of IAP endogenous retroviruses is constrained by cytosine methylation. Nat Genet *20*, 116-117.

Walter, M., Teissandier, A., Perez-Palacios, R., and Bourc'his, D. (2016). An epigenetic switch ensures transposon repression upon dynamic loss of DNA methylation in embryonic stem cells. Elife *5*.

Wamaitha, S.E., del Valle, I., Cho, L.T., Wei, Y., Fogarty, N.M., Blakeley, P., Sherwood, R.I., Ji, H., and Niakan, K.K. (2015). Gata6 potently initiates reprograming of pluripotent and differentiated cells to extraembryonic endoderm stem cells. Genes Dev *29*, 1239-1255.

Wang, J., Xie, G., Singh, M., Ghanbarian, A.T., Rasko, T., Szvetnik, A., Cai, H., Besser, D., Prigione, A., Fuchs, N.V.*, et al.* (2014). Primate-specific endogenous retrovirus-driven transcription defines naive-like stem cells. Nature *516*, 405-409.

Wiesner, T., Lee, W., Obenauf, A.C., Ran, L., Murali, R., Zhang, Q.F., Wong, E.W., Hu, W., Scott, S.N., Shah, R.H.*, et al.* (2015). Alternative transcription initiation leads to expression of a novel ALK isoform in cancer. Nature *526*, 453-457.

Wu, J., Huang, B., Chen, H., Yin, Q., Liu, Y., Xiang, Y., Zhang, B., Liu, B., Wang, Q., Xia, W.*, et al.* (2016). The landscape of accessible chromatin in mammalian preimplantation embryos. Nature *534*, 652-657.

Yasunaga, M., Tada, S., Torikai-Nishikawa, S., Nakano, Y., Okada, M., Jakt, L.M., Nishikawa, S., Chiba, T., Era, T., and Nishikawa, S. (2005). Induction and monitoring of definitive and visceral endoderm differentiation of mouse ES cells. Nat Biotechnol *23*, 1542-1550.

Yuan, P., Han, J., Guo, G., Orlov, Y.L., Huss, M., Loh, Y.H., Yaw, L.P., Robson, P., Lim, B., and Ng, H.H. (2009). Eset partners with Oct4 to restrict extraembryonic trophoblast lineage potential in embryonic stem cells. Genes Dev *23*, 2507-2520.

Zernicka-Goetz, M., Morris, S.A., and Bruce, A.W. (2009). Making a firm decision: multifaceted regulation of cell fate in the early mouse embryo. Nat Rev Genet *10*, 467-477.

Zhang, Y., Xiang, Y., Yin, Q., Du, Z., Peng, X., Wang, Q., Fidalgo, M., Xia, W., Li, Y., Zhao, Z.A.*, et al.* (2018). Dynamic epigenomic landscapes during early lineage specification in mouse embryos. Nat Genet *50*, 96-105.

Zhao, Q., Zhang, J., Chen, R., Wang, L., Li, B., Cheng, H., Duan, X., Zhu, H., Wei, W., Li, J.*, et al.* (2016). Dissecting the precise role of H3K9 methylation in crosstalk with DNA maintenance methylation in mammals. Nat Commun *7*, 12464.